University of Study of Messina

Department of Veterinary Sciences

PhD in Veterinary Sciences

Coordinator: Prof. Adriana Ferlazzo

Curriculum: Clinical Veterinary Sciences

EVALUATION OF VASCULAR PERFUSION OF ABDOMINAL ORGANS IN THE DOG USING CEUS (CONTRAST-ENHANCED ULTRASONOGRAPHY).

Author:
Cyndi Mangano, MVD

Tutor:
Prof. Massimo De Majo, MVD, PhD

Co-Tutor:
MVD Pavel Proks, PhD

XXX Cycle

To My Mom,
A Strong Woman
And
Always Close To Me

Thanks to all staff of:
- Veterinary Teaching Hospital of Department of Veterinary Sciences, University of Studies of Messina, Italy, in the person of Prof. Massimo De Majo.
- Clinica Veterinaria Camagna Spa, Reggio Calabria, Italy, in the person of Prof. Nicola Maria Iannelli.
- Department of Diagnostic Imaging of Veterinary Hospital of Veterinary and Pharmaceutical University of Brno, Czech Republic, in the person of Prof. Pavel Proks.
This research project was realized in accordance with the current legislation and only for medical purposes.

INDEX

Abstract

Contrast-enhanced ultrasound (CEUS) is an ultrasonographic technique that reveals the micro-vascularization of organs and is applied in veterinary medicine to study physiological and pathological conditions, focal or diffuse parenchymal lesions.
Clinical applications include the possibility to use CEUS in dogs to evaluate the perfusion of spleen, bladder, kidneys, testis, liver, gallbladder, adrenal, soft tissue lesions, pancreas, prostate and emergencies.

Aim of this study is to describe the use of CEUS in dogs for some organs, giving some new applications and analysing the literature knowledge.

SonoVue®, contrast medium agent, was used. Qualitative evaluation were done and quantitative computerized analysis of the contrast medium blood pool phase were performed using a dedicated commercial software.

Particular results were given about Benign Nodular Hyperplasia (BNH): 20 spleens affected by BNH were studied and qualitative analysis showed simultaneous wash-in of lesion, compared to normal parenchyma, and anticipated wash-out, with hypoechoic pattern than surrounding normal spleen. Quantitative results showed the same peak of enhancement of lesions to the surrounding normal parenchyma but the contrast remain into the lesion for shorter time. In few cases, Hemangiosarcoma, Lymphoma and Histiocytic Sarcoma had early wash-in and early wash-out, prominent inner vessels characterize the lesions, associated with malignancy according to literature.
Considering previous studies, our results suggest that hypoenhancing is not a specific pattern of malignancy in splenic lesions.
Bladder wall was studied in 10 normal dogs using CEUS; wash-in began around 18 seconds and enhancing the bladder wall. Six cases of Transitional Cell Carcinoma (TCC) were evaluated, involvement of muscular layer of bladder wall with hyperenhancement of infiltrating tumor tissue was demonstrated.
About kidney perfusion, CEUS showed lower values in case ok kidney failure compared to a control group, this aspect suggested a reduction of renal perfusion during kidney disease.
Testes were studied giving referral qualitative and quantitative parameters about Interstitial Cell Tumour in n°=12 non-sedated dogs to study a single type of tumor without any influence by anesthesia: wash-in was around 25 seconds at the same time with surrounding tissue with hyperenhancement of lesion, heterogeneity and inner vessels.
CEUS was used also in other organs (Special Section two) including: Liver, Gallbladder, Adrenal, Gastro-enteric tract, Ovary, Soft tissue lesions with few cases.
In conclusion, the evidence of hypoenhancement of BNH opens new considerations about CEUS characterization of malignant lesions that was demonstrated by previous studies. Based on our preliminary results about bladder lesions, a larger number of cases of TCC in comparison with inflammatory hyperplastic bladder lesions are needed to conclude if CEUS may be a feasible tool to study bladder wall lesions. Lower CEUS parameters of contrast medium diffusion in kidney of dogs affected by renal failure than normal dogs suggest a reduction of kidney perfusion in case of renal failure.
CEUS is a technique that gives important information about perfusion, even if previous data have produced variable results; CEUS may be used expanding the knowledge given by basic ultrasonography.

List of abbreviations

AIFA Italian Agency of Drugs
BNH Benign Nodular Hyperplasia
BPH Benign Prostatic Hyperplasia
CECT Contrast-Enhanced Computed Tomography
CEUS Contrast-Enhanced Ultrasound
CVC Caudal Vena Cava
CT Computed Tomography
EFSUMB European Federation of Societies for Ultrasound in Medicine and Biology
EMA European Medicine Agency
FDA Food and Drug Administration
GB Gallbladder
GE Gastro-Enteric
HCC Hepato-Cellular-Carcinoma
ICT Interstitial Cell Tumour
IFI Indirect Immunofluorescence
IRIS International Renal Interest Society
Leish Leishmaniasis – Leishmania
MI Mechanical Index
MR Magnetic Resonance
MTT average Time Transit
P Peak
PCR Polymerase Chain Reaction
PI Peak Intensity
PV Porta Vein
RBF Regional Blood Flow
RBV Regional Blood Volume
RES Reticle Endothelial System
RI Resistivity Index
ROI Region Of Interest
SCT Sertoli Cell Tumour
SD Standard Deviation
SEM Seminoma
TCC Transitional Cell Carcinoma
TIC Time Intensity Curve
TTP Time To Peak
UCA Ultrasound Contrast Agent
US Ultrasonography

---GENERAL SECTION---

1 Introduction

1.1 Contrast-enhanced ultrasound (CEUS)

Contrast-enhanced ultrasound (CEUS) is an ultrasonographic technique applied most widespread in human medicine at the beginning of 2000. (Piscaglia, et al., 2012)
In 2004, the European Federation of Societies for Ultrasound in Medicine and Biology (EFSUMB) released the first guidelines about use of CEUS for liver applications in human patients. (Albrecht, et al., 2004)
EFSUMB, between 2008 and 2011, enlarged CEUS guidelines for non-hepatic applications.
CEUS, based on safety and efficacy, can be performed everywhere and without losing time for preliminary laboratory testing and it operates in real time so that rapid changes can be captured.
The procedure provides that CEUS examination should be preceded by careful assessment of the target with conventional B-mode US and, when appropriate, with Doppler (Spectral and/or Colour - Power). *SonoVue*® (sulphur hexafluoride with a phospholipid shell) produced by Bracco International, Imaging Milan S.p.A®, introduced in 2001, is the UCA mostly used in Europe. Use of UCA is finalized to improve B-mode and Doppler information: the underlying conventional B-mode image is seen, Doppler shows the bigger vascularization and CEUS, in addition of colour Doppler information, shows micro-vascularization. The description of the behaviour of tissue or lesion under examination should be in terms of its enhancement, taking into consideration its temporal behaviour, degree of enhancement, and contrast distribution. (Piscaglia, et al., 2012)

The most important clarification about the use of UCAs regards the safety of use firstly in human medicine and then in veterinary medicine.
The UCAs are very safe with a low incidence of side effects.
Between December 2001 to December 2004, it was the period of data collection in 28 centres for a total number of 23188 investigations mostly for liver: total number of adverse events was 29 but just 2 seriously needed treatment and 27 not serious, not needed treatment. (Piscaglia & Bolondi, 2006). Cardiac evaluation, using MI 0,4 effects, appears to increase rapidly: studied effects include premature ventricular contractions, micro-vascular rupture and petechial haemorrhage;, these damages may be reparable but good practice suggests caution when using UCAs. (Haar ter, 2009)
Despite FDA in 2007 announced a stop for using UCAs after death of 4 patients, that was not directly related to UCA's administration, confirmed by the following study conducted for human patients and in veterinary as confirmed in Sailer et al, 2013. (Seiler, et al., 2013)
The interaction of diagnostic US with UCA could produce bio-effects, *in vitro* interactions between gas, bodies and cells; in fact, were observed alteration and cell death were observed. (EMA: European Medicines Agency, 2017)
In human medicine, there are important considerations are about using of CEUS in paediatric. Only the UCA *Levovist*® was approved for use in children and only for vesical-ureteral reflux; in fact, manufacturer's instructions declare that the safety and effectiveness of *SonoVue*® in patients under 18 years old has not been established and the product should not be used in these patients. (EMA: European Medicines Agency,

2017). However for CEUS paediatric applications remain of critical importance. (Piscaglia, et al., 2012)
In veterinary medicine some hypersensitivity or allergic events occur rarely and there is no evidence of nephrotoxicity or cardio-toxicity. However, there is the possibility of bio-effects such as micro-vascular rupture with the insonation of microbubbles. (Ohlerth & Obrien, 2007)
No side effects have been reported with the use of *Definity*®, *Imagent*®, *SonoVue*® and *Levovist*®, the most used UCAs, in none dogs and cats studied (O'Brien, et al., 2004 - Rademacher, et al., 2008).
Immune reactions have not been associated with the use of Optison® in humans. Although there are reports of uncomplicated use of Optison® in dogs and other small animals, anaphylactic response related to the human albumin component has been reported in two dogs. (Yamaya, et al., 2004)

In 2007 Ohlerth & OBrien, wrote about CEUS in veterinary medicine about basic concepts.
They defined that the ultrasound contrast agent is an exogenous substance, consisting of gas or air microbubbles encapsulated in a shell of different composition, that can be administered intravenously or into a body cavity to enhance ultrasonic signals and wrote about use of CEUS in veterinary medicine. (Ohlerth & OBrien, 2007)
Recently, another guideline on non-hepatic application in human medicine was published. In this review, they present updated knowledge on CEUS application in the following fields: urogenital system (kidney, prostate and testis), thyroid, small bowel and lymph nodes.(Cantisani, et al., 2015)

1.2 Ultrasound contrast agents (UCAs)

It is possible to classify different UCAs for different composition and diffusion, generation and utility (Table 1.1: UCAs).
Most UCAs do not diffuse across the endothelium and therefore, they basically are blood pool agents. Vascular enhancement usually lasts a few minutes.
Typically, the gas content in the contrast agent is eliminated by lungs, while the shell components are filtered by the kidneys and eliminated by liver (Quaia, 2005, p. 3-14).
This has led to the development of the first generation of trans-pulmonary contrast agents using air as the gas in the microbubbles covered by a shell. Third generation agents use the stabilization of a hard shell (polymer shells) and contain either air or perfluorocarbons, resulting in a much longer persistence time but are not still approved according to AIFA.
For example the *Levovist*® has been shown to have a late hepato-splenic-specific parenchymal phase with accumulation in human liver and spleen up to 20 min after intravenous (IV) bolus injection: accumulation may be mediated by the reticuloendothelial system, the Kupffer cells, or microbubbles are entrapped in the liver sinusoids (Quaia, 2005). Therefore, the late phase is also called sinusoidal phase.
SonoVue® or *Imavist*®, blood pool agents, were also subsequently found to have the sinusoidal phase: maybe the agents are trapped or slowed in the hepatic sinusoids, during the study of liver.
The microbubble behaviour is depending on the local acoustic power (Quaia, 2005, p. 15-30) and the output power is reflected by the mechanical index (MI) which originally measures the potential for mechanical damage to tissues exposed to intense ultrasound pulses: the higher is the MI, the greater are its destructive properties (Quaia, 2005, p. 15-30).
The linear effects of ultrasound contrast agents are utilized in the clinical setting by Doppler technologies. If the acoustic power of the ultrasound beam at the resonance frequency increases (intermediate MI: $0.1 < MI > 0.5$), microbubbles will show a longer expansion than contraction phase and begin nonlinear (not-sigmoidal shaped) oscillation (Quaia, 2005, p. 15-30). They start to emit the harmonics of the resonance frequency. The frequency of sub-harmonics is at half and that of higher harmonics is at multiples of the fundamental frequency. The second harmonic response is found at twice the fundamental frequency and usually has the highest intensity among the harmonic responses. The theoretical advantage of the harmonic over the fundamental frequency is that only microbubbles resonate with harmonics while adjacent tissues do not resonate or their harmonic resonation is very little. The increase of intensity of ultrasound beam disrupted the microbubbles: stimulated acoustic emission or loss of correlation.
Microbubble persistence and stability were increased by two principal ways: bubble encapsulation with or without surfactants and selection of gases with low diffusion coefficient. (Quaia, 2005, p. 3-14 - Ohlerth & OBrien, 2007)
The advantages to prefer sulphur hexafluoride-filled microbubbles, in comparison to the other UCAs are the prolonged stability in the vial (up to 6 h) and the peripheral blood (half-life of 6 min), and the uniformity of their size, which improves backscattering and harmonic behaviour at low acoustic power (Quaia, 2005, p. 3-14).
Similar to *Levovist*®, *SonoVue*® has also been shown to have a late hepatosplenic-specific parenchymal phase in humans. *SonoVue*® provides a non-linear response with production of a clinically useful signal at low acoustic pressures, and destruction of the microbubbles is limited. (Ohlerth & OBrien, 2007)

Table 1.1: UCAs. UCAs that are/ have been clinically approved and some characteristics. The table include UCAs differentiating according to name, generation, first approval for clinical use, shell material, gas, half-life, countries and distributor. (Paefgen, et al. 2015)

NAME	GENERATION	FIRST APROVED FOR CLINICAL USE	SHELL MATERIAL	GAS	HALF-LIFE	COUNTRIES	PROCEDURE/ DISTRIBUTOR
ALBUNEX	1	1993 WITHDRAW	SONICATED SERUM ALBUMIN	AIR	SHORT	JAPAN, US	MOLECULAR BIOSYSTEMS INC. SAN DIEGO, CA,USA
ECHOVIST	1	1991 WITHDRAW AIFA W	GALACTOSE MICROPARTICLES	AIR	SHORT	GERMANY, UK	SCHERING AG, BERLIN, DE
LEVOVIST	1	1995 WITHDRAW AIFA W	GALACTOSE MICROPARTICLES, PALMITIC ACID	AIR	SHORT	CANAD, EU, CHINA, JAPAN	SCHERING AG, BERLIN, DE
OPTISON	2	1998 AIFA APPROVED	CROSS-LINKED SERUM ALBUMIN	OCTAFLUOROPROPANE	LONG	US, EU	GE HEALTCARE, BUCKINGHAMSHIRE, UK
LUMASON / SONOVUE	2	2001/2004 AIFA APPROVED	PHOSPHOLIPID	SULPHURHEXAFLUORIDE	LONG	US, EU, CHINA	BRACCO INTERNATIONAL IMAGING MILAN S.p.A., ITALY
SONAZOID	2	2007	PHOSPHOLIPID	PERFLUOROBUTANE	LONG	JAPAN, SOUTH KOREA	GE HEALTCARE, BUCKINGHAMSHIRE, UK
DEFINITY/ LUMINITY	2	2001/2006 AIFA APPROVED	PHOSPHOLIPID	OCTAFLUOROPROPANE	LONG	NORTH AMERICA, EU	LANTHEUS MEDICAL IMAGING, NORTH BILLORICA, MA
IMAGENT/ IMAVIST	2	2002,WITHDRAW	PHOSPHOLIPID	PERFLUOROHEXANE, NITROGEN	LONG	US	SCHERING AG, BERLIN, DE
ECHOGEN	3	2000, WITHDRAW	COLLOID PERFLENAPENT	DODECAFLUOROPENTANE	LONG	EU	SONUS PHARMACEUTICALS

SonoVue® is composed by 8 microliters/ml of sulphur hexafluoride microbubbles in a kit that includes also the solvent for dispersion for injection: 1 ml of the resulting dispersion contains 8 µl sulphur hexafluoride in the microbubbles, equivalent to 45 micrograms. This kit is composed with 1 vial containing 25 mg of lyophilized powder, 1 pre-filled syringe containing 5 ml sodium chloride and 1 Mini-Spike transfer system.
According to the manufacturer's instructions, *SonoVue*® is

1. for use with ultrasound imaging to enhance the echogenicity of the blood, which results in an improved signal to noise ratio and should only be used in patients where study without contrast enhancement is not-conclusive.
2. is a trans pulmonary echocardiographic contrast agent for use in patients with suspected or established cardiovascular disease to provide opacification of cardiac chambers and enhance left ventricular endocardial border delineation.
3. increases the accuracy in detection or exclusion of abnormalities in cerebral arteries and extra cranial carotid or peripheral arteries by improving the Doppler signal to noise ratio.
4. increases the quality of the Doppler flow image and the duration of clinically-useful signal enhancement in portal vein assessment.
5. improves display of the vascularity of liver and breast lesions during Doppler sonography, leading to more specific lesion characterization.

In human medicine, the recommended doses of *SonoVue*® are: B-mode imaging of cardiac chambers, at rest or with stress: 2 ml and for vascular Doppler imaging: 2.4 ml. During a single examination, a second injection of the recommended dose can be made. (EMA: European Medicines Agency, 2017)
The microbubbles dispersion is prepared before use by injecting through the septum 5 ml of sodium chloride 9 mg/ml (0.9%) solution for injection to the contents of the vial. The vial is then shaken vigorously for a few seconds until the lyophilizate is completely dissolved. The desired volume of the dispersion can be drawn into a syringe any time up to six hours after reconstitution. Just before drawing into the syringe, the vial should be agitated to re-suspend the microbubbles. *SonoVue*® should be administered immediately after drawing into the syringe by injection into a peripheral vein. Every injection should be followed by a flush with 5 ml of sodium chloride 9 mg/ml (0.9%) solution for injection. (EMA: European Medicines Agency, 2017)

Some contraindications have been seen, such us hypersensitivity to the active substance(s) or to any of the excipients. *SonoVue*® is contraindicated in patients known to have right-to-left shunts, severe pulmonary hypertension (pulmonary artery pressure >90 mmHg), uncontrolled systemic hypertension, and in patients with adult respiratory distress syndrome.
SonoVue® should not be used in combination with dobutamine in patients with conditions suggesting cardiovascular instability where dobutamine is contraindicated.
ECG monitoring should be performed in high-risk patients as clinically indicated.
Use extreme caution when considering the administration of *SonoVue*® in patients with recent acute coronary syndrome or clinically unstable ischemic cardiac disease, including: evolving or ongoing myocardial infarction, typical angina at rest within last 7 days, significant worsening of cardiac symptoms within last 7 days, recent coronary artery intervention or other factors suggesting clinical instability (for example, recent deterioration of ECG, laboratory or clinical findings), acute cardiac failure, Class III/IV cardiac failure, or severe rhythm disorders because in these patients allergy like and/or vasodilatory reactions may lead to life threatening conditions.
SonoVue® should only be administered to such patients after careful risk/benefit assessment and a closely monitoring of vital signs should be performed during and after administration.
Emergency equipment and personnel trained in its use must be readily available.
In the event of an anaphylactic reaction, beta blockers (including eye drop preparations) may aggravate the reaction. Patients may be unresponsive to the usual doses of adrenaline used to treat the allergic reactions.
Caution is advised when *SonoVue*® is administered to patients with clinically significant pulmonary disease, including severe chronic obstructive pulmonary disease.
It is recommended to keep the patient under close medical supervision during and for at least 30 minutes following the administration of *SonoVue*®.
The number of patients with the following conditions who were exposed to *SonoVue*® in the clinical trials has been limited, and therefore, caution is advisable when administering the product to patients with: acute endocarditis, prosthetic valves, acute systemic inflammation and/or sepsis, hyperactive coagulation states and/or recent thromboembolism, and end-stage renal or hepatic disease.
SonoVue® is not suitable for use in ventilated patients, and those with unstable neurological diseases.
In animal studies, the application of echo-contrast agents revealed biological side effects (e.g. endothelial cell injury, capillary rupture) by interaction with the ultrasound beam. Although these biological side effects have not been reported in humans, the use of a low mechanical index is recommended.
No interaction studies have been performed.
No clinical data on exposed pregnancies are available about use in pregnancy cases.
The safety of *SonoVue*® was evaluated in 4653 adult patients who participated in 58 clinical trials.
The adverse reactions are classified by System Organ Class and frequency, using the following convention: Very common (≥ 1/10), Common (≥ 1/100 to < 1/10), Uncommon (≥ 1/1,000 to < /100), Rare (≥ 1/10,000 to < 1/1,000), Very rare (< 1/10,000), not known (cannot be estimated from the available data)
In very rare cases, fatal outcomes have been reported in temporal association with the use of *SonoVue*®.
In all these patients, there was a high underlying risk for major cardiac complications, which could have lied to the fatal outcome.

Reporting suspected adverse reactions after authorization of the medicinal product is important. It allows continued monitoring of the benefit/risk balance of the medicinal product.
The addition of sodium chloride 9 mg/ml (0.9%) solution for injection to the lyophilised powder followed by vigorous shaking results in the production of the microbubbles of sulphur hexafluoride.
The microbubbles have a mean diameter of about 2.5 μm, with 90% having a diameter less than 6 μm and 99% having a diameter less than 11 μm. Each millilitre of *SonoVue*® contains 8 μl of the microbubbles. The interface between the sulphur hexafluoride bubble and the aqueous medium acts as a reflector of the ultrasound beam thus enhancing blood echogenicity and increasing contrast between the blood and the surrounding tissues.
The intensity of the reflected signal is dependent on concentration of the microbubbles and frequency of the ultrasound beam. At the proposed clinical doses, *SonoVue*® has been shown to provide marked increase of more than 2 minutes in signal intensity for B-mode imaging in echocardiography and of 3 to 8 minutes for Doppler imaging of the macrovasculature and microvasculature.
Sulphur hexafluoride is an inert, innocuous gas, poorly soluble in aqueous solutions. There are literature reports of the use of the gas in the study of respiratory physiology and in pneumatic retinopexy.
The total amount of sulphur hexafluoride administered in a clinical dose is extremely small, (in a 2 ml dose the microbubbles contain 16 μl of gas). The sulphur hexafluoride dissolves in the blood and is subsequently exhaled.
After a single intravenous injection of 0.03 or 0.3 ml of *SonoVue*®/kg (approximately 1 and 10 times the maximum clinical dose) to human volunteers, the sulphur hexafluoride was cleared rapidly. The mean terminal half-life was 12 minutes (range 2 to 33 minutes). More than 80% of the administered sulphur hexafluoride was recovered in exhaled air within 2 minutes after injection and almost 100% after 15 minutes.
In patients with diffuse interstitial pulmonary fibrosis, the percentage of dose recovered in expired air averaged 100% and the terminal half-life was similar to that measured in healthy volunteers.
Non-clinical data reveal no special hazard for humans based on conventional studies of safety pharmacology, genotoxicity and toxicity to reproduction.
Shelf life is 2 years.
Once reconstituted, chemical and physical stability has been demonstrated for 6 hours. From a microbiological point of view, the product should be used immediately. If not used immediately, in use storage times and conditions prior to use are the responsibility of the user.
Before use examine the product to ensure that the container and closure have not been damaged.
Do not use if the liquid obtained is clear and/or if solid parts of the lyophilisate are seen in the suspension.
SonoVue® should be administered immediately by injection into a peripheral vein.
If *SonoVue*® is not used immediately after reconstitution the microbubble dispersion should be shaken again before being drawn up into a syringe. Chemical and physical stability of the microbubble dispersion has been demonstrated for 6 hours.
The vial is for a single examination only. Any unused medicinal product or waste material must be discarded in accordance with local requirements. (EMA: European Medicines Agency, 2017)

1.3 The technique

Contrast-specific US modes are required and are generally based on the cancellation and/or separation of linear US signals from tissue and the use of the non-linear response from microbubbles. The non-linear response from microbubbles arises from non-linear response from microbubbles oscillations at low acoustic pressure, chosen to minimize the disruption of the microbubbles and high-energy broadband non-linear response arising from microbubbles disruption.
Non-linear harmonic US signals also arise in tissues themselves from distortion of the sound wave during its propagation through the tissue. The extent of this tissue harmonic response increases with the acoustic pressure, which is proportional to the MI. The precise unit of measurement for acoustic pressure is the Pascal, but the most common reference unit is the MI.
Minimization of bubble disruption is the main reason for using low MIs for real time imaging but it also reduces tissue harmonics and artefacts, thus facilitating the separation of signals from UCAs from those of tissue. Low MI is typically below 0.3.
CEUS is defined as low MI real time contrast specific imaging, unless otherwise specified. This is in agreement with the terminology of the vast majority of the literature.
EFSUMB characterized the quality of the equipment used for CEUS examinations.
Sensitivity reflects the ability of a system to detect extremely small amounts of microbubbles. Good sensitivity extends the duration of useful enhancement. The ability to image small differences in local contrast concentration is a component of sensitivity.
Tissue suppression is mandatory to differentiate contrast enhancement from tissue echoes. Strongly reflective structures such as vessel walls, the abdominal wall and gas-filled structures can break through and appear on the CEUS part of the screen.
Temporal resolution is defined by the frame rate at a given line density, depth and width. A high frame rate allows visualization of the flow direction in arteries. It may also produce more rapid destruction of bubbles within the acoustic field. Spatial resolution mainly refers to the ability to display bubble echoes with optimal detail. Additionally, the image should be homogeneous throughout. The MI is the most important setting for CEUS and gain is the second one.
Competence ensured by adequate training is a prerequisite to achieve correct diagnoses when using ultrasonography and especially CEUS. EFSUMB has defined three levels of training. (Piscaglia, et al., 2012)

CEUS has some artefacts, mainly caused by incorrect machine settings or UCA dosages, particularly: acoustic power (mechanical index) and other aspects resulting in micro bubble destruction; the possibility of false positive contrast signals in non-vascularized areas; attenuation caused by too high contrast agent dose; influence of the frame rate on the spatial resolution; dealing with deep located lesions; differences in focus positioning in detection and characterization studies; advantages and disadvantages of replenishment studies; reliability of contrast enhanced spectral Doppler measurements. (Dietrich, et al., 2011)

The CEUS interpretation of results is done from a qualitative and a quantitative analysis of the video clips images.
Significant variations exist in the imaging results, and the lack of understanding regarding their origin of acquisition data when performing CEUS. This is related to potential sources of variability in the quantification of tissue perfusion based on microbubbles contrast-enhanced ultrasound images. These depends from factors relating

to the scanner setting, which include transmission power, transmission focal depth, dynamic range, signal gain and transmission frequency; factors relating to the patient, which include body physical differences, physiological interaction of body with bubbles, propagation and attenuation through tissue, and tissue motion, and factors relating to the microbubbles, which include the type of bubbles and their stability, preparation and injection and dosage. It has been shown that the factors can significantly affect the imaging results and contribute to the variations observed. (Tang, et al., 2011)

The bubble contrast agents are especially sensitive to the local deposition of sound energy. Sufficient energy (sound amplitude) must be provided to generate an adequate signal-to noise ratio for agent detection, but not so high that bubble destruction occurs, preventing real-time display of perfusion. It is necessary one energy balance that includes adjustment of MI (output power), frame rate, number and location of focal zones, and transmitted frequency. Included in the pulse sequence adjustments are specific optimization of grey scale maps, frame averaging and edge enhancement.
Technologies now exist to image contrast agents in both the fundamental (1st harmonic) and harmonic (2nd harmonic) frequencies by differing applications and manufacturers.
Ultrasound contrast agents can be used with conventional B-mode and Doppler sonography. Contrast agents cause significant enhancement of Doppler signals and have been used for many years for vascular studies.
Before the introduction of UCAs some studies were based on Doppler use but Conventional contrast-enhanced power Doppler ultrasound has been shown to be more sensitive for detecting low velocities and small parenchymal vessels than power Doppler alone or colour Doppler with or without the use of a microbubbles contrast agent (Bude, et al., 1994) (Eriksson, et al., 1991).
To avoid interpretative errors, during performing CEUS, artefacts need to be recognized and the following settings should be adapted; reduction of colour gain, persistence and MI, slower infusion of contrast agent, and increasing the wall filter and pulse repetition frequency (Quaia, 2005, p. 15-30)
By varying the phase and amplitude of multiple pulse interactions the contrast agent signal can be separated from the tissue signals.
The system should be optimized for both low and high MI studies, as clinically indicated. Contrast enhancement in most parenchymal organs is divided into early and late phases. The late phase is approximately up to 20 min after introduction of the contrast material and after elimination of the majority of the blood pool portion of contrast agent.
The remaining contrast agent is described variably within the sinusoids or RES of the liver and spleen (Quaia, 2005, p. 3-14).
Low MI studies allow a real-time display of arteriolar perfusion and venous portions of early phase contrast imaging. As discussed later in the clinical applications section, the perfusion portion of the early phase imaging is especially important for determining the characteristic of liver nodules in the differential between malignant and benign nodules.
Contrast-enhanced colour and power Doppler ultrasound images may be subjectively evaluated for vascularity (number of vessels per unit tissue volume), distribution of vessels within a lesion (vascular pattern) and vessel morphology.
Subjective quantification of vascularity can be performed by using a score. Altered vessel morphology such as stenosis, occlusion, trifurcations, abnormal branching patterns and loop formation may also be assessed.

For previously identified nodules, masses or abnormal organs (especially lymph nodes), characterization of the size, shape, number and location (vascular pattern) of afferent vessels provides important information.
During the perfusion portion of the early phase, regional hypo-perfusion can be detected and, when compared to timing of perfusion in the surrounding normal tissue, it is vital for characterization of malignancy. All of this is performed in real-time and assessed subjectively. Similarly, occult malignant nodules can be detected by methodical scanning through an organ during the peak of the normal tissue perfusion.
Regional hypo-perfusion can be detected in cases of infarction, thrombosis or necrosis by comparison to more normal regions.

Important considerations have to be done about the influence of the pharmacological agents used for sedation or anesthesia on contrast medium diffusion.
In a study about kidney perfusion, was clearly explained that use of Propofol and Butorphanol did not influenced UCA diffusion (Stock, et al., 2014).
Also for kidney was confirmed that tiletamine-zolazepam don't give changes (Choi, et al., 2016).
The action of dexmedetomidine implies a decrease of the PI in the renal cortex but not in the spleen, liver and intestines (Restitutti, et al., 2013); a significant reduction of splenic enhancement was observed with dexmedetomidine and contraindicate the use as sedative for splenic CEUS procedures in the dog (Rossi et al., 2016).

Most manufacturers provide online image analysis packages for post-imaging quantitative analysis. This is especially important for research applications. Contrast-enhanced colour and power Doppler ultrasound.
Basically, a region of interest (ROI) is applied to the image, and the percentage of coloured pixels within the ROI determines a vascularity index indicating the percentage area of the tumour occupied by blood vessels. Taking the colour level of each pixel, determined by the hue, saturation and brightness values, into account, a measure of blood volume or perfusion within the tissue may be derived.
With the onset of injection of an ultrasound contrast agent, time intensity curves can be generated over an appropriate time by applications of ROIs to assess perfusion within tissue volumes or individual vessels. The following quantitative haemodynamic indices are most commonly obtained: peak enhancement, time to peak enhancement, up-slope, down-slope and area under the curve (Nyman, et al., 2005 - Ziegler, et al., 2003).
By this method, baseline data for normal organ perfusion but also disease processes can be obtained. One caveat for determination of these indices is accounting for respiratory motion. Regardless of the MI, all imaging leads to destruction of contrast agent.
Movement of the liver with respiration presents previously non- imaged liver with naive bubbles for analysis.
Estimations of baseline and peak values are affected by patient motion. Time to absolute peak may introduce too many motion and bubble integrity variables in the analysis, falsely prolonging time-to-peak and lowering wash-in rate indices. A better method may be to calculate values of time to Peak or indices of washout based on the times associated with 20% above baseline (as a better baseline value) and 90% (or other objective suboptimal value) of peak for the various indices, as appropriate for the organ and species (Ziegler, et al., 2003 - Ohlerth & Obrien, 2007).
If *Levovist*® is used, after blood pool clearance, is visible an underlying mechanism is not fully understood consisting in a late hepatosplenic-specific parenchymal phase with accumulation that may be mediated by the reticuloendothelial system (RES), e.g. the

Kupffer cells, or microbubbles are entrapped in the liver sinusoids. (Quaia, 2005, p. 3-14)

Differently, *SonoVue*® was also subsequently found to have the "sinusoidal phase" because it is believed to be trapped or slowed in the hepatic sinusoids.

1.4 Clinical applications

According to literature, CEUS can be utilized for Clinical applications.
The first organ mostly studied by this technique was liver (Albrecht, et al., 2004) and after some years, the applications in other organs were showed (Claudon, et al., 2008 - Piscaglia, et al., 2012 - Cantisani, et al., 2015).

An excursus of literature for spleen includes the use of CEUS to evaluate the physiological parenchyma (Nakamura, et al., 2009 - Ohlerth, et al., 2007), and to differentiate between malignant and benign parenchymal lesions, both in humans (Piscaglia, et al., 2012) and in veterinary medicine (Nakamura, et al., 2010 - Ohlerth, et al., 2008 - Rossi, et al., 2008 - Ivančić, et al., 2009 - Taeymans & Penninck, 2011).

For Bladder CEUS studies were finalized to evaluate the bladder wall alteration, including TCC (Piscaglia, et al., 2012 - Caruso, et al., 2010 - Wang, et al., 2011 - Nicolau, et al., 2011 - Drudi, et al., 2014 - Drudi, et al., 2012 - Pollard, et al., 2017)

Referring to human applications of CEUS in kidneys (Piscaglia, et al., 2012 - Cantisani, et al., 2015 - Oh, et al., 2014 - Xue, et al., 2014 - Schneider, et al., 2014 - Girometti, et al., 2017), some studies were discussed for dogs with final objective to study kidney failure and kidneys tumour (Haers, et al., 2010 - Kinns, et al., 2010 - Waller, et al., 2007 - Dong, et al., 2013 - Stock, et al., 2014 - Haers, et al., 2013 - Stock, et al., 2016 - Tsuruoka, et al., 2010 - Choi, et al., 2016)
Particular relevance was given to canine testis affected by tumours studied before in human (Piscaglia, et al., 2012 - Cantisani, et al., 2015) and veterinary medicine (Volta, et al., 2014).

Liver applications (Albrecht, et al., 2004) are finalized to evaluate the parenchyma perfusion (Ziegler, et al., 2003) and lesions differentiating between benign and malignant (Jang, et al., 2009 - O'Brien, et al., 2004 - Nyman, et al., 2005 - Trillaud, et al., 2009 - Nakamura, et al., 2010 - Yang, et al., 2015)

About gallbladder, in our knowledge, CEUS was used for surgical planning in dogs with suspected gallbladder necrosis/ rupture. (Bargellini, et al., 2016). Can be use also to detect lesions(Wang, et al., 2016 - Tsuji, et al., 2012). Possible diagnosis on CEUS of wall correspond to biliary lithiasis, gallbladder polyp, tumours. (Liu, et al, 2015 - Si, et al., 2013 - Tang, et al., 2013 - Spârchez & Radu, 2012 - Liu, et al., 2012).

Adrenal glands were studied with CEUS in human medicine (Piscaglia, et al., 2012) and in case of tumours use of CEUS was considered a big tool for malignant differentiation (Friedrich-Rust, et al., 2011). Bargellini et al. (2013) studied CEUS characteristics of adrenal glands in dogs with pituitary dependent hyperadrenocorticism giving an important contribute to literature. (Bargellini, et al., 2013). Important considerations about use of CEUS in case of adrenal masses were established by Bargellini, et al. (2016).

For the gastro-enteric tract the guidelines have been given only in human medicine (Piscaglia, et al., 2012 - Cantisani, et al., 2015) and one study has been done in veterinary medicine to study duodenal perfusion in 8 beagle (Nisa, et al., 2017): it could be a big diagnostic tool in dogs.

The ovary can be studied with CEUS in dogs where it should be increased the vascularization during ovulatory phase (Barbosa, et al., 2013 - Polisca, et al., 2013). In human medicine, since 2010, they used CEUS to detect ovarian lesions. (Sconfienza, et al., 2010 - Wang, et al., 2011 - Qiao, et al., 2015). All these applications could be a good objective of research.

A soft tissue lesion can be evaluated by CEUS according to human literature. (Piscaglia, et al., 2012 - Coran, et al., 2015).

Important CEUS applications, for pancreas, in human medicine, were established from EFSUMB.
Focal pancreatic lesions identified with US can be studied by CEUS in order to improve: characterisation of ductal adenocarcinoma, differential diagnosis between pseudocysts and cystic tumours, differentiation of vascular (solid) from avascular (liquid/necrotic) components of a lesion, defining dimensions and margins of a lesion, including its relationship with adjacent vessels, management of the lesion with a better distinction between solid and cystic lesions, thus providing information for the choice of the next imaging modality , diagnosis in cases that are indeterminate on CT (vascularization of solid pancreatic lesions; differential diagnosis between pseudocysts and pancreatic cystic tumours, especially mucinous cystic tumour). (Piscaglia, et al., 2012 - Recaldini, et al., 2008 - D'Onofrio, et al., 2010). CEUS using bolus injection and continuous infusion can be used in dogs to image the pancreas and duodenum (Lim, et al., 2013). In case of acute pancreatitis using quantitative CEUS should be helpful to detect pancreatic perfusional changes (Lim, et al., 2014).
Using contrast-enhanced ultrasonography (CEUS) were obtained different images of insulinoma (Nakamura, et al., 2015). Recently was studied using CEUS the pattern of ultrasonographic contrast enhancement of the pancreatic body and left lobe of 10 clinically healthy cats using *SonoVue*®: this perfusion pattern of normal pancreatic parenchyma may be useful for characterizing cats with exocrine pancreatic disorders (Diana, et al., 2015). Pancreatitis was studied using CEUS in eight dogs in comparison to healthy dogs. CEUS can be utilized to diagnose pancreatitis, pancreatic necrosis, and disease monitoring following therapy in dogs. (Rademacher, et al., 2016)

In human medicine, several studies investigated the potential of CEUS to identify prostate cancer.
Preliminary investigations show that CEUS can also be useful in evaluating prostate hemodynamics in response to medical treatment in patients with BPH. (Cantisani, et al., 2015)
CEUS, in dogs, through quantitative hemodynamic parameters, is useful in distinguishing between physiological and pathologic prostates. The quantitative study showed that through both techniques, TTP and MTT values were significantly lower in pathologic prostates than those in normal prostates (Troisi, et al., 2015)

Useful application of CEUS should be to evaluate lymph-nodes.
CEUS can be used for detecting sentinel lymph nodes in cancer patients: CEUS appears to be capable of discriminating benign from malignant superficial lymph nodes only in special clinical settings and CEUS with subcutaneous injection of contrast agent to identify the sentinel lymph node is a field of ongoing research and can therefore not be recommended for clinical practice to date (Piscaglia, et al., 2012). Some veterinary information is given in 2007 (Salwei, et al., 2005 - Ohlerth & OBrien, 2007).

New prospectives include use of CEUS to evaluate Articular changes: CEUS can be utilized for further assessment of the degree of vascularisation in joints of patients with rheumatoid arthritis and repeat contrast enhanced Doppler US may provide useful information on the response to treatment, to guide therapeutic strategy. The technique has the potential to be utilized within dedicated centres using standardized methodology. (Piscaglia, et al., 2012 - Löffler, et al., 2016 - Zhao, et al., 2017).

CEUS can be employed consistently in trauma imaging, considering the wide spectrum of scenarios encountered in clinical practice (Piscaglia, et al., 2012 - Miele, et al., 2016) also in veterinary medicine (Zhou, et al., 2013).

2 General Procedures

All medical procedures were performed after signature of Informed Consent by owners, in accordance with the official laws on animal welfare and only for medical necessity, in the period between 2015 and 2017.

The devices used were ultrasound *Esaote Mylab40Vet*®, *Esaote Mylab60*® and *Esaote7*®; the scanner was equipped with a contrast-tuned imaging technology. These facilities were supplied and the CEUS was performed respectively at Veterinary Teaching Hospital of the University of the Study of Messina - Department of Veterinary Sciences, Italy, at Clinica Veterinaria Camagna in Reggio Calabria, Italy and at Department of Diagnostic Imaging of Veterinary and Pharmaceutical University of Brno, Czech Republic.

At the beginning, for all exams, B-mode and Doppler US were performed.
The UCAs used was sulphur hexafluoride (*SonoVue*®, Bracco International Imaging, Milan, Italy).
The organs were examined in B-mode with linear probe (7.5 to 12 MHz) and Micro-convex transducer (5-8 MHz) for different scans. Immediately after B-mode ultrasonography, was performed Doppler study of the organs, and the study with ultrasound contrast (CEUS).
The contrast, prepared before use and shaken vigorously for 20 seconds, was rapidly infused at a dose of 0.03-0.05 ml/kg bodyweight through a three-way valve connected to an intravenous catheter of 18/20 G, inserted at the level of the cephalic vein, followed by 5 ml of physiological saline (NaCl 0.9%), injected immediately after contrast as "push" in to the venous circulation.

The dogs received two bolus injections, with a minimum interval between each injection at least 7-10 minutes, even if the residual bubbles were destroyed by a scan of the organ and the aorta in fundamental mode with an output power adjusted to 100%.
The administration was carried out in a standardized way by the same person during the course of the study. All studies were carried out by two operators. The first operator injected the contrast through the cephalic vein, while the second will perform the ultrasound exam.
The second-one video clips obtained (not the first one because maybe needed adjustment of the settings to better perform the CEUS), were analysed for qualitative and quantitative analysis using a dedicated software (*Qontrast*®, Bracco International, Imaging Milan S.p.A®), supplied Veterinary Teaching Hospital, in Messina.
For each organ, were established some criteria to interpret the video clips, after excursus of literature.

The time-intensity curve (TIC), generated by two regions of interest (ROI), as large as possible, was analysed.
The software for analysis of TIC inside the ROI produced Peak perfusion intensity (%) that was defined as the percentage increase in SI, from baseline intensity to maximal SI, Time To Peak (TTP, sec)perfusion that was defined as the time of arrival of UCA to its maximum SI, Mean transit time (MTT, sec) was defined as the time interval between half of the maximum SI of the UCA in the ascending phase of the curve (wash in) and the same value of SI in the descending phase (wash out), Regional Blood Volume (RBV) that was defined as the integral of the video SI (%) changes during the the extrapolated transition time without recirculation, Regional Blood Flow (RBF) that was

defined as the ratio between regional blood volume and mean transit time, and the Signal Intensity (average).
Parametric Maps and Error Maps were evaluated. Calculated curves are then fitted to parametric curves and, as a result, parametric maps are obtained. Parametric maps are visualized as easy-to-interpret colour coded images describing different aspects of perfusion. Error Map is a new map will be than displayed where the pixels are depicted as a 4 levels iso-intensity gradient map and where the colour coded bar represents respectively high fitting errors (red areas), medium fitting errors (dark red areas), low fitting errors (dark green areas) and very low fitting errors (light green areas).
All results obtained were analyzed with a statistical commercial software (*GraphPad software, InStat®)*

As regards the timing of enhancement, should be recognized two phases: the arterial phase, starting from the first arrival of contrast (usually in 10 – 20 seconds) until around 30 – 45 seconds, during which the degree of enhancement increases progressively, and the venous phase, which starts from approximately 30 – 45 seconds after contrast injection, during which the degree of enhancement shows a plateau and then decreases progressively. Most organs have a single blood supply with a single inflow (arterial) phase, the exceptions being the liver, which is supplied by its artery and the portal vein, leading to two distinct inflow phases (arterial and portal venous) and the lungs, which are supplied by pulmonary and bronchial arteries with different arrival times. Liver and spleen are also exceptions since they tend to retain microbubbles longer than other organs, probably due to the trapping of microbubbles in their unique microcirculations after clearance from the remainder of the macro-vasculature.
Consequently, the wash-out phase in most organs is shorter than in liver and spleen, whose prolonged retention is termed the late phase. There is no precisely definable event that allows an exact distinction between the arterial and venous and late phases.
The time of contrast arrival is usually 10 to 20 seconds after intravenous injection, but factors such as a slow injection of microbubbles in to very peripheral small veins or cardiac diseases may prolong it, whereas intra-cardiac or pulmonary shunting or a hyper-dynamic circulation may shorten it.
The degree of enhancement is difficult to assess. Generally, when the target of the study is a focal region in a parenchymal organ, the degree of enhancement should be compared to the surrounding parenchyma or to the paired organ when available. The lesion might be relatively hyper-enhancing, iso-enhancing, hypo-enhancing or non-enhancing and the pattern should be described separately for the arterial and venous phases. The transition from hyper- or iso-enhancement to hypo-enhancement is commonly referred to as “wash-out”.

Contrast distribution regards the description of whether the enhancement is homogeneous or heterogeneous and, in the latter case, if non-perfused regions exist, should be included. In general terms, the CEUS depiction of non-perfused (potentially necrotic or liquid) areas might be relevant prior to any US-guided biopsy in order to better identify the target.(Piscaglia, et al., 2012)

The subjects of all groups should have an assessment of the appearance of any side effects due to the CEUS up to 2 months after the procedure.

---SPECIAL SECTION ONE: RESEARCH APPLICATIONS---

3 Spleen

3.1 CEUS knowledge

The spleen is one parenchymal organ of the left hypo-gastric region composed by a white and a red pulp (the real blood reservoir) (Evans & De Lahunta, 2013, p. 558-559), and it is studied mostly with US, in B-mode and Doppler, that are used to detect, also like incidental findings, diffuse splenic abnormalities, focal or multifocal lesions of spleen parenchyma. (Mattoon & Nyland, 2015, p. 400-405 - Penninck & D'Anjou, 2015, p. 242)

The spleen is the second organ (first the liver) most studied with Contrast-enhanced Ultrasonography (CEUS) in human medicine (Piscaglia, et al., 2012).
To understand the application of CEUS in canine spleen it is important to explain splenic physiological parenchymal vascularization. The splenic artery derives from celiac artery while the splenic vein drains into the gastrosplenic vein. The blood enters by up to 25 splenic branches: rami lienales that pass through the long hilus. The branches continue in the trabeculae, branching repeatedly and becoming smaller when they go surrounded by the white pulp and continue entering in the red pulp, where they branch in to penicilli. The venous side begins in the venous sinuses (sinus lienis) playing an active role for the RES. The sinuses coalesce into veins of the red pulp, and these finally merge to become the trabecular veins. Most of the erythrocytes are contained in large, thin-walled splenic sinusoids, that are supplied by the penicillar arterioles of the adjacent splenic cords and continue into the pulpar and trabecular veins. The time interval for each cycle of passage of blood in spleen varies from a few minutes to as long 10 hours. (Evans & De Lahunta, 2013, p. 558-559).

Benign Nodular Hyperplasia (BNH) was identified in the group of the most frequent benign lesions of the spleen of dogs in case of splenomegaly. (Corbin, et al., 2017).
In case of BNH, it is identified with nodules typically seen on B-mode ultrasonography like hypoechoic to essentially isoechoic or sometimes the nodules are not always observed ultrasonographically and in such cases, it can be suspected when the border of the spleen is smoothly irregular if parenchymal abnormalities are not detected. (Mattoon & Nyland, 2015, p. 409)
Colour and power Doppler evaluation of blood flow to splenic masses in dogs are not helpful to distinguish benign from malignant splenic masses in dogs (Sharpley, et al., 2012).
Using CEUS, it is possible to show this splenic perfusion, in fact, the splenic enhancement after injection of contrast medium should derive from the presence of such a large vascular space with slow blood passage. (Rossi, et al.,2008)

Using *SonoVue*®, normal perfusion values were determined for the canine spleen and it was observed that the small splenic arteries radiating from the splenic hilus opacified rapidly after injection of the contrast. There was heterogeneous enhancement of the splenic parenchyma, the splenic parenchyma became homogeneously enhanced before a gradual homogeneous decrease of opacification and persistent enhancement was not seen during the late phase: there was no evidence of tissue specificity in the canine spleen.(Ohlerth, et al., 2007)

Compared to *SonoVue*®, *Sonazoid*® had long-lasting contrast enhancement of canine spleen parenchyma: the optimal time for splenic parenchymal imaging in the dog would be from 7 to 30 min after injection. In splenic arteries, the time to upslope from injection (5.2-0.4 s) and time to peak from initial upslope (2.7-1.0 s) afforded only a narrow window.
In beagles injected with *Sonazoid*®, the appropriate timing for examining the arterial phase of the spleen ranges from 5 to 22 s after injection. (Nakamura, et al., 2009)

BNH (lymphoid hyperplasia) is one of the most frequent benign lesions of spleen of dogs, particularly old ones, in case of splenomegaly. (Corbin, et al., 2017). Ultrasonography is the method of choice to detect splenic lesions, but it is not specific in their diagnosis. BNH is identified with nodules typically seen on B-mode ultrasonography like hypoechoic to essentially isoechoic lesions, sometimes the nodules are not immediately detected in normal parenchyma and, in such cases, can be suspected only as solid nodule bulging from a regular border of the capsule. (Mattoon & Nyland, 2015, p. 409).
Colour and Power Doppler study of splenic focal lesions in dogs showed that detection of tortuous or aberrant vessels, entering or within them, is nearly significant to distinguish benign from malignant lesions (Sharpley, et al., 2012).
Different studies were finalized to characterize benign and malignant lesions in spleen using Contrast Enhanced Ultrasonography (CEUS) and a hypoechoic pattern to the surrounding parenchyma during wash-in, peak enhancement and wash-out phases was significantly associated with malignancy (Rossi, et al., 2008 - Ohlerth, et al., 2008 - Nakamura, et al., 2010). CEUS pattern in BNH had predominantly similar wash-in and wash-out to the surrounding spleen, so that, after a few seconds the nodules were isoechoic and diffusely homogeneous with the remainder; a normal architecture of the vascular network in benign hyperplastic conditions is supposed to explain this pattern (Rossi, et al., 2008). Histologic examination had showed a common relationship between splenic hyperplastic nodules and hematomas and this is suggested as a consequence of alteration of circulation in and around hyperplastic nodules with failure of marginal zone flow and accumulation of blood (Spangler & Culbertson, 1992 - Cole, 2012).

CEUS was used to differentiate benign from malignant lesions: it was clear that the accuracy of contrast-enhanced ultrasonography in differentiating benign from malignant splenic lesions in dogs is conflicting but the results from early washin-/early washout-based interpretation reported were characterized by poor sensitivity and specificity. (Ivančić, et al. 2009 - Nakamura, et al., 2009 - Nakamura, et al., 2010 - Taeymans & Penninck, 2011).
Qualitative assessment of tortuous feeding vessels and persistence of visualization of the vessels throughout all perfusion phases may improve the accuracy in characterizing benign vs. malignant splenic lesions (Taeymans & Penninck, 2011).

CEUS was a highly accurate method of characterizing nodule images as malignant or benign in dogs with hemangiosarcoma, with an accuracy of 100%. (Ivančić, et al., 2009)
General principles, that referring to cytological or histological final diagnosis, give to CEUS a not invasive role for a not invasive differentiation of malignant splenic tumours from haematomas or benign nodules like a valuable method since fine needle aspirates of splenic lesions are often not diagnostic and tissue core biopsies may cause further bleeding. (Ohlerth & OBrien, 2007)

Hemangiosarcomas are included in the group of canine splenic malignant neoplasm.
Detected in B-mode, CEUS was applied giving in all phases by homogeneous anechoic (not perfused) areas with highly vascularized surrounding parenchyma (peripheral irregular perfusion pattern), with presence of thin septae and tortuous vessels were visible on the periphery of the lesion ; based on the time–intensity curves, there was no enhancement in the large anechoic lesions, and pixel intensity did not change from the baseline. (Rossi, et al., 2008)
Hemangiosarcoma showed characteristic hypoechoic pattern during the early vascular phase using *Sonazoid*® in (Nakamura, et al., 2010). This hypoechoic area may correspond to the haemorrhagic or necrotic areas commonly associated with hemangiosarcoma. However, differentiation between hemangiosarcoma and hematoma is referred to the presence of aberrant wide vessels and none of the other malignant or benign lesions, including hematoma, had such vessels. Hematoma derives from BNH like evolution of disease and its always more rejected the traumatic nature, becoming hematoma an evolution of benign diseases: the presence of lymphoid hyperplasia is supportive of a diagnosis of hematoma, although not diagnostic in itself and only this appeared to be useful for increasing confidence that a lesion is truly a hematoma and that hemangiosarcoma had not been overlooked. (Cole, 2012)
Considering the presence of tortuous feeding vessels in the arterial phase, together with persistence of these feeding vessels in the parenchymal phase as an indicator of malignancy resulted in an accuracy of 100%. (Taeymans & Penninck, 2011)

In one examination using *Sonazoid*® on 7 of the 8 malignant nodules other than hemangiosarcoma were isoechoic in the early phase. However, CEUS in these 7 nodules rapidly decreased, and they became hypoechoic in the late vascular phase. Finally, all 8 lesions became hypoechoic in the parenchymal phase. It means that there is no significant difference between benign and malignant lesions in the parenchymal phase instead on the liver the parenchymal phase is suggestive of malignant tumours. The splenic nodular hyperplasia became hypoechoic during the parenchymal phase in this study. The contrast defect during the parenchymal phase created by splenic nodular hyperplasia might be because of a decrease of splenic macrophages. Therefore, the parenchymal phase imaging was not useful for differentiation between benign and malignant splenic lesions. In some cases, however, nodules that could not be visualized with conventional ultrasonography became clearly hypoechoic in the parenchymal phase: the parenchymal phase imaging could be useful for the detection of focal splenic lesions.
They speculate that the lack of normal sinusoids combined with neoplastic angiogenesis might be one of the causes of a malignant hypoechoic pattern during the late vascular phase.
The early vascular phase could also differentiate malignant and benign lesions with high specificity: hemangiosarcoma showed characteristic hypoechoic pattern during the early vascular phase that may correspond to the haemorrhagic or necrotic areas commonly associated with hemangiosarcoma. (Nakamura, et al., 2010)
In dogs, however, it was demonstrated that sulphur hexafluoride microbubbles allowed for vascular phase imaging but not for parenchymal phase imaging. (Ohlerth, et al., 2007) The vascular phase imaging with sulphur hexafluoride microbubbles could differentiate benign and malignant focal splenic lesions based on the finding that malignant tumours were hypoechoic to the surrounding normal spleen parenchyma in the wash-out phase (30 seconds after injection of sulphur hexafluoride microbubbles). (Rossi, et al., 2008)

CEUS allows detection of abnormal perfusion patterns associated with splenic malignancies. In some cases of lymphosarcoma, CEUS had early wash-in and wash-out phases, and this possibly reflects the lack of normal sinusoidal vessels of the red pulp combined with neoplastic angiogenesis. (Rossi, et al., 2008)

Aim of our study is to evaluate diffuse and nodular canine spleen lesions, differentiating between benign and malignant lesions. A focus was done about BNH, particularly on qualitative and quantitative analysis and according to final diagnosis done with cytology and histology: the hypothesis was that benign hyperplastic nodules, having an altered vascular pattern, would have, consequently, a different microbubbles distribution related to normal spleen parenchyma.

3.2 Materials and Methods

Equipment staff was composed according to general procedures established and summarized in the following table. (chapter 2 and Table: General Procedures).

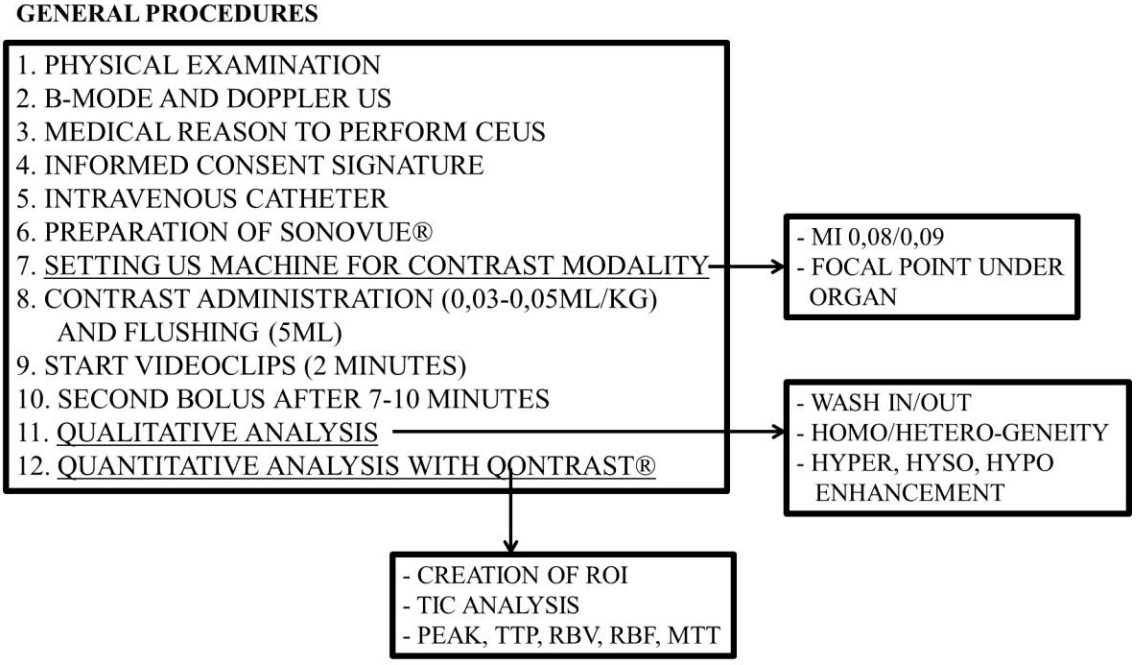

Patients included all dogs with focal or diffuse splenic lesions detected by Basic ultrasonography.

This procedure was used to study 20 cases of BNH and cases of malignant lesions including Hemangiosarcoma, Lymphoma and Histiocytic Sarcoma.

Qualitative criteria for interpretation of the results were:

- Doppler: The presence of a wide or tortuous vessel within the mass is suggestive of malignancy. (Note: dogs) (Sharpley, et al., 2012)
- Differentiation between benign and malignant lesions: qualitative assessment of tortuous feeding vessels and persistence of visualization of these vessels throughout all perfusion phases may improve the accuracy in characterizing benign vs. malignant splenic lesions. (Note: *SonoVue*® - dogs) (Taeymans & Penninck, 2011)

It is suggested the use of early vascular phase to differentiate malignant and benign lesions with high specificity. (Note: *Sonazoid*® - dogs) (Nakamura, et al., 2010)

- Hemangiosarcoma: hypoechoic pattern during the early vascular phase that may correspond to the haemorrhagic or necrotic areas. (Note: *Sonazoid*® - dogs) (Nakamura, et al., 2010)

  Benign lesions: no contrast enhancement or rapid wash-in, followed by persistent enhancement in the late phase.
- Malignant lesions (metastases or lymphoma): the combination of contrast enhancement (diffuse or peripheral) in the arterial phase followed by rapid and marked wash-out.

  (Note: EFSUMB recommendation - *SonoVue*® - human) (Piscaglia, et al., 2012)
- BNH in B-mode, included: size and shape, echo pattern (homogeneous or heterogeneous) and location. Spleen masses were recorded as "homogeneous" or "heterogeneous" according to echogenicity. Doppler evaluation was assessed comparing perfusion Colour appearance of lesion to surrounding tissue in homogeneous or heterogeneous, with prominent inner vessels and with rim enhancement. (Penninck & D'Anjou, 2015) (Mattoon & Nyland, 2015)

  For lesions with CEUS: hyperenhancing (brighter than surrounding tissue), isoenhancing (no more visible during contrast ultrasound) or hypoenhancing (hypoechoic to the surrounding tissue) compared to the surrounding tissue. Presence of heterogeneity, rim enhancement or prominent inner vessels was also evaluated. Important consideration is done for individuation of wash-in (arrival time of contrast medium) and wash-out (outgoing time of contrast medium) in comparison between lesion and surrounding tissue. (Rossi, et al., 2008)

Quantitative evaluation of results using *Qontrast*®, software analysis, included:

- Creation of two ROI as similar as possible dimensions: one ROI for lesion and one for surrounding parenchyma
- Evaluation of following parameters generated from TIC: P, TTP, RBF, RBV, MTT, Parametric maps and Error Maps.

Between January, 2015 until February, 2017, at the Veterinary Teaching Hospital of the University of Messina (Italy), a CEUS prospective study was performed in dogs with focal or multifocal splenic lesions detected during routine abdominal ultrasonography. In this part of study, dogs were included only if a diagnostic ultrasound-guided aspiration or histo-pathologic samples taken during surgery for splenectomy were performed after ultrasonography contrast enhanced exams and conclusive diagnosis was benign nodular hyperplasia. For the dogs that did not undergo surgery, a ultrasound follow up exam was scheduled 1 month after CEUS exam. Each dog underwent a physical examination and blood analysis.

B-mode and Colour Doppler Ultrasonography of all abdominal cavity was performed by the same operator B-mode and Doppler ultrasonography of the spleen was performed with microconvex (5.0 to 8.0-MHz) and linear (10 to 12-MHz) transducers. Lesions of the spleen were assessed for their size, number and echogenicity in comparison with the normal spleen (hypoechoic, hyperechoic, mixed), and presence of cavitary areas (anechoic areas surrounded by irregular parenchyma with distal acoustic enhancement). Colour and Power Doppler evaluation was performed to describe vascularisation, evaluating the path of blood vessels in and around the lesions.

The CEUS procedure started after that informed owners consent was obtained. CEUS examinations was performed by the same investigators using a system equipped with contrast-tuned imaging technology in non-sedated dogs by the same operator. After assessing lesion characteristics with standard ultrasound , a CEUS examination was performed with a linear (5.0 MHz) transducer with contrast agent capability, mechanical index (MI) was set from 0.08 to 0.11 and focal zone was placed at the deepest part of the lesion. Part of the normal splenic parenchyma surrounding the lesion was included in the image to compare the flow in the two areas. The contrast agent used was *SonoVue*®, prepared in accordance with the manufacturer's recommendations. Each vial of contrast agent, containing 25 mg of freeze-dried powder, was reconstituted by injection of 5 mL of 0.9% sodium chloride and shaken vigorously for 20 seconds. An aliquot (0,04 mL/kg of body weight) of the contrast medium was rapidly injected through a 3-way valve connected to a 18-20 Gauge catheter inserted in the cephalic vein. The contrast injection was immediately followed by a 5 mL saline flush. Each dog received two bolus injections of contrast agent at 7-10 minutes apart from each other and after the first inoculation microbubbles were destroyed with high MI flash on the abdominal aorta. During the first bolus examination, if necessary machine settings (i.e. total gain, time-gain compensation) were optimized and not modified for the second injection. The activation of a timer was performed simultaneously with the contrast agent dose inoculation. Good-quality video clips for approximately 2 minutes, only obtained during the second contrast enhanced examination, were stored digitally on a hard disk and subsequently they were analysed by the same operator.

The focal lesion in the spleen was classified in hyperenhancing (brighter than surrounding tissue), isoenhancing (isoechoic with surrounding tissue) or hypoenhancing (hypoechoic to the surrounding tissue) or not enhancing (anechoic). Presence of homogeneous or heterogeneous lesion pattern, rim enhancement or inner vessels was also evaluated.

Post processing quantitative analysis of video-clips was done using a dedicated image-analysis software (QontrastTM , Bracco, Milan, Italy). For each dog, one Region Of Interest (ROI), as big as possible, was manually drawn around the entire lesion. A second one ROI, with the most similar possible dimension to the first, was created on the normal parenchyma, to compare the first one. Contrast-enhanced Time Intensity Curves (TICs) were generated for each ROI. Analysis of tissue perfusion was based on video Signal Intensity (SI) changes over time using CEUS. The SI of a white band in the grey scale bar (8 bit) was defined as maximal (100%) SI. Other pixels in the image were then assigned SI values based on this reference. Within the selected ROI, during the period of enhancement, the following parameters were computed and considered: Peak Intensity % (PI), Time to Peak (TTPs) measured from T0 (injection time) as the time to arrive to the maximal PI, Regional Blood Volume (RBV), Regional Blood Flow (RBF), and Mean Transit Time (MTTs).

All data obtained were statistical described expressing as mean ± standard deviation (SD) and ROI's data from lesion and surrounding tissue were compared with Student's t-test. To assess the association between the difference of enhancement (hypo) with benign hyperplastic nodules during wash-in, at peak and during wash-out, sensitivity with 95% confidence intervals were calculated. Values were considered significant when $P < 0.05$. Statistical analysis was performed with a standard computer software program (*GraphPad InStat*®).

3.3 Results

BENIGN NODULAR HYPERPLASIA.

There was one each Yorkshire, Pomeranian, Weimaraner, Hound, West Highland and fifteen mixed breeds. There were 13 males and 7 females, median age was 9 years (range 6-13 years) and median weight 14 kg (range 5-28 kg). Dogs blood count and serum biochemistry were within normal range. Twenty dogs had a diagnosis of benign nodular hyperplasia by cytology (n=16) and histology (n°=4); histologic evaluation showed in 3 cases multiple nodules of lymphocytes within a hematoma.

On B-mode examination, all dogs had a single lesion; respect splenic parenchyma, 10/20 were homogeneous hypoechoic, 8/20 had mixed echogenicity, only 2 was isoechoic with small hypoechoic areas; mean lesion diameter was 1,86 cm (0.45-3.04 cm) and 5/20 were near splenic capsule, giving an altered splenic border. Colour and Power Doppler showed detectable vessels only in 10/20 lesions, with small vessels entering the lesion and in 3/10 with vessels followed the contour of the lesion.

Contrast-enhanced ultrasound of the normal spleen showed rapid enhancement of the small splenic arteries (10-13 s), a heterogeneous phase of enhancement of the spleen that became homogeneous at peak enhancement and a slow decrease of enhancement.

About benign hyperplastic lesions, in the rapid wash-in phase, 11 nodules had a homogeneous pattern and were isoechoic with the normal spleen, 8 nodules had heterogeneous pattern with small not enhancing areas and only 1nodule was isoechoic with the normal spleen. After a time of about 15-40 s, 19/20 (95%) benign nodules became markedly hypoechoic with inner thin vessels enhancement that were gradually not more visible in the wash-out phase of the normal spleen (Fig. 1-2-3). The only nodule isoechoic in the wash-in phase remained such during all blood pool phases of the CEUS exam. Sensitivity of early hypoechoic pattern for benign nodular hyperplasia was 95% with a 95%CI (86-100%).

Quantitative analysis of lesions 19/20 lesions showed TICs characterized by a faster wash-in and an anticipated washout than normal parenchyma (Fig. 5). Mean PI% in lesions was 16.06 +/- 5.45 (range 6.9-23.7) and in non-pathologic tissue was 21,93 +/- 5.05 (range 14,9-31,6) . Mean TTPs was 42.31 +/-30.7 (range 10.55-94.723) for lesion and 50.86 +/-21 (range 25.77-97.67) for normal parenchyma. Mean RBV in lesion was 925.10 +/-708 (range 196.44-2426.97) while in normal tissue 1952,496 +/-1073 (range 616.83-4109.37). Mean RBF in lesions was 17.08 +/-6.2 (range 5.26-28.68) and 25.7 +/-7.22 (range 16.65-40.53) in surrounding tissue. MTTs mean values included 54.55 +/-34.83 (range 16.47-114.85) for lesions and 70.57 +/- 26.55 (range 34.33-114.38) for normal parenchyma. Quantitative parameters of enhancement of ROIs in benign hyperplastic nodules compared with ROIs of the normal spleen gave significant difference in the following data: PI% 0.0001, TTPs 0.01, RBV 0.0001, RBF 0,0001, MTTs 0.0001.

No one dog had adverse reaction during and until one month later the procedure. B-mode follow up examination showed unremarkable changes than the previous time.

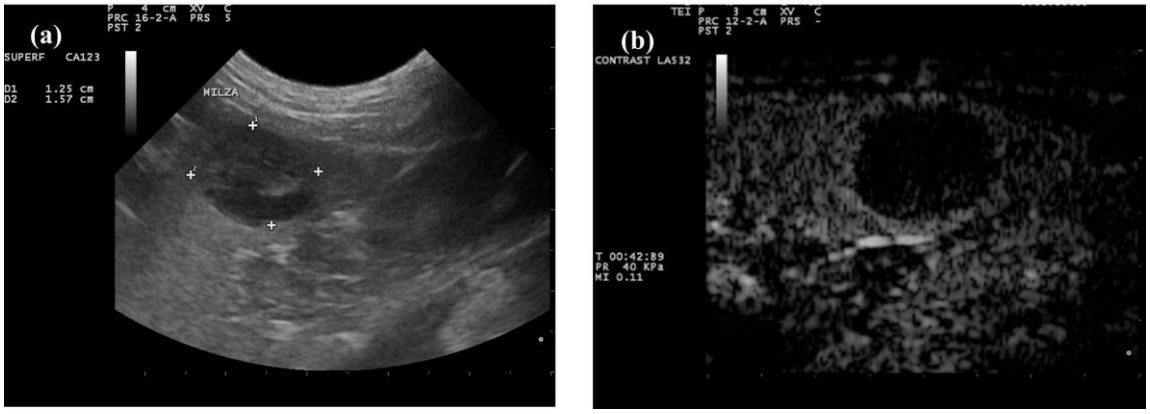

Figure 3.1 BNH of spleen in clinical case n°=8. B-mode ultrasonography of spleen (a) where is visible a hypo-echoic part in comparison to the surrounding parenchyma corresponding to the lesion. CEUS representation of lesion in spleen (b) at 42 seconds after injection of contrast: hypo-enhancing area corresponding to the lesion and comparing to the surrounding tissue, that means that the contrast medium persists in to the lesion for shorter time.

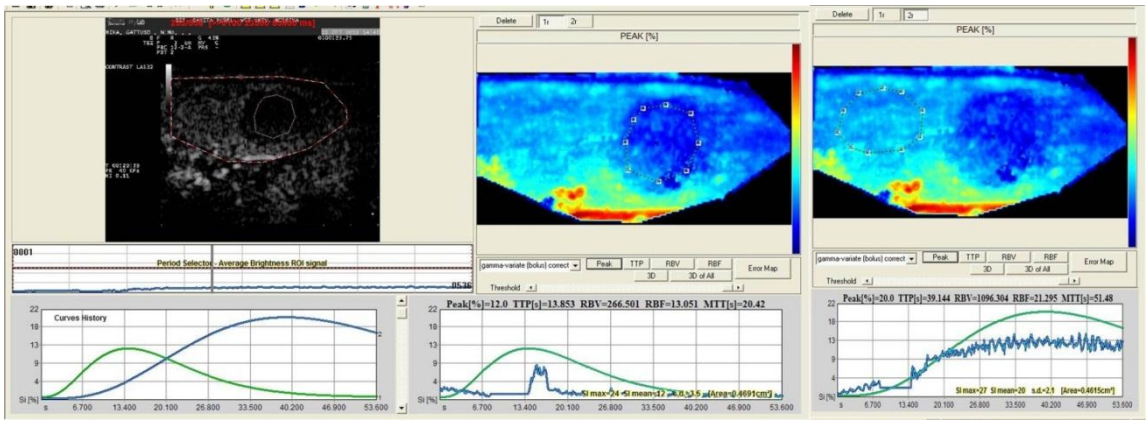

Figure 3.2 Quantitative analysis using *Qontrast*® of BNH in clinical case n°=8. Two ROIs are created and generate different TICs: one ROI is located in to the lesion and another one, with similar dimension, in the normal parenchyma. From this analysis derive values for Peak, TTP, RBV, RBF, MTT.

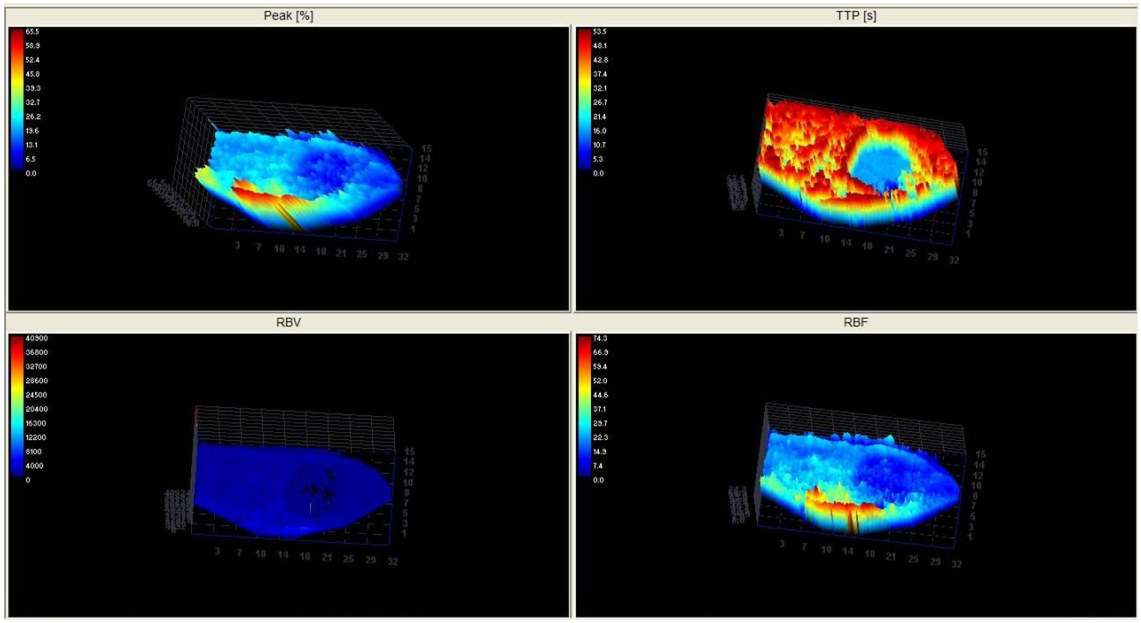

Figure 3.3 *Qontrast*® creation of Parametric Maps (clinical case n°=8). Parametric Maps are a spatial 3-D reconstruction of Peak, TTP, RBV, RBF. In each reconstruction is visible the lesion corresponding with an area of alteration of spleen parenchyma.

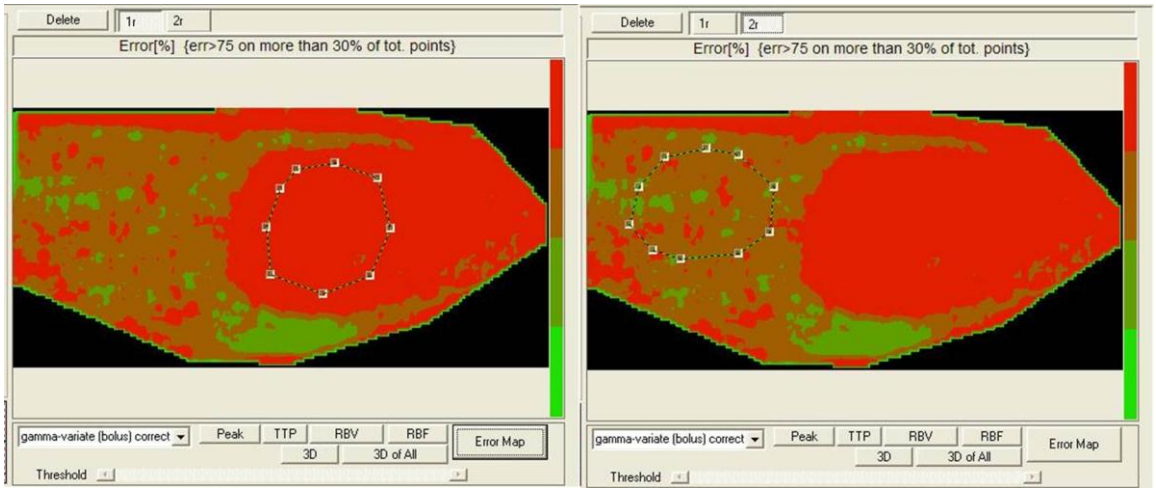

Figure 3.4 *Qontrast*® creation of Error Maps (clinical case n°=8). Error maps analysis of two different ROI; it displayed where the pixels are depicted as a 4 levels iso-intensity gradient map and where the colour coded bar represents respectively high fitting errors (red areas), medium fitting errors (dark red areas), low fitting errors (dark green areas) and very low fitting errors (light green areas).

Table 3.1: Data collection of 20 cases of BNH. Data were obtained with quantitative analysis (*Qontrast*®) after creation of TICs (generated from two ROI: one each in lesion and normal parenchyma) , using *Qontrast*®, software for contrast analysis. All data are ordered based to Peak, TTP, RBV, RBF, MTT respectively for lesion (L) and normal (N) parenchyma.

CASE	PEAK L	PEAK N	TTP L	TTP N	RBV L	RBV N	RBF L	RBF N	MTT L	MTT N
1	17,5	23,1	23,681	49,923	508,977	1495,285	15,475	25,038	32,89	59,72
2	17,1	19,2	17,469	28,684	288,67	859,752	14,477	21,965	19,94	39,14
3	8,5	18,4	94,575	97,674	744,43	1904,097	6,758	16,647	110,16	114,38
4	6,9	18,5	94,723	96,186	571,861	1947,123	5,265	17,128	108,61	113,68
5	23,7	23	65,494	51,131	2256,102	2294,787	25,489	28,373	88,51	80,88
6	23	30	60,479	59,388	1735,372	3486,198	22,799	37,148	76,12	93,82
7	15,3	19,8	22,937	42,166	555,954	1134,771	16,32	20,759	34,07	54,66
8	12	20	13,853	39,144	266,501	1096,304	13,051	21,295	20,42	51,42
9	10,6	15,4	13,363	25,769	216,287	616,835	12,222	17,966	17,84	34,33
10	10,3	14,9	12,283	30,336	196,44	648,994	11,927	16,847	16,47	38,52
11	14,5	15	13,99	36,665	594,876	983,776	18,671	18,086	31,86	54,39
12	11,8	23,6	10,546	35,305	328,048	1631,008	15,066	29,54	21,77	55,2
13	13,6	18,1	51,822	49,14	1080,321	1923,533	15,394	23,299	70,18	82,56
14	10,1	19,7	30,592	51,602	437,526	2241,543	10,884	25,538	40,2	87,7
15	23,5	28,7	19,516	31,827	814,37	1526,407	28,676	33,442	28,4	45,6
16	20	20,3	22,456	31,015	799,611	1131,244	23,775	24,406	33,63	46,35
17	19,1	29,1	44,67	58,324	1155,981	3124,389	21,271	35,266	54,35	88,6
18	18,6	31,6	54,001	58,248	1381,399	4109,368	20,601	40,529	67,05	101,32
19	22,6	25,5	91,82	78,05	2426,966	4006,191	22,855	31,714	114,85	126, 32
20	22,6	24,7	87,912	66,685	2142,42	2888,322	20,644	29,275	103,75	98,62
MEAN	16,065	21,93	42,3091	50,8631	925,1056	1952,49635	17,081	25,71305	54,5535	70,57316
SD	5,453466	5,046739	30,66001	20,99894	707,9044	1072,64514	6,194213	7,220255	34,83539	26,55538
MAX	23,7	31,6	94,723	97,674	2426,966	4109,368	28,676	40,529	114,85	114,38
MIN	6,9	14,9	10,546	25,769	196,44	616,835	5,265	16,647	16,47	34,33

HEMANGIOSARCOMA.

Our case of hemangiosarcoma is a visible differentiating lesion on B-mode with hypoechoic parenchyma and few detections of flow in Doppler, in comparison to the surrounding parenchyma. On CEUS, prominent vessels are confirmed, but, in this clinical case, just small anechoic areas are visible: this should be a good observation about the possibilities of evolution of the lesion for parenchymal necrosis during time. (Figure 3.5)

Quantitative analysis was performed using *Qontrast*® with creation of two ROI: from the analysis of these two TICs is clear the presence of different perfusion and parameters confirm the data obtained in lesion lower than in normal parenchyma. Lesion data include Peak 14.1%, TTP 21.067s, RBV 415.150, RBF 15.261, MTT 27.20, while in normal parenchyma they were Peak 17.8%, TTP 32.083s, RBV 954,243, RBF 21.123, MTT 45.18. (Figure 3.6)

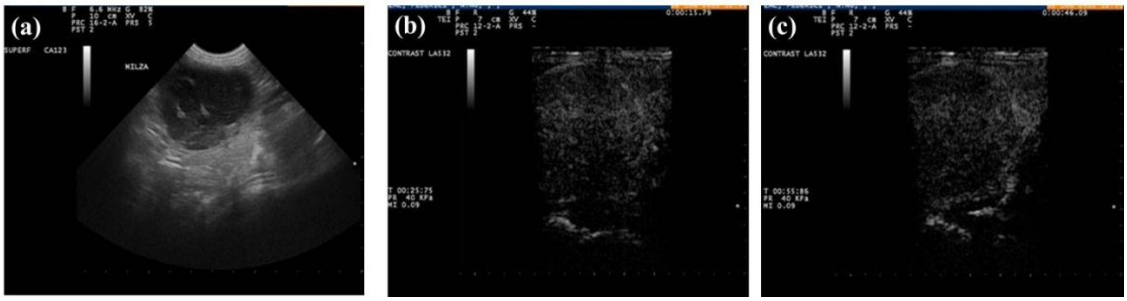

Figure 3.5 Hemangiosarcoma of spleen. B-mode US of hemangiosarcoma (a): the lesion is hypo-echoic and well differentiated to the surrounding parenchyma. CEUS hemangiosarcoma at 25seconds(b) and at 55seconds(c): the perfusion is visible and mantained during time inside the lesion.

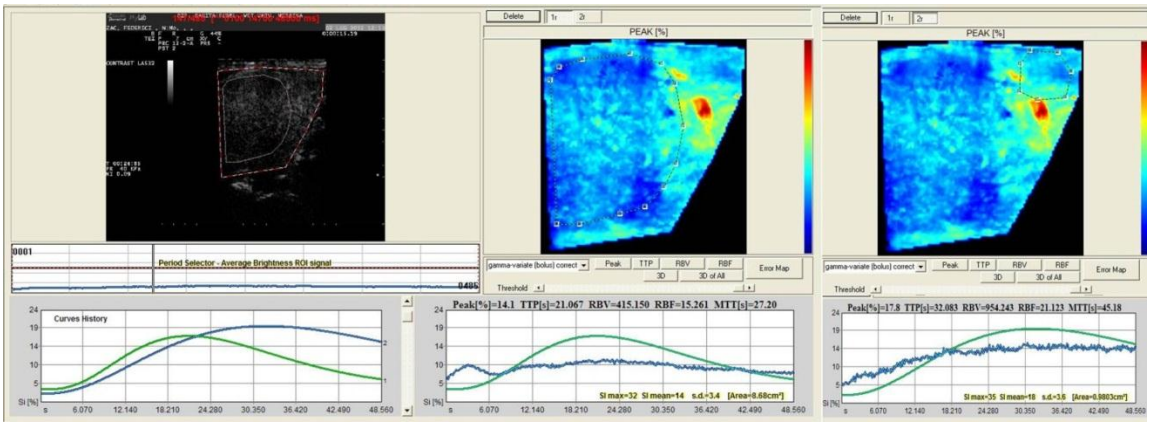

Figure 3.6 Hemangiosarcoma quantitative analysis using *Qontrast*®. One ROI is located in lesion and one in normal parenchyma: two different TICs were obtained and different data for Peak, TTP, RBV, RBF, MTT.

LYMPHOMA.

About malignant lesions, was studied a clinical case of lymphoma. In this case the lymphoma showed a classical malignant appearance on CEUS differentiating from benign with evident enhancement of heterogeneity, prominent inner vessels and some hypoechoic areas. (Figure 3.7) *Qontrast*® analysis was done confirming higher parameters for neoplastic parenchyma. Lesion data obtained from analysis were: Peak 20.0%, TTP 33.277s, RBV 975.016, RBF 22.464, MTT 43.40. Normal parenchyma parameters include: Peak 16.8%, TTP 25.882s, RBV 698.446, RBF 19.730, MTT 35.40. (Figure 3.8)

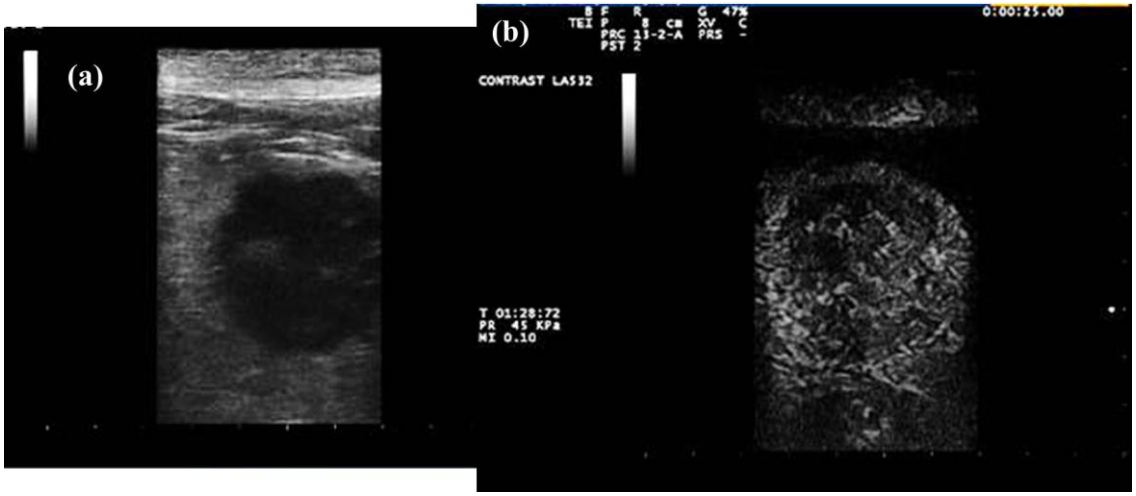

Figure 3.7 Lymphoma in spleen. B-mode (a) evaluation of spleen mass: well differentiated, hypo-echoic lesion. CEUS (b) Malignant appearance of splenic lesions: prominent vessels and small avascular areas.

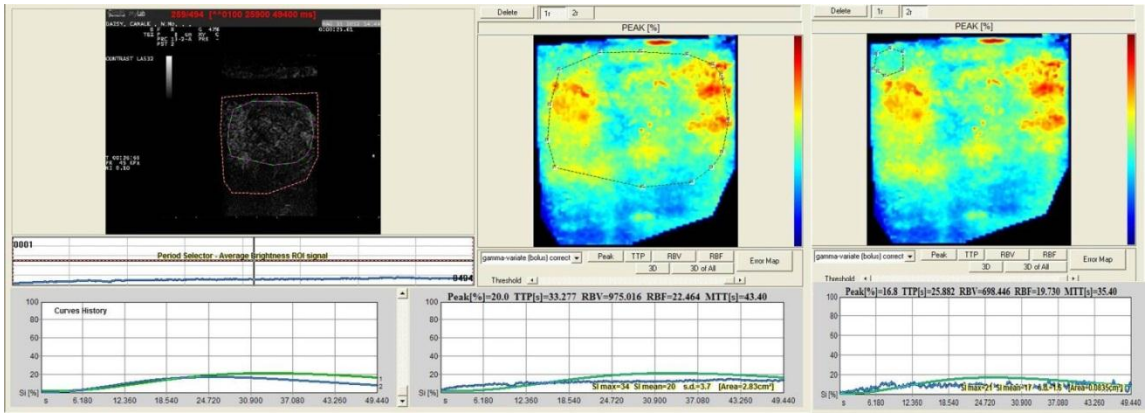

Figure 3.8 Quantitative analysis of Lymphoma in spleen. Quantitative analysis using *Qontrast*®: two ROI were applied one in lesion and one in normal parenchyma, different TICs were generated giving different data for Peak, TTP, RBV, RBF and MTT.

HISTIOCITIC SARCOMA.

Histiocytic sarcoma also confirms the malignant appearance. This neoplasm has diffuse multi-nodular appearance first detected in B-mode than in CEUS.

Histiocytic sarcoma was isoechoic in the wash-in phase, with a diffuse homogeneous enhancement and a rapid time to peak. At peak, it became hypoechoic to the surrounding spleen. The lesion wash-out phase started before the splenic peak (early wash-out phase) and all nodules became hypoechoic during this phase. The contrast medium washed out progressively from the lesions, leaving a round hypoechoic lesion characterized by small round anechoic areas giving the honeycomb pattern. (Figure 3.9).

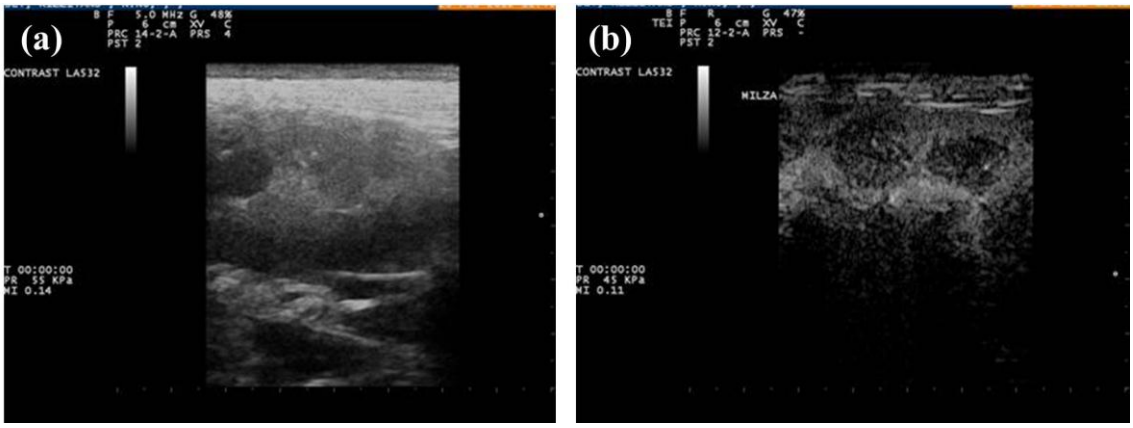

Figure 3.9 Histiocytic Sarcoma in spleen. B-mode appearance of nodular lesions: diffuse and hypo-echoic (a) confirmed on CEUS like a diffuse hypo enhancement of nodular areas (b).

3.4 Discussion

The spleen is one of the organs, together with the liver, most studied with Contrast-Enhanced Ultrasonography (CEUS) in veterinary medicine. Using *SonoVue*®, normal perfusion values were determined for the canine spleen and was observed that the small splenic arteries, radiating from the splenic hilus, rapidly opacify after injection of the contrast; after a heterogeneous enhancement of the splenic parenchyma, it became homogeneously enhanced before a gradual homogeneous decrease of opacification and persistent enhancement was not seen during the late phase; there was no evidence of tissue uptake of *SonoVue*® in the canine spleen (Ohlerth, et al., 2007).
CEUS has been used for characterization of focal splenic lesions. In one study, most benign lesions (six nodular hyperplasia) had a perfusion pattern similar to the surrounding parenchyma, so that the lesions were isoechoic in wash-in and wash-out phases; in the same study malignant lesions (lymphosarcoma, malignant fibrous histiocytoma, histiocytic sarcoma, mast cell tumour, metastasis) became extensively and homogeneously hypoenhanced to the adjacent parenchyma in the wash-out phase. Hemangiosarcoma, undifferentiated sarcoma and liposarcoma had an inhomogeneous wash-out (Rossi, et al., 2008). Also, in another study, extensive to moderate hypoechogenicity of a splenic lesion during all blood pool phases was highly associated with malignancy; benign lesions (ten nodular hyperplasia) were predominantly isoechoic with the surrounding parenchyma in wash-in and peak enhancement phases; only 5 lesions were mildly hypoechoic in wash-out phase (Ohlerth, et al., 2008). A different consideration must be made about a third study using perflubutane microbubbles-enhanced ultrasonography, another second-generation contrast agent with a parenchymal uptake until 7-10 minutes after injection; in the early (5-10 s) and the late (25-30 s) vascular phases a hypoechoic pattern was significantly associated with malignancy. In that study, nodular hyperplasia (n°=8) was the most common benign lesion and 6/8 remained isoechoic in the late vascular phase. In the parenchymal phase 15/16 malignant lesions and 8/8 benign nodular hyperplasia had a hypoechoic pattern without significant differences (Nakamura, et al., 2010).
The results of our study, focused on 20 benign nodular hyperplasia, are very different from those have already published: 11 nodules had a homogeneous pattern and were isoechoic with the normal spleen, 8 nodules had heterogeneous pattern with small not enhancing areas and only 1nodule was isoechoic with the normal spleen during all enhancement phases. After a time of 15-40 s, again in splenic wash-in phase, 19/20 lesions showed rapid wash-out, with evidence of inner thin vessels enhancement that gradually disappeared in the wash-out phase of the normal spleen. Evidence of transit of ultrasound contrast agent into these small vessels during the splenic wash-in phase makes us think they can be the small follicular arteries inside the lymphatic follicles of the white pulp.
To understand the application of CEUS in spleen it's important to know the splenic physiological vascular network. The splenic artery derives from celiac artery while the splenic vein drains into the gastrosplenic vein. The blood enters by up to 25 splenic branches: rami lienales that pass throught the long hilus. The branches continuous in the trabeculae, branching repeatedly and becoming smaller pulpar and then follicular arteries (central arterioles) when progresses inside "a tunnel" where the splenic reticular fibers support blood elements of the white line and the peri-arterial lymphatic sheets (PALS). These arteries continue to subdivide entering in the red pulp, where they give rise to terminal vessels, defined as penicillary arterioles (Rossi, et al., 2008)
Most of the erythrocytes are contained in large, thin-walled splenic sinusoids, that are supplied by the penicillary arterioles of the adjacent splenic cords and continue into the

pulpar and trabecular veins. The time interval for each cycle of passage of blood in spleen varied from a few minutes to as long 10 hours. (Evans & De Lahunta, 2013, p. 558-559) (Rossi, et al., 2008).

Scanning Electron Microscopy (SEM) technique for microvascular corrosion casts shows radial ramification of central arterioles of the white pulp, some of them open into sinusoids and others open inside the white pulp and are responsible for irrigating the white pulp and for opening in the marginal zone. Association of hematomas and lymphoid hyperplasia is based on documented alteration of the blood flow by changes in the lymphoid tissue, such as marginal zone distorsion and failure of circulation (Cole, 2012 - Spangler & Culbertson, 1992).

We hypotize that alterations of the sleeve of sinusoids with reduction of vascular space with slow blood flow, due to lymphoid hyperplasia, may be one explanation of the reduction of the mean transit time of contrast agent with rapid wash-out after a normal wash-in that we found in so high number of benign nodular hyperplasia. Such alterations of splenic sinusoids may be responsible of rearrangement of the venous system with an abrupt development of veins. A similar modification has been documented in SEM observations of corrosion cast of spleens of dogs infected with visceral Leish and was speculated to justify the malignant hypoechoic pattern during the late vascular phase (Nakamura, et al., 2010).

Quantitative data showed faster time to peak and mean transit time of ROI lesion, regional blood flow was lesser than normal splenic ROI and, although qualitative evaluation was of iso-enhancement to normal parenchyma, also PI % was significantly lesser in benign nodular hyperplasia.

Again, the evidence of hypoenhancement of benign nodular lesions in our study can open new considerations about the specificity of this pattern in malignant splenic lesions. Probably, alterations of vascular system responsible of the same detection of this perfusion pattern may be not exclusive of neoplastic lesions. In fact, we think that new investigations on benign nodular hyperplasia vascularization may help CEUS patterns interpretation.

Our study has some limits, the first is the scarcity of histologic evaluations vs cytologic ones and, consequently, the lack of information about tissue architecture in all benign hyperplastic nodules. The conservative choice was made by the owners who, in the hypothesis of benign pathology and in view of the age of the animal, preferred not to undergo surgery.

Second limitation is the short gray-scale ultrasound follow up, it did not permit us to have more informations about remarkable modifications of their pattern and, eventually, to gave us possibility to repeat contrast-enhancement examination.

Nowadays malignant lesions are mostly identified for the presence of tortuous feeding vessels according to (Taeymans & Penninck, 2011) what found confirm in our experience.

Limit of this study were the few number of cases studied for malignant lesions, that however, confirm the literature knowledge of malignant appearance.

Further studies have to be done using CEUS for the other spleen alterations trying to give a standardization of data, like ours for BNH.

4 Bladder

4.1 CEUS knowledge

CEUS was applied to study bladder wall perfusion in human medicine. (Piscaglia, et al., 2012)
Our objective was to characterize the physiological bladder wall perfusion, to give referral parameters and to evaluate the wall alteration of bladder by inflammatory or neoplastic lesions (Transitional Cell Carcinoma, TCC) in dogs, for which the gold standard is cytology or histology.

The most useful application of CEUS is the differential diagnosis of bladder cancer from clots in human patients with haematuria when the diagnosis is equivocal on conventional B-mode and Doppler US (Piscaglia, et al., 2012)

In 2010 in human medicine, CEUS was used to study bladder tumours showing preliminary results: CEUS is more accurate than conventional sonography in staging tumours of the urinary bladder. At grey-scale examination, the main diagnostic criterion used to diagnose tumour infiltration of the muscular layer of the bladder wall was interruption of the hyperechoic bladder wall by the less-echogenic tumour tissue; disruption of the muscle layer by enhancing tumour tissue was considered diagnostic of infiltration. Important findings were the use of a 5-degree scale to classified the lesions: 1, definitely absent; 2, probably absent; 3, indeterminate; 4, probably present; 5, definitely present. Scores of 1 and 2 indicated negative results (absence of muscle infiltration) and scores of 4 and 5, positive results (presence of muscle infiltration). A score of 3 indicated that the presence or absence of muscle infiltration could not be determined. (Caruso, et al., 2010)

Wang, Wang, & Lei, 2011, studied lesions occupying kidney and bladder with *SonoVue*®. The overall CEUS manifestations of bladder cancer was characterized by fast wash-in, fast wash-out, and hyperenhancement. Further confirming that bladder carcinomas are tumours with rich blood supply. In general, CEUS presents clear sonograms of bladder occupying lesions: it is clearly displayed the demarcation and morphology of bladder tumours and outline particularly levels of tumour invasion to its surrounding tissues, suggesting invasion degree and staging of tumours, which is of great value for selecting treatment regimens and predicting prognosis. Besides, bladder tumours are susceptible to recurrence: CEUS in postoperative follow-ups is more likely to obtain important information contributing to early detection of lesions instead of trans-abdominal ultrasonography. (Wang, et al., 2011)

In a human medicine study was demonstrated the high bladder cancer detection rate of CEUS, which had a very high sensitivity for the presence of bladder cancer (90.9%). The bladder cancer is a hyper-vascular tumour that shows strong enhancement in the arterial phase, followed by a plateau of enhancement and a slow washout. A limitation of CEUS is the detection of flat lesions smaller than 1 cm. (Nicolau, et al., 2011)

In human medicine lesion classification was done based on enhancement pattern and was assigned a score: 1 (mild enhancement) or 2 (strong enhancement) as compared to the surrounding urinary bladder wall. Time-intensity curves (TICs) were extracted from regions of interest in the lesion and the closest bladder wall individuating three TICs shapes: shape A.- Z with wash-in phase followed by a plateau (normal bladder wall);

shape B - Z with wash-in phase followed by a slow wash-out phase (low-grade carcinoma); shape C - Z with wash-in phase followed by a rapidly descending curve (high-grade carcinoma).
Although both low- and high-grade malignant lesions are hyper-vascular, some characteristic features are helpful in differentiating them, such as enhancement score and particularly TIC shapes.
CEUS is a reliable non-invasive method for differentiating low- and high-grade bladder carcinomas since it provides typical enhancement patterns as well as specific contrast-sonographic perfusion curves. (Drudi, et al., 2012)

Drudi, et al., 2014, individuated that CEUS has limited ability to detect flat lesions. Another major limitation is that CEUS provides no tissue for histological evaluation. However, the combination of enhancement pattern, contrast-graphic parameters and the TIC shapes could indicate the histopathology of bladder lesions, thus increasing the specificity of Colour-Doppler US without a statistically significant reduction of sensitivity. (Drudi, et al., 2014)

A recent study evaluates the feasibility of using contrast-enhanced cadence contrast pulse sequencing ultrasound estimates of micro-vascular density to predict clinical and angiogenic response to treatment in dogs affected by bladder tumours undergoing to chemotherapy (Pollard, et al., 2017)

4.2 Materials and Methods

Use of CEUS in our clinical cases (n°=10 physiological cases) was organized to evaluate firstly the normal physiological parameters to give referral data. The method, applied according to General Procedures (see chapter 2) as in the follow table, provides the urine analysis of all subjects included, following by B-mode and Doppler US. Finally, was performed CEUS giving a qualitative and quantitative evaluation. Statistical analysis was done with Student's t test (*GraphPad InStat®)*

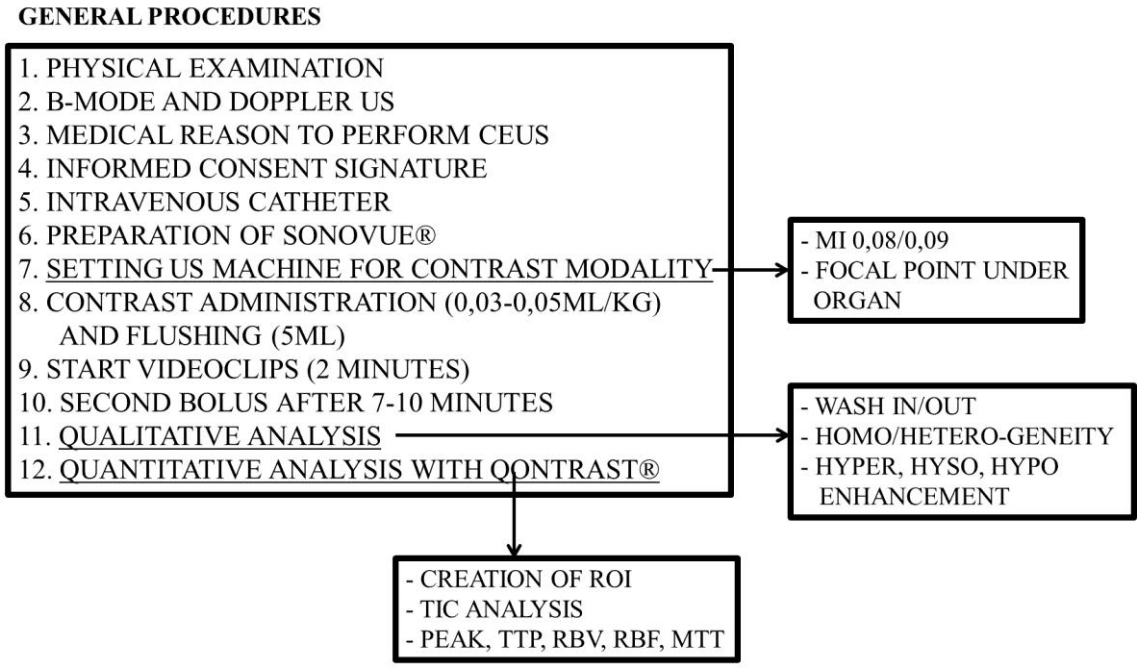

According to this procedure, were also studied with CEUS an inflammatory wall lesion and some TCC. In this case cytology diagnosis was done with collecting sample by catheter biopsy.

According to human literature qualitative criteria for interpretation of the results were:

- CEUS is superior to conventional B-mode US to identify infiltration of the muscular layer. (Note: *SonoVue*® - human) (Piscaglia, et al., 2012)
- Bladder lesions: classification of lesion using a 5- scale. Tumour infiltration of the muscular layer of the bladder wall corresponds to the interruption of the hyperechoic bladder wall by the less-echogenic tumour tissue. Disruption of the muscle layer by enhancing tumour tissue was considered diagnostic of infiltration. (Note: *SonoVue*® - human) (Caruso, et al., 2010)
- Bladder Cancer: on CEUS fast in, fast out, and hyperenhancement. Bladder carcinomas are tumours with rich blood supply. (Note: *SonoVue*® - human) (Wang, et al., 2011)
- Bladder cancer is a hyper-vascular tumour that shows strong enhancement in the arterial phase, followed by a plateau of enhancement and a slow washout. (Note: *SonoVue*® - human) (Nicolau, et al., 2011)
- A limitation of CEUS is the detection of flat lesions smaller than 1 cm. (Note: *SonoVue*® - human) (Drudi, et al., 2014) (Nicolau, et al., 2011)

Quantitative evaluation of results using *Qontrast*®, software analysis, included:

- Organization of different data derived from three different ROIs: one general, including wall (sierosa, muscular layer and sub-mucosa) and mucosa, and the other two respectively for wall (W) and mucosa (M) separately.
- Evaluation of following parameters generated from TIC: P, TTP, RBF, RBV, MTT.

4.3 Results

Ten dogs were evaluated between 2015 and 2017: in six cases the urinary analysis was normal, in three cases there was just a not significant crystalluria, and in one case there were small calculi. On B-mode and Colour Doppler US performed was evaluated the shape, the content and the border of the bladder, all in normal appearance, but not significant information was given from Colour Doppler. CEUS enhanced the wall of the bladders in which there was normal shape of wall and totally absence of lesions.
The video clips were analysed for qualitative interpretation: contrast medium arrived around 30 seconds and start to enhance sierosa and sub-mucosa similar to two parallel lines, then, with perpendicular direction to the previous lines, started to enhance the small vessels into the muscular layer. Wash-out phase is slow with enhancement still at 90 seconds (Figure 4.1).

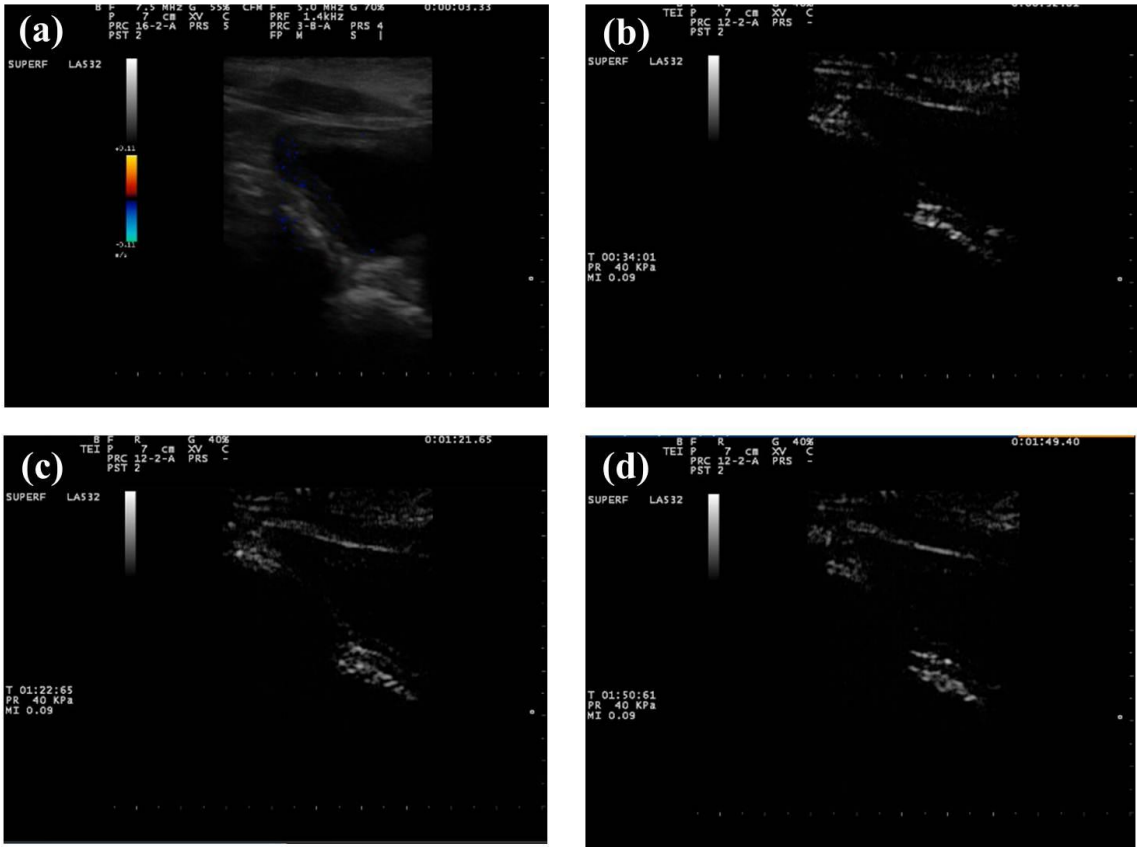

Figure 4.1 Physiological appearance of bladder wall on CEUS (clinical case n=3). B-mode-Doppler signal of bladder wall in which the content was totally urine with normal condition (a). CEUS examination at 34seconds (b), 82seconds (c), and 110seconds (d).

Quantitative study was done and data were organized as following giving statistical results: see Table 4.1 and Figures 4.2-4.3-4.4.

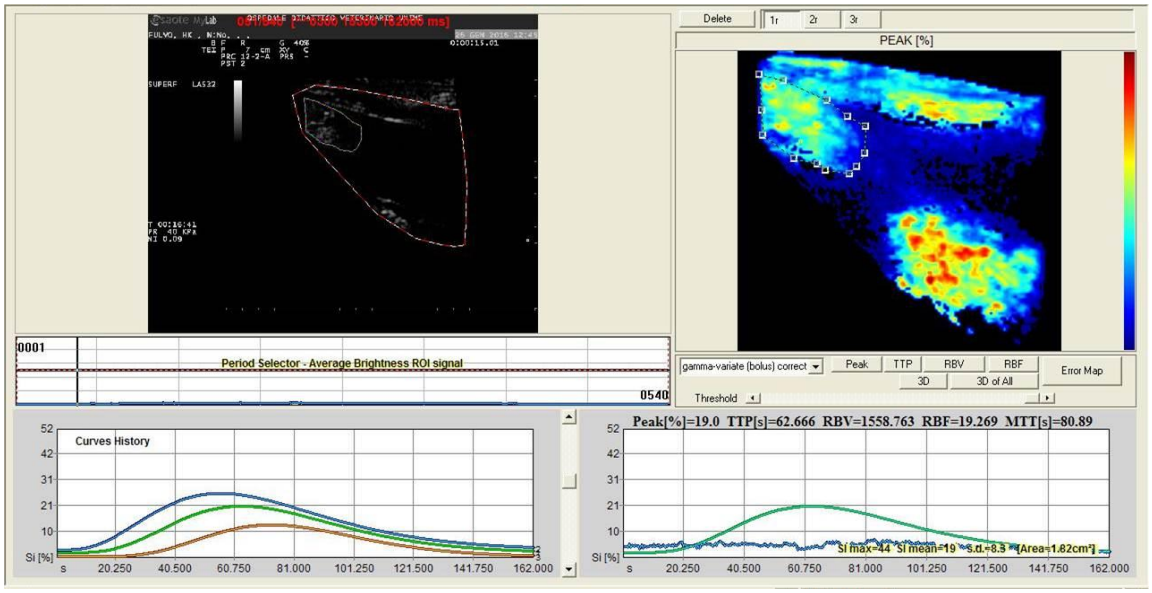

Figure 4.2 Quantitative analysis of physiological bladder cases (clinical case n=3). Quantitative analysis of Wall and Mucosa of a physiologic example, with creation of one ROI including both. The green TIC indicate the perfusion of ROI including both

Wall and Mucosa, while the blu TIC indicate the ROI perfusion just for Wall and the brown one just in Mucosa.

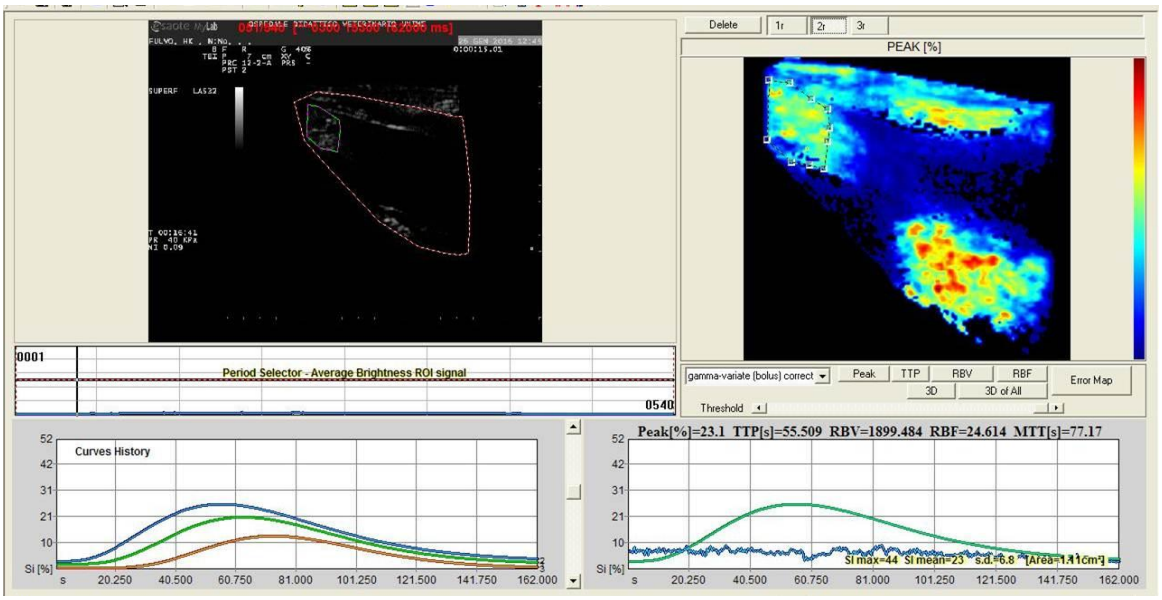

Figure 4.3 Quantitative analysis of physiological bladder cases (clinical case n=3). *Qontrast*® Quantitative analysis of wall with creation of one ROI, just in wall. The green TIC indicate the perfusion of ROI including both Wall and Mucosa, while the blu TIC indicate the ROI perfusion just for Wall and the brown one just in Mucosa.

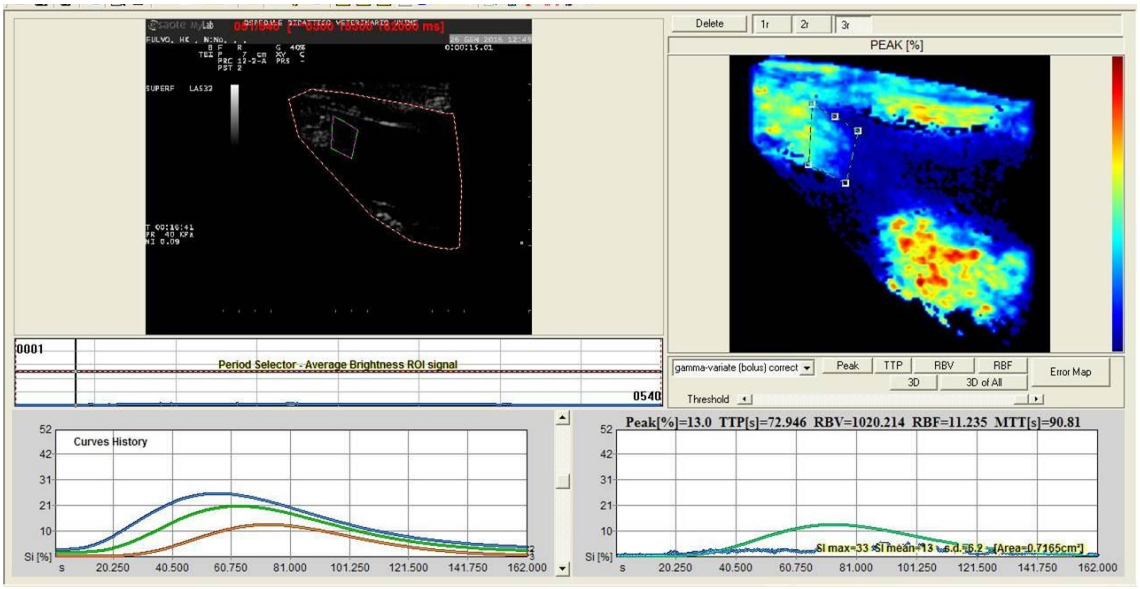

Figure 4.4 Quantitative analysis of physiological bladder cases (clinical case n=3). *Qontrast*® Quantitative analysis of mucosa with creation of one ROI, just in mucosa. The green TIC indicate the perfusion of ROI including both Wall and Mucosa, while the blu TIC indicate the ROI perfusion just for Wall and the brown one just in Mucosa.

Table 4.1 Analysis of 10 physiological wall bladder cases. These data derive from the quantitative analysis of CEUS using *Qontrast*®, the parameters are: Peak, TTP, RBV, RBF, MTT. Mean, Standard Deviation (SD) and Minimum and Maximum values are showed respectively for General ROI (Wall and Mucosa), ROI of Wall and ROI of Mucosa.

CASE	PEAK	PEAK W	PEAK M	TTP	TTP W	TTP M	RBV	RBV W	RBV M	RBF	RBV W	RBV M	MTT	MTT W	MTT M
1	22,7	30	12,8	30,107	31,856	20,891	1172,853	1551,121	317,371	24,001	32,76	10,978	48,87	47,35	28,91
2	9,6	15,6	6,1	58,595	50,423	57,265	724,687	1227,775	402,609	10,363	17,814	6,316	69,93	68,92	63,74
3	19	23,1	13	62,666	55,509	72,946	1558,763	1899,484	1020,214	19,269	24,614	11,235	80,89	77,17	90,81
4	12,1	20,7	5,7	46,091	33,565	58,376	742,076	1298,107	367,819	13,326	24,608	5,063	55,68	52,75	72,64
5	14,3	19	5,1	38,71	43,514	25,283	869,452	1204,892	153,21	14,986	20,142	5,136	58,02	59,82	29,83
6	7,7	9,5	4,8	34,263	33,899	34,807	351,482	437,039	180,653	8,261	10,507	4,404	42,55	41,59	41,02
7	11,7	15,9	9	44,155	33,041	54,412	618,613	726,152	572,873	12,444	18,35	8,234	49,72	39,57	69,58
8	17,3	21,3	10,5	53,527	32,898	65,571	1407,954	1192,853	866,042	20,347	25,487	11,57	69,2	46,8	74,85
9	11,9	13,2	10,4	50,916	43,511	58,655	687,053	679,993	703,155	11,925	13,467	9,935	57,61	50,49	70,77
10	9,8	11,1	6,8	48,705	50,133	47,015	525,351	605,172	341,429	9,176	10,316	6,343	57,25	58,66	53,83
MEAN	13,61	17,94	8,42	46,7735	40,8349	49,5221	865,8284	1082,259	492,5375	14,4098	19,8065	7,9214	58,972	54,312	59,598
SD	4,715801	6,166432	3,131844	10,35722	8,903012	17,26269	391,1698	461,3115	290,2749	5,206572	7,220121	2,81182	11,44545	11,95477	20,61503
MIN	7,7	9,5	4,8	30,107	31,856	20,891	351,482	437,039	153,21	8,261	10,316	4,404	42,55	39,57	28,91
MAX	22,7	30	13	62,666	55,509	72,946	1558,763	1899,484	1020,214	24,001	32,76	11,57	80,89	77,17	90,81

The quantitative data showed three TICs deriving from the three different ROIs. All three TICs obtained had similar morphology: the green-one, representing a unique ROI including Wall and Mucosa, showed intermediate data between the TICs deriving from the separated ROIs corresponded by Wall (blue-one) and Mucosa (brown-one). The blue TIC had higher Peak Intensity to the brown-one indicating higher perfusion in wall than in mucosa.

A case of inflammatory bladder lesion was studied with CEUS (Figure 4.5).
This lesion was an inflammatory lesion with upon a superficial mineralized part, giving shadow artefact, confirmed by cytology (catheter biopsy).
Our consideration about B-mode and Doppler were, of course, not conclusive and not sufficient to confirm the benign or malignant nature of this structure. Basic US was important to detect the lesion: on B-mode and Doppler there were a not vascularized nodule with shadow artefact.
CEUS showed the benign nature of this lesion: no compromising of wall was evidenced and it mantained normal enhancement. (Figure 4.5)

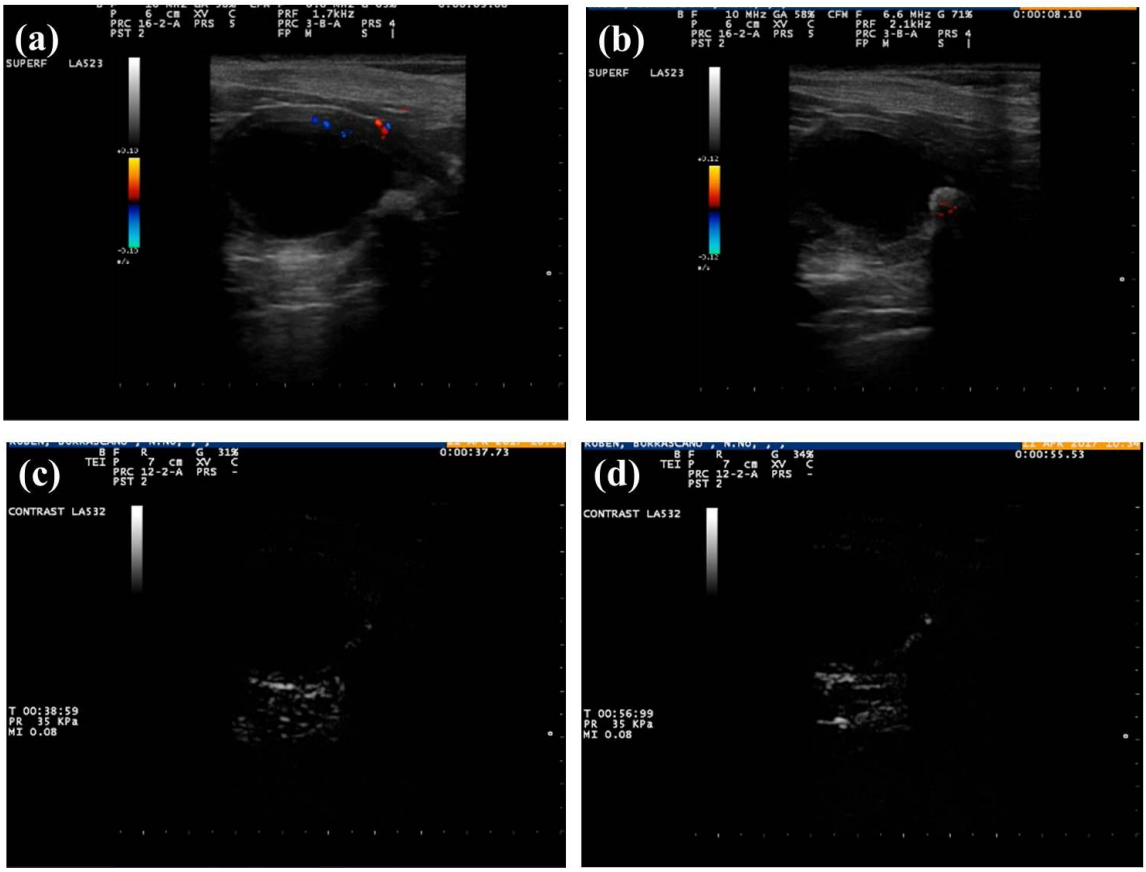

Figure 4.5 Inflammatory lesion case in bladder wall. B-mode and Colour Doppler image is showed and reveal the presence of a lesion in bladder wall hyper-echoic with shadow and with a low Doppler signal(a)(b) and CEUS reveal the bladder wall without abnormal changes(c)(d).

CEUS was used, after performing B-mode and Doppler, to study six patient with haematuria, not responsive to treatment.
Final diagnosis of TCC was done with cytology performed by catheter biopsy.
On B-mode was visible a parenchymal structure located in the bladder lumen and connected to the bladder wall, perfused on Colour Doppler with inner vessels.
CEUS revealed the wall (muscular layer) involved of bladder by lesion that was totally vascularized. (Figure 4.6)
Descriptive statistical analysis of the quantitative CEUS-derived parameters revealed a normal distribution for each value of its mean and standard deviation, provided below: peak enhancement was 22,05±1,73 %; TTP was 30,38±4,78 seconds; RBV was 1064.15±184,39 L/min; RBF was 25,17±3.29 L/min; MTT was 42,19±3,81 seconds.

As example, in one clinical case, showed as follows, the lesion was characterized from wall involvement on CEUS giving these quantitative parameters: Peak 26.6%, TTP 33.958s, RBV 1660.543, RBF 32.605, MTT 50.93.

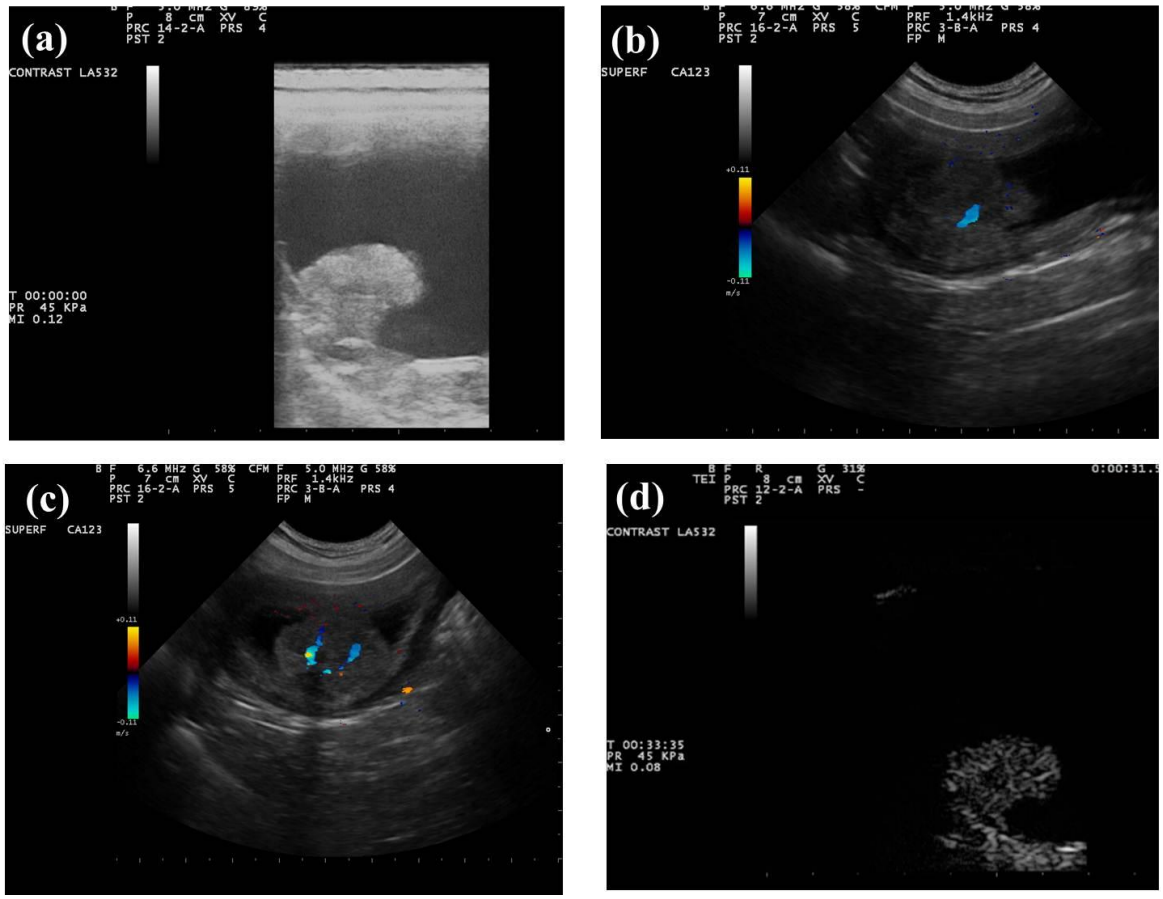

Figure 4.6 TCC in bladder (case n°=2). Image of lesion emerging from the bladder wall with homogeneous parenchyma and regular shape (a). Doppler detection of flow inside lesion (b)(c). CEUS enhancement of lesion at 33seconds after injection: the lesion reveals a diffuse perfusion of lesion and a disruption of the muscular layer of wall (d).

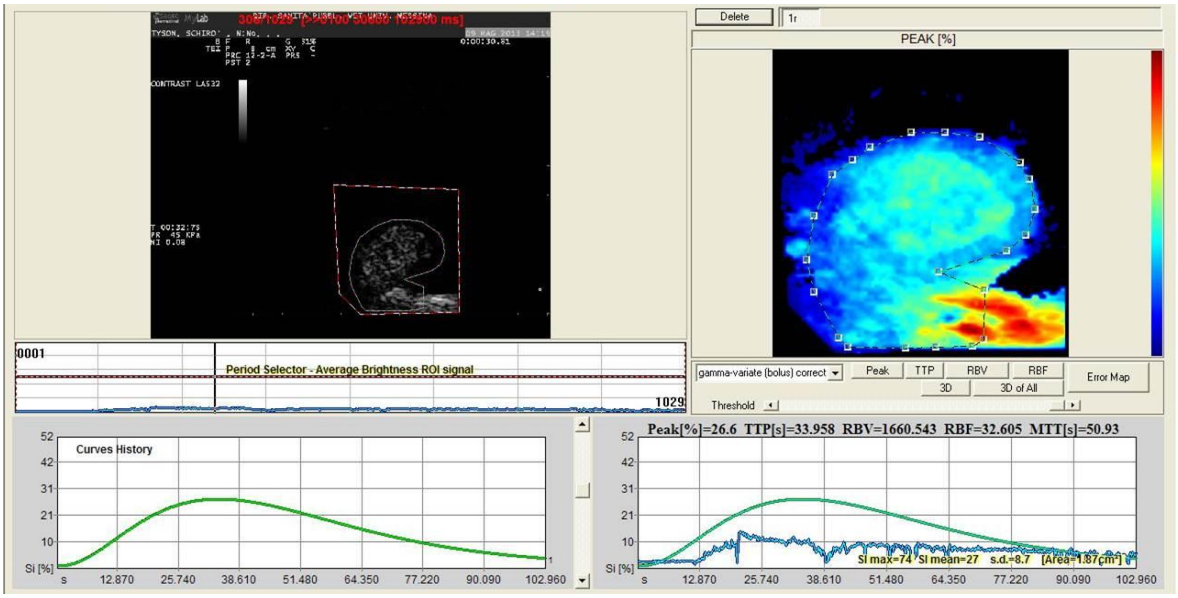

Figure 4.7 Quantitative analysis of TCC lesion. *Qontrast*® analysis of ROI including lesion and involved wall. Peak(%) was 26.6% and TTP was of 34seconds.

4.4 Discussion

Important considerations have to be done making comparisons about use of CEUS to individuate the involvement of bladder wall from malignant lesions (TCC) respect to benign (inflammatory case).
The urinary bladder receives its major blood supply through the caudal vesical arteries. These are branches of the vaginal or prostatic arteries that are branches of the internal pudendals from the internal iliac arteries. The small cranial vesical artery from the umbilical supplies the bladder apex. The venous plexus on the urinary bladder drains primarily into the internal pudendal veins. (Evans & De Lahunta, 2013, p. 360-367)
With CEUS we are able to analyse the wall perfusion, especially the vascularization of muscular layer that give the difference between a lesion infiltrating to an inflammatory simple lesion.
Using these criteria, it will be easy differentiate between benign and malignant lesions in bladder.
In the present study, the diagnostic criteria of the canine TCC were based on a cyto-pathologic evaluation of a sample of cancerous cells obtained through an ultrasound-guided suction biopsy.
Ultrasonography is commonly used as the first-line imaging modality in order to diagnose a bladder cancer. Furthermore, the detection of neoplastic angiogenesis using an imaging technique is very important to achieve a diagnosis of malignant cancers. So, imaging techniques performed with the injection of intravascular contrast agents become the gold standard to fully study an invasive bladder tumours in humans as well as in animals.
CEUS may play a role in urinary bladder diagnostic field.
In our study, using a contrast-tuned imaging technology, CEUS provided useful clinical information and allowed discrimination of perfusion vascular patterns of the urinary bladder for dogs affected by TCC. The purely intravascular contrast agent provides detailed viewing of the micro-vascular pattern of the tumour lesion and a more accurate reading of ultrasound images. The qualitative analysis showed a hyperenhancing vascular pattern of the tissue tumour and the loss of the hypoenhancing muscle layer of the bladder wall at base of the mass. Furthermore, it was possible the direct visualization of the hyperenhancing vascularized tumour tissue that pass through the bladder wall. These findings allowed us to underline the infiltrative pattern, as malignant feature, of this neoplastic disease.
The quantification of blood flow parameters was also reported, although the qualitative analysis of perfusion pattern is more reliable in arriving to a definitive diagnosis. In fact, the ultrasound enhancement measurements may be influenced by several patient-related (i.e. cardiac output, blood pressure, respiratory rate and interactions with the contrast medium) and technical variables related factors (i.e. scanner setting, gain setting, type, preparation and injection protocol of the contrast medium), all of which are potential source of variability.
In our experience CEUS allows to differentiate inflammatory lesions from neoplastic like showed before, with limitations given by few cases.
In conclusion, although the relatively small number of dogs enrolled, we believe that CEUS can improve diagnostic accuracy in characterization of the canine bladder wall in physiological condition or in case of TCC through the specific vascularization pattern and the bladder wall involvement. It may be a useful, non-invasive and reproducible diagnostic tool for detecting tumours that infiltrate the muscle layer of the bladder wall.

5 Kidney

5.1 CEUS knowledge

To clarify the contrast medium passage it is important to focus on the physiological anatomy of vascularization. Blood enters the renal artery from the aorta, goes through end arteries, interlobar vessels, arcuate vessels, interlobular arteries, and finally to glomeruli through afferent arterioles. Efferent arterioles leave the glomeruli and course directly into the outer layer of the medulla, giving rise to long capillary nets that extend to the apical end of the pyramid, or they branch directly into inter-tubular capillary networks.
The renal artery bifurcates into dorsal and ventral branches. The two primary branches of the renal artery, end branches, divide into two to four interlobar arteries. These branch into arcuate arteries at the corticomedullary junction. The arcuate arteries radiate toward the periphery of the cortex, where they redivide into numerous interlobular arteries. Afferent arterioles leave these to supply the glomeruli and thence the efferent arterioles.
Venous drainage of the kidney stems from the numerous stellate veins in the fibrous capsule. These connect with veins of the adipose capsule and empty into interlobular, arcuate and interlobar veins before entering the main trunk of the renal vein, which joins the CVC. Venous arcuate vessels, unlike their arterial counterparts, unite to form elaborate arches. Arcuate veins span the medulla to join the dorsal and ventral parts of the kidney. (Evans & De Lahunta, 2013, p. 361-364)

US gives important information to evaluate shape, dimension, parenchyma and vascularization. On B-mode the renal medulla is hypoechoic when compared with the cortex, which is usually hypoechoic or isoechoic to the liver and typically hypoechoic to the spleen. The medulla appears separated into several lobulated segments by the presence of linear echogenicities representing borders of the interlobar vessels and diverticuli.
The renal crest is the prolongation of the renal medulla and is in contact with the pelvis.
The walls of the arcuate arteries can be observed as paired, short, hyperechoic lines at the corticomedullary junction, which can sometimes generate an acoustic shadow and must be differentiated from mineralization. These vessels, as well as the larger renal and intralobar vessels, can also be evaluated with colour Doppler or power Doppler.
The renal arteries and veins, usually single on each side, can be followed from the hilus to the aorta and CVC, respectively. These vessels must be differentiated from dilated ureters.(Penninck & D'Anjou, 2015, p. 331-333)

CEUS is well tolerated and gives information about perfusion of kidneys according to humans EFSUMB guidelines (2012).
Kidneys enhance quickly and intensively after microbubble administration. The arterial pedicle and main branches enhance first, followed within a few seconds by complete fill-in of the cortex. There is no microbubble excretion into the urinary tract. As contrast concentration in the general circulation decreases, enhancement fades. Contrast enhancement is less intense and fades earlier in patients with chronic renal disease.
CEUS, for human patients, is recommended in the following clinical situations:
1. Suspected vascular disorders, including renal infarction and cortical necrosis.
2. Differential diagnosis between solid lesions and cysts presenting with equivocal appearance at conventional US.

3. Differentiation between renal tumours and anatomical variations mimicking a renal tumour ("pseudo-tumours") when conventional US is equivocal. However, both CEUS and CECT have limitations in rare very small isoenhancing tumours.
4. Characterisation of complex cystic masses as benign, indeterminate or malignant to provide information for the surgical strategy.
5. Additional aid, when necessary, in the follow-up of non-surgical complex masses.
6. Identification of clinically-suspected renal abscesses in patients with complicated urinary tract infection.
7. In patients undergoing renal tumour ablation under US guidance, CEUS may be used to improve lesion visualization in difficult cases and to detect residual tumour either immediately or later after ablation. When CEUS is planned, pre-ablation assessment of lesion vascularity is important. (Piscaglia, et al., 2012)

A clinical study with cats evaluates the renal hemodynamics of kidneys, reproducible Resistivity Index and Peak Intensity measurements in awake, non-sedated cats is feasible, making this a potentially valuable technique in the evaluation of renal disease in cats using US.(Mitchell, et al., 1998)
In 2010 were studied the normal characteristics of feline kidney using CEUS (*Definity*®): there was an initial uniform rapid enhancement of the renal cortex followed by a more gradual enhancement of the renal medulla. At peak medullary enhancement, there was a subjective loss of demarcation between the cortex and medulla. Important comparison was using contrast enhanced power Doppler ultrasound there was rapid increased Doppler signal from the interlobar, arcuate, and interlobular vessels and also within the peripheral cortex. The medulla could not be evaluated as a separate structure due to blooming artefact from the major vessels. Mean time to peak contrast enhancement for the whole kidney was longer using contrast-enhanced harmonic ultrasound than contrast enhanced power Doppler ultrasound. The time to peak enhancement for the cortex alone in contrast-enhanced harmonic ultrasound was 13s (SD 3.2s), and for the renal medulla was 25.5s (SD 8.7s). The half time for washout of contrast agent was 39s (SD 14.5s) for contrast-enhanced harmonic ultrasound. Contrast-enhanced harmonic ultrasound and contrast-enhanced power Doppler ultrasound allow improved non-invasive examination of feline renal perfusion compared with conventional Doppler imaging. (Kinns, et al., 2010)

A baseline of normal renal perfusion was studied in 8 dogs with *Definity*®.
The fast-early cortex inflow is a reflection of the blood flow to the glomeruli. The delayed peak may represent tubular perfusion in the second capillary bed concurrent with the more gradual inflow to the medulla. The overall decreased intensity of the medulla compared with the cortex at peak medulla intensity may be due to overall increased vascular space in the cortex, cortical bubble destruction, or venous drainage from the cortex tubules directly to the interlobular veins. There are multiple factors influencing the curves within the renal cortex or medulla. Factors such as gain and signal processing choices are expected to equally affect echo-signal amplitudes from the renal cortex, medulla, and contrast medium. Although they affect overall curve, they do not change with time and therefore, do not strongly affect the slope or time to peak. Mechanical factors, such as the use of a stopcock, volume of saline flush, and/or how rapidly it is administered, may influence the time to peak. Other factors are intrinsic to the contrast medium or to the patient. (Waller, et al., 2007)

In a study of human medicine for cystic renal lesions, CEUS images depicted additional septa, thicker wall and septa, and more solid components in than US or CECT. This

resulted in a grade of cystic malignant tumours higher than that was identified either by US or CECT, and a lower grade in benign lesions than by US. CEUS performed better than US in the diagnosis of renal cystic lesions, and played a similar role to CECT. (Xue, et al., 2014)

In human medicine CEUS features of diffuse heterogeneous enhancement, washout in the late phase, and peri-lesional rim-like enhancement allow confirmation of renal cell carcinoma, distinguishing renal cell carcinoma from angio myelolipoma, in small renal masses. CEUS improves the diagnostic efficacy of conventional US.
It may decrease the necessity of additional diagnostic studies and support decisions about treatment strategy in patients with small renal masses. (Oh, et al., 2014)

Important consideration about anaesthesia have to be done. We can refer to a study on cats where were performed three different protocols: (1) awake, (2) butorphanol (0.4 mg/kg IM), and (3) Propofol (3.5–7.7 mg/kg IV boluses to effect). Time–intensity curves were created from two regions-of-interest drawn in the renal cortex. The curves were analysed for blood flow parameters representing blood volume (base intensity, peak intensity, area-under-curve) and blood velocity (arrival time, time-to-peak, wash-in/out). There was no difference in the subjective enhancement pattern between the three protocols. No significant effect of butorphanol was observed in any of the perfusion parameters ($P > 0.05$). Propofol did not influence the most important perfusion parameter, area-under-the-curve, and is adequate for use in contrast-enhanced ultrasound studies. (Stock, et al., 2014)

In human medicine CEUS was also used to estimate the effect of an increase in mean arterial pressure induced by noradrenaline infusion on renal micro-vascular cortical perfusion in critically ill patients: noradrenaline-induced increase in mean arterial pressure was not associated with an overall increase in renal cortical perfusion as estimated by CEUS. However, at individual level, such response was heterogeneous and unpredictable suggesting great variability in pressure responsiveness within a cohort with a similar clinical phenotype. (Schneider, et al., 2014)

In 2015 Cantisani, et al., (2015) describe CEUS in human kidney. Investigations, however, have shown that CEUS is more sensitive than CT in detecting blood flow in hypovascular lesions and can be used to differentiate between lesions with equivocal enhancement at CT Ultrasonography and especially CEUS are reliable tools in characterizing simple cysts and in describing their complicated character. Many studies have demonstrated that CEUS often upgrades the Bosniak classification, thus indicating the need for surgical treatment, a clear benefit of CEUS. (Cantisani, et al., 2015)

Choi, et al. (2016), compared the normal kidney perfusion patterns in conscious and anaesthetized dogs using CEUS in eight healthy beagles.
The protocol used for anaesthesia was tiletamine-zolazepam and medetomidine (TZM group) or only medetomidine (M group): renal cortical perfusion pattern under TZM anaesthesia was not significantly different with conscious status, except for TTP0. However, perfusion factors in the renal medulla were affected by anesthesia during CEUS. Therefore, the TZM combination may be a useful anaesthetic protocol for evaluating renal cortical perfusion, and data obtained in this study may serve as reference values for evaluation of renal perfusion using CEUS in dogs under the injectable anaesthesia. (Choi, et al., 2016)

In veterinary medicine, some characteristics of kidney's lesions, studied with CEUS using SonoVue®, are described in the following table.

Table 5.1 Some kidney's lesions characteristics according to Haers, et al. (2010). Were classified lesions and described B-mode, Doppler and CEUS appearance.

LESION	B-MODE AND DOPPLER	CEUS
Trauma-induced hematoma	large heterogeneous mass that contained a moderately sized ill-defined hypoechoic cavity	Large, smoothly outlined, not-vascularized cavity that contained only a few echoic spots
Idiopathic hematoma	Smaller, heterogeneous slightly hyperechoic nodule that contained several small anechoic areas, located at the renal pelvis	No vascularity, well-defined anechoic to slightly hypoechoic nodule
Haemorrhagic and necrotic area	hypoechoic renal mass with randomly organized internal echoes	well-defined avascular anechoic mass, with a vascularized rim and small diverticuli within the lesion
Abscesses	Heterogeneous predominantly hypoechoic rounded nodular lesion that contained hyperechoic debris (n¼1) or as a large subcapsular irregular and sharply outlined hypoechoic pocket containing small echoes, compressing the adjacent renal parenchyma	(As for hematoma) vascularity was not apparent and appeared as smoothly outlined anechoic to hypoechoic masses
Small abscess	Multiple echogenic foci within the abscess cavity	Avascular lesions
Small renal cysts	Smoothly	Round avascular lesions
Renal cell carcinomas	Single iso- to hypoechoic heterogeneous mass as a larger heterogeneous mass in the cranial pole and a smaller hypoechoic nodular lesion at the caudal pole of the affected kidney, or as multiple variable-sized slightly hypoechoic nodules	Large intralesional tortuous arterial vessels during the early phase of enhancement, that were enhancing at the same time or slightly earlier than vessels in the surrounding normal kidney. The late corticomedullary phase was characterized by either a diffuse heterogeneous or homogeneous pattern with gradually decreasing enhancement
Histiocytic sarcoma	Large heterogeneous hypoechoic renal mass with a large number of calcifications or as a homogeneously hypoechoic cortical nodule	It had arterial vessels within the lesion during the early phase of enhancement, being smaller and less well defined than in the renal cell carcinomas, which had large tortuous vessels in every lesion, irrespective of size. During the late cortico-medullary phase of enhancement, the histiocytic sarcomas were characterized by a diffuse and homogeneously hypoechoic contrast pattern with gradually decreasing enhancement
Renal lymphoma	multiple confluent iso- to hypoechoic nodules and masses	During the early arterial phase of enhancement, there was rapid and obvious vascularization surrounding the lesions followed by centripetal filling of small vessels at the periphery of these lesions. This arterial phase was rapidly disappearing when compared with the renal cell carcinomas. During the late cortico-medullary phase, the lesions became hypoechoic, similar to the renal cell carcinomas and the histiocytic sarcoma, with the duration of intralesional enhancement being less than in the renal cell carcinomas and comparable with the histiocytic sarcomas.
Hemangiosarcoma metastases	single hyperechoic or multiple hypoechoic nodules in the renal cortex	non-enhancing nodules during both the early arterial and late corticomedullary phase of enhancement
Renal chemodectoma metastases	iso- to slightly hyperechoic nodule at the level of the renal pelvis	no clear arterial feeding vessels were seen, and the lesion had gradual and homogeneously increasing enhancement. The late corticomedullary phase of enhancement was characterized by a diffuse and homogeneous, slightly hypoechoic nodule, with gradually decreasing enhancement

The assessment of renal perfusion plays a big role in evaluating the kidney disease: renal perfusion changes occur in early state of the disease progress (Tsuruoka, et al., 2010).

Since 2000, it was introduced the chronic hypoxia hypothesis (Fine, et al., 2000) for which the hypoxia increases the chronic ischemic damage, final pathway of end-stage kidney injury.
The hypoxia causes loss of peritubular capillaries, decreased oxygen diffusion from peritubular capillaries to tubular and interstitial cells as a result of fibrosis of the kidney, stagnation of peritubular capillary blood flow induced by sclerosis of "parent" glomeruli, decreased peritubular capillary blood flow as a result of imbalance of vasoactive substances, inappropriate energy usage as a result of uncoupling of mitochondrial respiration induced by oxidative stress, increased metabolic demands of tubular cells and decreased oxygen delivery as a result of anaemia (Nangaku, 2006).
Overtaken the initiating insult, chronic kidney diseases (in which the renal fibrosis is given from the accumulation of extracellular matrix disrupting the normal tissue architecture and giving kidney failure) present a common pathology of glomerulosclerosis and tubulo-interstitial fibrosis and it is well established that tubulo-interstitial fibrosis provides the best predictive indicator of progression to end-stage disease giving also rarefaction of peritubular capillaries (Fine & Norman, 2008).
Different tests can be used to evaluate the renal perfusion such as the estimation of the renal plasma flow with the determination of para-amino hippuric acid (PAH) clearance, but technically laborious, or the evaluation can be done using radioactive tracers like ortho-iodo-hippuric acid and mercaptoacethyltriglycerine, but with high cost and radiations (Stock, et al., 2016).
Currently , nuclear renogram, CT, and MR are the most common imaging tests to quantitatively assess renal perfusion, but with significant limitations for quantifying renal blood flow in case of chronic kidney disease: invasive for radiation, highly costly, cannot reveal glomerular filtration (Dong, et al., 2013).
In this contest, CEUS can be used because it allows assessment of both macro- and micro- circulation giving good representation in case of diagnosis of diffuse renal disorders and early assessment of chronic kidney dysfunction.
CEUS can quantitatively evaluate the perfusion changes of the kidney in case of chronic ischemic renal disease.
To determine the usefulness of CEUS in the visualization of peritubular capillaries and changes in enhancement with progression of renal dysfunction, in a study using *Sonazoid*® in normal subjects and patients with chronic kidney disease, were evaluated the correlations between glomerular filtration rate and enhancement in the renal cortex and medulla: the attenuation consisted of a delay in the rise in echogenicity, reduction of peak intensity, and acceleration of decay of enhancement in both cortex and medulla; it seems likely that the increase in renal resistance due to the decrease in number of glomeruli and peritubular capillaries as well as narrowing of arterioles contributes to the delay in rising and reduction of peak intensity with progression of chronic kidney disease stage. Can be also observed the attenuation of visualization of interlobular arteries and sluggish efflux of enhancement from interlobar arteries with progression of renal dysfunction. (Tsuruoka, et al., 2010)

In one study were used healthy dogs, by placing the Ameroid ring constrictors on the distal portion of right renal artery through operation, was performed CEUS monitoring the right kidney perfusion using *SonoVue*® every week after operation. With the progression of chronic ischemic renal disease, dogs showed delayed enhancement and perfusion in renal CEUS curve. CEUS can display the perfusion changes of chronic ischemic renal disease in the early period. Earlier significant changes were observed in blood perfusion indexes from 4,7 weeks after operation, but changes in creatinine and azotaemia occurred in 11 weeks. As it was described in the literature, during the

decompensation period of renal dysfunction, the occurrence of a characteristic increase of creatinine and azotaemia becomes apparent only when renal filtration decreases to half of normal level (Dong, et al., 2013).
This concept, about detection by CEUS of kidney failure was used to study the technique in healthy cats infused with Angiotensin II to induce perfusion changes: they found a significant decrease in peak enhancement and a tendency towards a lower wash-in perfusion index compared to control measurements (Stock, et al., 2016)
In case of renal function impairment, CEUS was used to study acute renal failure of suspicious vascular origin or suspicious renal lesions. Imaging in human patients with renal function impairment is challenging because of well-known limitations of conventional colour Doppler ultrasound or risks related to the use of contrast media on CT and MR. CEUS is a safer imaging tool in patients with RFI, showing 36% detection rate of renal infarction in patients with acute renal failure of suspicious vascular origin, and the capability of characterizing renal lesions in order to address patients to most proper treatment (Girometti, et al., 2017).

According to reported literature knowledge about importance of CEUS technique to show micro-vascularization in kidney failure, the aim of our preliminary study is to evaluate this alteration in case of canine kidney failure compared to a control group.
Again, one clinical case of Carcinoma and one of Histiocytic Sarcoma were studied.

5.2 Materials and Methods

The procedure was applied according to General Procedures (see chapter 2) as in the follow scheme.

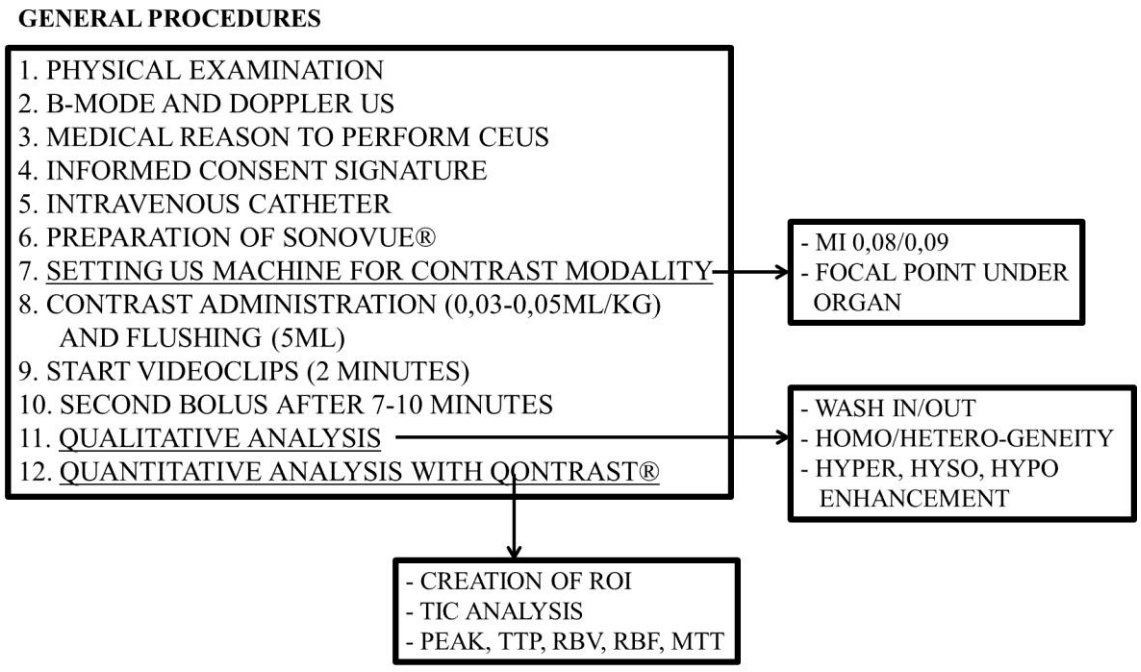

Patient with kidney's parameters in the range of normality were studied with contrast medium giving referral points to compare patients with kidney failure.
To classify the stage of chronic kidney disease was followed the official staging of the International Renal Interest Society (IRIS).
Considering the high prevalence of canine Leishmaniasis in our area giving kidney damage, the patients follow a diagnostic iter to diagnose Leish through Indirect

Immunofluorescence (IFI) title, direct microscopy Polymerase Chain Reaction (PCR), with material lymph-node and clinical evaluation. The serological test was considered with the title "positive" for values upper to 80 and classified according to LeishVet guidelines (Solano-Gallego, et al., 2011). For all subjects were done blood and urine analysis. Were excluded patients that have ultrasound examination positive for focal lesions or hydronephrosis.
Were organized two group, a control group and a kidney failure group.
In particular, in all analysed kidneys, arterial and venous flows was displayed using colour Doppler ultrasound and will make a recording of flows interlobar artery and arched. A level of the interlobar will evaluate the Renal perfusion, assessed by the study CEUS, in sagittal scanning was recorded in real-time for 2 minutes.
The kidneys were monitored continuously during arterial immediate and the late phase cortico-medullary with a mechanical index at a low level (0.09); It was used only one focal point located just below the organ.
One qualitative and quantitative analysis (manually drawn two ROIs, one located in cortex and one in medulla (Macrì, et al., 2016)) was done and the data obtained from the two group were compared with a Student's t test (two tailed P).

5.3 Results

The control group was constituted by 10 normal dogs and the kidney failure group included 7 dogs.

The following Table shows signalment and IRIS stage of the subjects of kidney failure group.

Table 5.2 IRIS classification of kidney failure. The 7 clinical cases of kidney failure are classified based on creatinine values according to IRIS guidelines. Are showed: breed, gender (male (M) or female (F)), age (years (Y) or months (M)), Crea (creatinine, range 0.5-1.8 mg/dL), Bun (azotaemia value, range 7-27 mg/dL) and IRIS stage.

CASE	BREED	GENDER	AGE	CREA	BUN	IRIS
1	CROSS	M	15Y	11	110	4
2	GREAT DANE	M	3Y	4	35	3
3	ENGLISH SETTER	M	10Y	6	130	4
4	SPRINGER SPANIEL	M	2Y	2,1	60	3
5	CROSS	F	10Y	3,1	100	3
6	LABRADOR	M	6M	6,48	320	4
7	DACHSHUND	M	5Y	5,5	120	4

B-mode and Doppler US in all control group dogs showed normal shape, borders, cortex-medulla limit, echogenicity and vascularization. CEUS showed early wash-in in cortex, followed by medulla and slow wash out (Figure 5.1).
In comparison to failure group, renal cortex was hyper-echoic in B-mode and lower perfused with CEUS (Figure 5.2).

From *Qontrast*® analysis of control group, mean data were obtained: Peak C 24.2% and Peak M 21.3%, TTP C 24.4s and TTP M 35.3, RBV C 1509.3 and RBV M 1231.6, RBF C 31.2 and RBF M 24.1, MTT C 45.7 and MTTM 48.736. Peak values were higher in cortex than in medulla (P=0,31), TTP values were significantly lower for cortex than in medulla (P=0.01), RBV (P=0.4) and RBF (P=0.11) values were higher for cortex than in medulla, MTT (P=0.62) values were higher for medulla than in cortex.

In the same analysis for failure group (Figures 5.3 – 5.4), mean values were: Peak C 12.8% and Peak M 17.5%, TTP C 31.8s and TTP M 42,3s; RBV C 734.5 and RBV M 1092.7, RBF C 15.5 and RBF M 19.5, MTT C 46.3 and MTT M 56.1. Peak values were higher in medulla than in cortex (P=0.17), TTP values were higher in medulla than in cortex (P=0.13), RBV (P=0.35), RBF (P=0.34) and MTT (P=0.31) values were lower in cortex than in medulla.

Comparing data obtained between control group and kidney failure cases, mean values for Peak in cortex were significantly lower in patients with kidney failure (P=0.003) and the time to Peak was slower in kidney failure group (P=0.17). Mean values of RBV of cortex in kidney failure group were near significantly lower than control group (P=0.08) and mean values RBF of cortex were significantly lower in failure group than in control group with P=0.003.

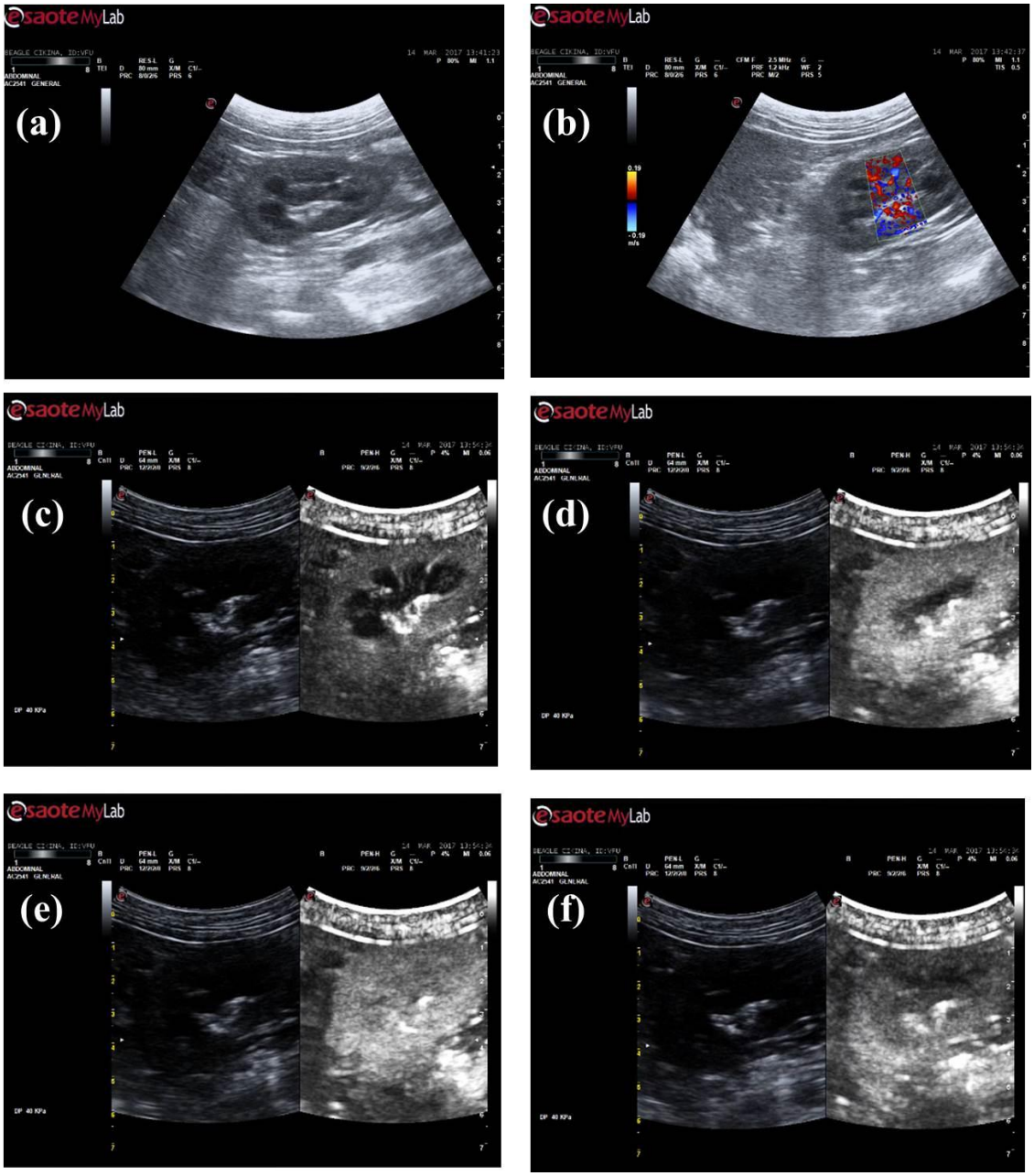

Figure 5.1 Physiological appearance of kidney with CEUS. Physiological example of US in B-mode(a) Doppler(b) and CEUS enhancing cortex(c) medulla(d) and wash-out phase(e-f).

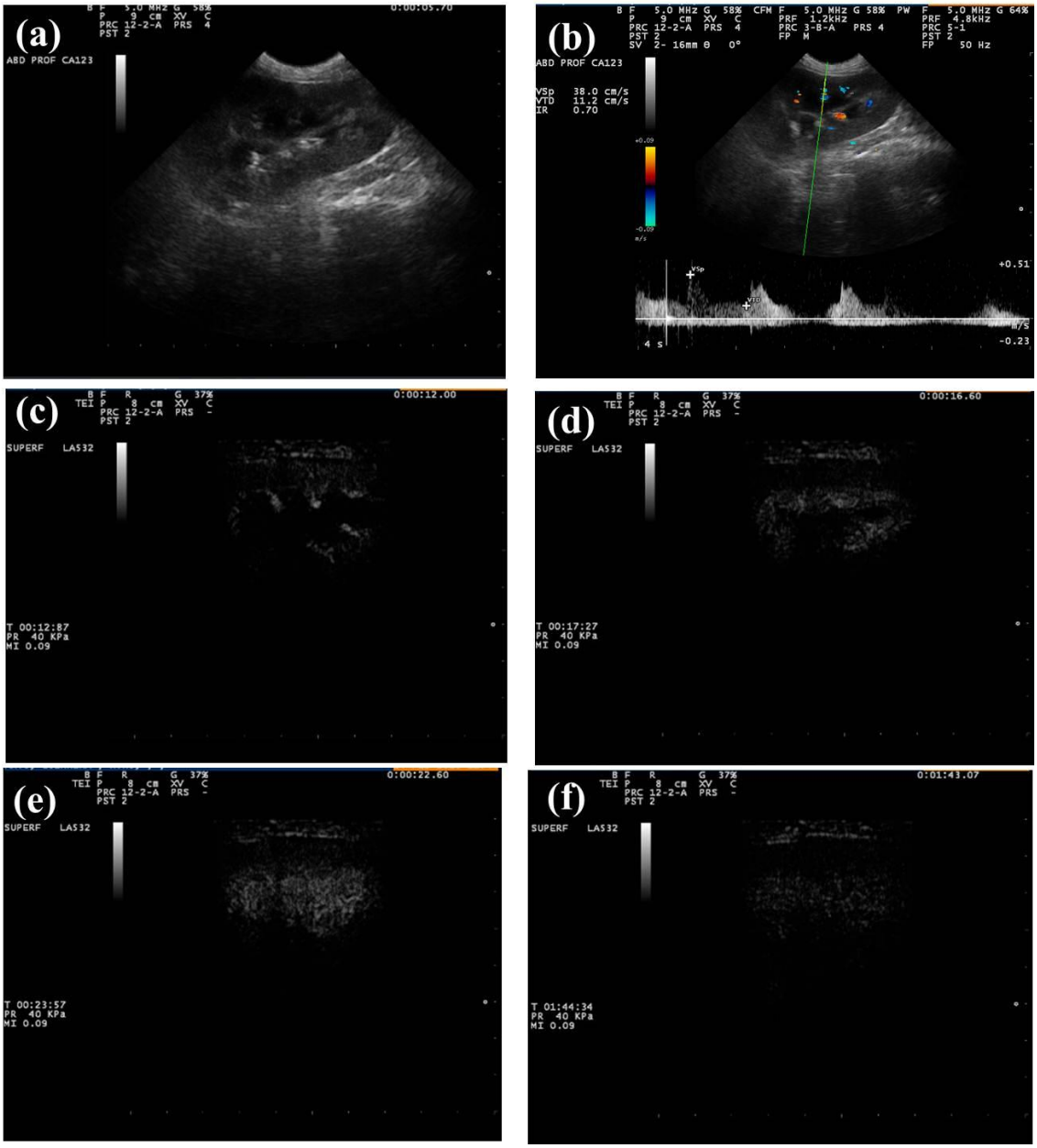

Figure 5.2 Kidney failure appearance with CEUS. Clinical case n°4: kidney failure in case of Leish. B-mode US (a) – Doppler US and Resistivity Index 0.7 (b) – CEUS at 12 seconds with cortex perfusion (c) – CEUS at 17 seconds with medulla perfusion (d) – CEUS at 23 seconds still in medulla (e) – CEUS wash-out (f).

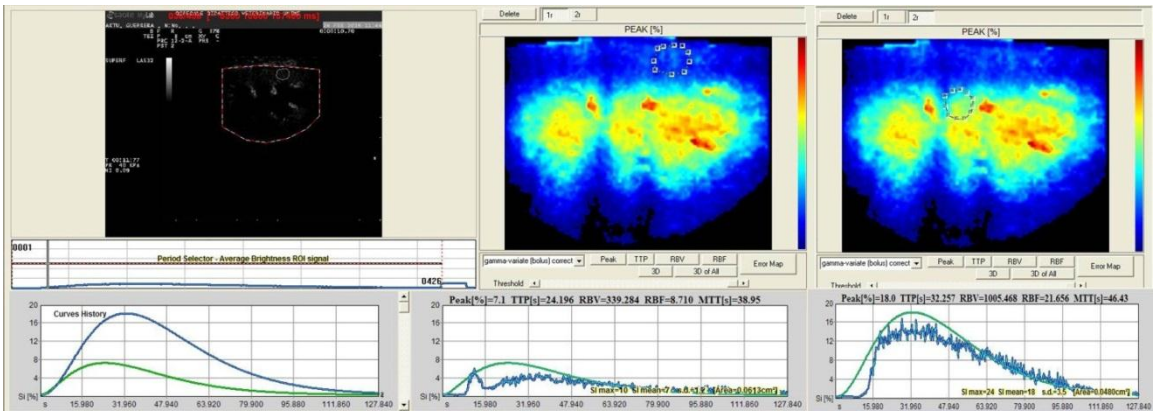

Figure 5.3 Quantitative analysis of kidney failure. Clinical case n°=4. Quantitative analysis using *Qontrast*® was done using two ROIs, one located in cortex and one located in medulla, different TICs were generated giving different parameters for Peak, TTP, RBV, RBF, MTT.

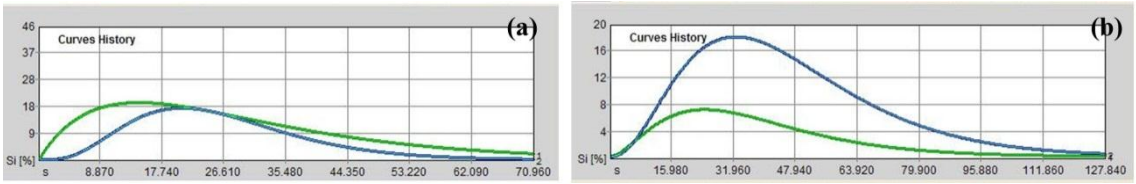

Figure 5.4 Tics comparison between control group and failure group. Tic of control group (a) is compared with Tic of failure group (b) in which green line is cortex and blue one is medulla: it is visible lower Peak of cortex in the second group.

Table 5.3 Quantitative analysis data of physiological kidney (Control group). Quantitative data deriving from *Qontrast*® analysis of CEUS of Physiological Control group (n°10). Were analysed Peak, TTP, RBV, RBF and MTT deriving from two ROIs, one in cortex and one in medulla. Mean, Standard Deviation (SD), Minimum and Maximum were calculated.

CASE	PEAK C	PEAK M	TTP C	TTP M	RBV C	RBV M	RBF C	RBF M	MTT C	MTT M
1	26,9	23,2	22,711	44,368	1540,765	1385,196	35,147	24,262	43,84	57,09
2	33,6	32,6	37,543	42,076	3238,106	2631,033	45,039	40,433	71,9	65,07
3	19,9	18	14,264	20,456	793,168	501,787	26,958	19,046	29,42	26,35
4	14,6	14,1	20,501	40,416	671,254	558,836	19,059	12,48	35,22	44,78
5	23,3	22,5	17,559	23,815	927,465	1162,012	30,508	29,089	30,4	39,95
6	30	29,3	18,952	23,911	2012,253	1996,623	41,157	39,795	48,89	50,17
7	29,3	20,9	34,574	40,917	1690,638	889,87	34,044	18,727	49,66	47,52
8	22,2	17,1	16,39	37,672	1648,376	1302,171	30,312	21,698	54,38	60,04
9	16	10,6	23,472	31,281	524,002	386,226	16,701	10,917	31,38	35,38
10	26,2	24,3	37,968	47,603	2046,666	1501,781	32,891	24,615	62,23	61,01
MEAN	24,2	21,26	24,3934	35,2515	1509,269	1231,554	31,1816	24,1062	45,732	48,736
SD	6,164414	6,672864	8,960615	9,66635	823,8271	704,4904	8,781735	10,04036	14,44665	12,43166
MIN	14,6	10,6	14,264	20,456	524,002	386,226	16,701	10,917	29,42	26,35
MAX	33,6	32,6	37,968	47,603	3238,106	2631,033	45,039	40,433	71,9	65,07

Table 5.4 Quantitative analysis data of kidney failure group. Quantitative data deriving from *Qontrast*® analysis of CEUS of kidney failure group (n°7). Were analysed Peak, TTP, RBV, RBF and MTT deriving from two ROIs, one in cortex and one in medulla. Mean, Standard Deviation (SD), Minimum and Maximum were calculated.

CASE	PEAK C	PEAK M	TTP C	TTP M	RBV C	RBV M	RBF C	RBF M	MTT C	MTT M
1	15,7	19,6	15,282	22,31	377,778	578,788	17,954	20,974	21,04	27,6
2	18,9	17,9	29,185	49,825	1364,87	1537,91	25,005	21,303	54,58	72,19
3	6,7	18,3	39,852	61,134	365,273	1494,35	7,312	19,166	49,95	77,97
4	7,1	18	24,196	32,257	339,284	1005,47	8,71	21,656	38,95	46,43
5	5,1	10,1	36,113	45,472	249,52	641,312	5,369	10,881	46,47	58,94
6	11	14,8	24,731	39,778	44,485	825,538	12,865	16,271	34,32	50,74
7	25,3	24,1	53,01	45,263	2463,06	1565,8	31,323	26,523	78,63	59,04
MEAN	12,8286	17,5429	31,767	42,2913	743,468	1092,74	15,5054	19,5391	46,2771	56,13
SD	7,46206	4,30227	12,3879	12,4967	867,548	434,01	9,74219	4,90253	18,0866	16,7749
MIN	5,1	10,1	15,282	22,31	44,485	578,788	5,369	10,881	21,04	27,6
MAX	25,3	24,1	53,01	61,134	2463,063	1565,798	31,323	26,523	78,63	77,97

In kidney failure group, 4 dogs were affected by Leish: 2 dogs were classified in LeishVet stage 4 and 2 dogs were classified in stage 3.

Was studied a clinical case of Carcinoma, confirmed by cytology. In B-mode were detected the lesion: kidney was totally altered in shape, border, cortex-medullary limit was not visible; by Doppler the perfusion was not detected homogeneously. CEUS appearance included hypoenhancement areas not homogenously perfused by tortuous arterial vessels (Figure 5.5).

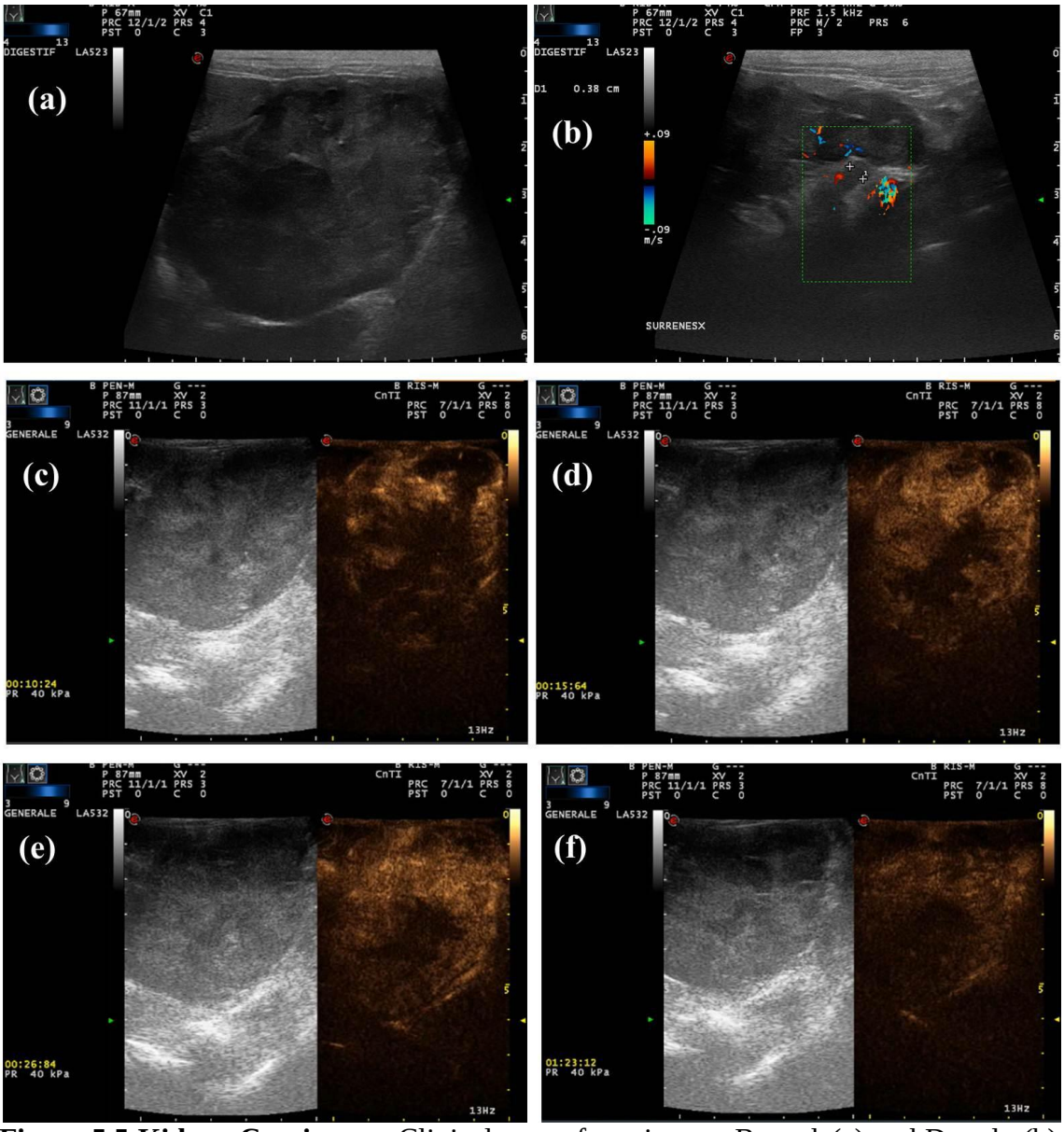

Figure 5.5 Kidney Carcinoma. Clinical case of carcinoma. B-mode(a) and Doppler(b) study revealed shape, volume and cortex/medulla alteration. On CEUS was showed the parenchymal kidney perfusion at 10-15-26seconds where is visible a lack of perfusion in cortex in big and some smaller areas; wash-out phase at 83seconds.

Histiocytic Sarcoma, confirmed by cytology, showed on B-mode and Doppler a big lesion destroying the border of kidneys and some smaller, not vascularized on Doppler. On CEUS all parenchymal kidney perfusional structure had fast wash-in and loose fast contrast becoming early hypo-enhanced comparing to kidney parenchyma with typical malignant appearance (Figure 5.6).

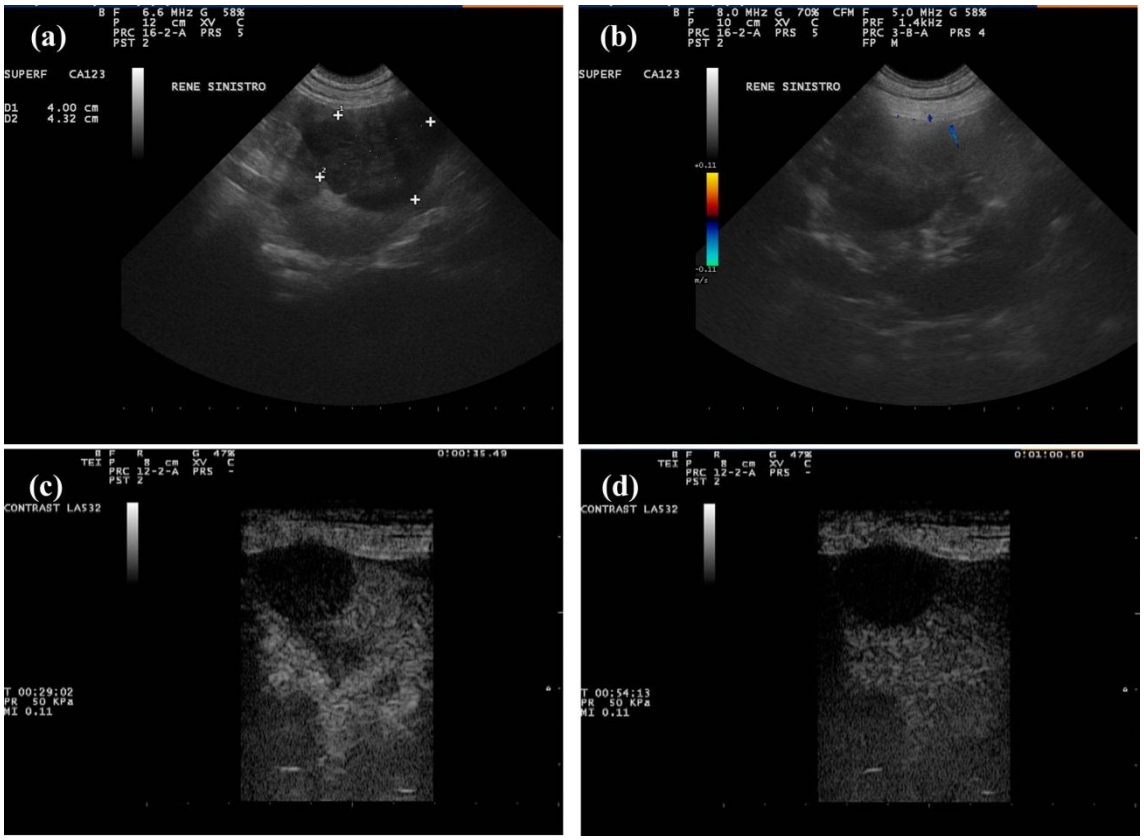

Figure 5.6 Histiocytic Sarcoma of kidney. B-mode (a) appearance of a nodular lesion deforming the kidney shape with low vascularization on Doppler (b). CEUS appearance of lesion loosing faster contrast compared to the rest of parenchyma (c)(d).

5.4 Discussion

As reported in other studies in human medicine and in veterinary medicine, our data have shown the feasibility to use CEUS in the assessment of renal perfusion also in clinical practice (Tsuruoka, et al., 2010) (Dong, et al., 2013) (Haers, et al., 2013)(Stock, et al., 2016).

The evaluation of renal perfusion is very important because these changes occur earlier than biochemical parameters of renal function (Dong, et al., 2013).

In comparison with a clinical study in in human patients with chronic kidney disease, in which analysis of CEUS images showed a delay in the rise of enhancement, reduction of peak intensity in cortex and medulla and acceleration of decay of enhancement in both cortex and medulla, in our study TTP of cortex and medulla are higher in kidney failure group, respectively P=0.17 e P=0.20, but are not statistically significant than control (Tsuruoka, et al., 2010).

The ability of CEUS and renal scintigraphy with contrast to detect changes in renal perfusion in healthy cats at baseline and during infusion of angiotensin II was evaluated in a recent study (Stock, et al., 2016). In that study, the cats were in anaesthesia and quantitative perfusion parameters resulted from ROIs drawn in cortex, in medulla; one ROI contained the entire kidney. A decrease in peak enhancement was significant for the entire kidney and near to statistical significance in renal cortex; no changes were observed in any of the perfusion parameters for the renal medulla. That study has shown that CEUS is more capable to find perfusion changes induced by angiotensin II infusion than renal scintigraphy (Stock, et al., 2016).

In this study, we have found significant lower values of Peak in cortex and RBF and nearly significant lower for RBV showed a lower perfusion in cortex: these values became significant according that more than 90% of total renal blood flow entering in kidney and supplies the renal cortex; therefore, a change in cortical microbubbles volume and velocity was used as a surrogate for alteration in total renal perfusion.

These are promising results to using CEUS as a feasible tool to evaluate alterations in kidney perfusion during renal failure as acute than chronic, or monitoring therapy with ACE-inhibitors.

The main limitation of our research was the small number of patients in kidney failure, so that it was not possible to grouping them according to IRIS staging, thus we considered to have only preliminary results.

Again, considering that clinical manifestations of Leish include renal disease that may be the only one sign of Leish and it can progress from mild proteinuria to the nephrotic syndrome or to an end stage renal disease (Solano-Gallego, et al., 2011 - Costa, et al., 2003 - Zatelli, et al., 2003), it could be a useful tool studing with CEUS the kidney perfusion in a large number of dogs affected by Leish.

One cases of Carcinoma and Histiocytic Sarcoma were showed: in both cases were showed malignant characteristic of lesions appearing on CEUS, as reported in literature (Haers, et al., 2010).

6 Testis

6.1 CEUS knowledge

The canine testes are oval structure located in to the scrotum. Testis and epididymis are supply by testicular artery and artery of the ductus deferens branch of the prostatic artery from the internal pudenda. The testicular vein follows the arterial pattern but forms an extensive pampiniform in the spermatic cord. The right testicular vein empties into the CVC at the level of the origin of its arterial counterpart. The left drains into the left renal vein. (Evans & De Lahunta, 2013, p. 371)
US is the diagnostic method most used to study testis, and testicular tumours are common findings, but B-mode and Doppler are not able to distinguish the type classification. (Penninck & D'Anjou, 2015, p. 423 - 445)

EFSUMB guidelines give information about the study of scrotum and testis with CEUS for human patient. CEUS provides a practical solution by increasing the confidence of the interpretation of lesion vascularity and of scrotal cord vessels, allowing for appropriate clinical management.
The arterial phase at CEUS is the most important aspect of the examination: the testis and epididymis enhance rapidly but the arrival time varies among individuals. The arteries enhance first, followed within seconds by complete parenchymal enhancement. The scrotal wall tends to enhance to a lesser degree than the contents. There is no accumulation of microbubbles in the parenchyma of the testis and the enhancement declines over a variable period of time such that there is minimal residual enhancement by 3 minutes. (Piscaglia, et al., 2012)

Testicular tumours are the most common neoplasms in male dogs, representing more than 90% of all canine male genital tumours (Hayes & Pendergrass, 1976). According to the World Health Organization classification, the main three types reported in dogs are Interstitial Cell Tumour (ICT), Seminoma (SEM) and Sertoli Cell Tumour (SCT) (Kennedy & al., 1998). In a previous study on 232 tumour-affected dogs, ICT was the most common tumour (Grieco, et al., 2008).

The most important knowledge in veterinary medicine are from study of Volta, et al., (2014) that considered sedates dogs, 14 non-pathologic and 60 pathologic testes. They individuated as following: Forty testes were neoplastic (24 interstitial cell tumours, 9 seminomas, 7 Sertoli cell tumours), 20 were non-neoplastic (16 testicular degenerations, 2 chronic orchitis, 1 testicular atrophy, 1 interstitial cell hyperplasia). In healthy dogs, the contrast medium flow had a rapid homogeneous wash-in and wash-out, with a short peak phase. With contrast ultrasound, testes those were inhomogeneous with a hyperenhancing pattern were associated with neoplasia (sensitivity: 87.5%, specificity: 100%). Lesions with persistent inner vessels and a hypo- iso-echoic background were significantly associated with seminomas (sensitivity: 77.8%, specificity: 100%). Testes with non-neoplastic lesions were characterized by a scant/moderate homogeneous enhancement. Perfusion parameters were higher in neoplastic lesions.
The procedure followed, classified a lesion as hyperenhancing, if it was brighter than surrounding tissue either homogeneously or heterogeneously or with rim enhancement or with prominent inner vessels. A lesion was considered hyso-enhancing when it was no more visible during contrast ultrasound. A lesion was considered hypoenhancing when it was hypoechoic to the surrounding tissue.

Table 6.1 Testis tumours characteristics. Some lesion's characteristics on B-Mode and CEUS are showed according to Volta et al. (2014)

LESION	B-MODE AND DOPPLE	CEUS
Interstitial cell tumours (11 were classified as solid and 13 as angiomatous)	Solid interstitial cell tumours were either hypo or hyperechoic nodules Angiomatous interstitial cell tumours had a similar appearance, but two cases showed up as cystic-like nodular lesions	21 of the testes were inhomogeneous, with the focal lesions showing a hyperenhancing pattern (13 homogeneous, 5 heterogenous, 3 with rim enhancement), and 3 were inhomogeneous with the focal lesions showing a hypoenhancing pattern
Seminomas (7 were diffuse, while 2 were intratubular type)	Diffuse were hypoechoic solid nodules with thin hyperechoic striations Intratubular were not detected	Diffuse were inhomogeneous with the focal lesion showing a hypo-isoechoic background and several prominent inner vessels, which were still distinguishable in the wash-out phase Intratubular enhancement was homogeneous
Sertoli cell tumours (solid type)	nodules with different echogenicity, in two cases, they had hypoechoic cystic-like cavities	inhomogeneous with the focal lesions showing a hyperenhancing pattern (3 homogeneous, 3 heterogeneous and 1 with rim enhancement)
Degenerated testes	a normal or increased echogenicity, normal or reduced dimensions, and in two cases, several parenchymal hyperechoic foci were present, which histologically corresponded to small areas of fibrosis.	homogeneous pattern with an enhancement subjectively lower than non-pathologic tissue

Most of the testicular tumours were hyperenhancing to the surrounding tissue, when examined with contrast ultrasound. Prominent and persistent inner vessels within a hypoechoic background lesion were peculiar features of diffuse seminomas, which are not reported in humans. Interstitial cell and Sertoli cell tumours could not be differentiated with contrast ultrasound as most of them appeared as hyperenhanced lesions, which were well visualized in the early wash-in phase. (Volta, et al., 2014)

Important knowledge derives from human medicine such as an important evaluation of testis by Cantisani, et al., (2015). Ultrasonography is the imaging modality of choice for examination of the scrotum but to differentiate between hypovascular and avascular lesions, for instance, may be difficult at colour Doppler interrogation. So, CEUS is extremely effective in assessing presence or lack of organ perfusion. In principle, it is able to detect and display echoes from individual bubbles, and therefore it is able to assess whether an organ or a lesion is completely avascular or not.
ICT being the most frequent histo-type. CEUS is valuable to distinguish between vascularized and avascular testicular lesions, characterization of the former as benign or malignant is challenging. In their experience, however, cystic tumours display vascularized regions after microbubble injection, while not neoplastic complex cysts do not. (Cantisani, et al., 2015)

The current understanding is that testicular tumours with a diameter of less than 1.5cm may not show flow on colour Doppler US and thus may be misinterpreted as a benign lesion, the purported hallmark of malignancy being an increase in vascularity. (Piscaglia, et al., 2012)

The objective of our research is to evaluate qualitative and quantitative perfusion with CEUS of a single type of tumour (ICT) in conscious dogs to exclude any influence of pharmacological agents on vascular flow.

ICT is related to the presence of single or multiple nodules inside the testicular parenchyma, detected by palpation, or often it is an incidental finding by screening

ultrasonography (Grieco, et al., 2008). Examination of the testis with B-mode and Doppler ultrasound also allows to describe and, if possible, to characterize focal lesions. A previous study described an inhomogeneous lesion with hyperenhancing pattern as an important feature in the diagnosis of testicular neoplasms, but only SEM was characterized by prominent and persistent inner vessels in a hypo-isoechoic background (Volta et al. 2014). All dogs in that study were sedated and cardiovascular system and consequently CEUS perfusion parameters may be or not strongly influenced by sedative drug administration (Restitutti, et al., 2013 - Leinonen, et al., 2011 - Stock, et al., 2014 - Rossi, et al., 2016).

6.2 Materials and Methods

The study was conducted, between February 2015 until March 2017, including dogs (n=30) with focal or diffuse testicular lesions found by palpation and/or by ultrasound (B-mode and Doppler) examination were selected; CEUS were performed only in subjects that presented testicular focal lesions. After orchiectomy, testes were submitted to histological evaluation and we recruited only dogs with histological diagnosis of ICT. Written informed owners consents were obtained. Prior to include in the study, a complete general physical examination, serum chemistry profile and complete blood cell count were performed.

Dogs were excluded if they had evidence of cardiac disease or a history of anaphylactic reactions to vaccines or other medications, to avoid adverse reactions due to the micro-bubble contrast agent. Informed owners consent was obtained.

Conventional ultrasonography and CEUS examinations were performed according to General Procedures (chapter 4).

Ultrasonographic assessments of testes masses included: size and shape, echo pattern (homogeneous or heterogeneous) and location. Testes masses having uniform echogenicity or mixed echogenicity with hyperechoic and hypoechoic areas were recorded as “homogeneous” or “heterogeneous”, respectively. Presence of rim or inner vessels was also evaluated by Colour Doppler evaluation.

CEUS examination was performed immediately following B-mode ultrasonography, using a linear (5.0-7.5-MHz) transducer with contrast agent capability. The mechanical index (MI) was set from 0.08 at 0.09; a single focal zone was placed at the deepest part of the lesion.

The focal lesion in testis was classified in hyperenhancing (brighter than surrounding tissue either homogeneously or not homogeneously or with rim enhancement or with prominent inner vessels), isoenhancing (no more visible during contrast ultrasound) or hypoenhancing (hypoechoic to the surrounding tissue) compared to the surrounding testes tissue, as described by Volta et al. (2014).

Post processing quantitative analysis of video-clips was performed by use of image-analysis software (*Qontrast*® , Bracco International Imaging, Milan S.p.A.®). For each dog, one Region Of Interest (ROI) was manually drawn around the entire tumour; a second ROI, if possible, as large as the lesion’s ROI and at approximately the same depth, was drawn in the normal parenchyma.

Time Intensity Curves (TICs) were generated for each ROI. Analysis of tissue perfusion was based on video Signal Intensity (SI) changes over time using CEUS. The SI of a white band in the grey scale bar (8 bit) was defined as maximal (100%). Other pixels in the image were then assigned SI values based on this reference. Within the selected ROI, during the period of enhancement, the following parameters were computed and considered: Peak Intensity (PI %), Time to Peak (TTP) measured from T0 (injection time), Mean Transit Time (MTT), Regional Blood Volume (RBV) and Regional Blood

Flow (RBF). Peak Intensity is defined as the percentage increase in SI - from 0 to 100 as maximal intensity - reached during transit of the contrast agent at a specific time point. The RBF is defined as the ratio between Regional Blood Volume (RBV: proportional to the area under the curve) and Mean Transit Time (MTT: the circulation time of contrast agent in the tissue/lesion/structure under investigation).
All data obtained were statistical described expressing as mean (M) ± standard deviation (SD) and ROI's data from lesion and surrounding tissue were compared with Student's t-test. Values were considered significant when $P < 0.05$ (*GraphPad InStat*®)

6.3 Results

There was one each Boxer, Cocker, two each German Shepard, Hound, and six mixed breeds. The age of the twelve enrolled dogs was 9,8 (±1,4) years (range: 7 to 12 y). Blood count and serum biochemistry were within normal range.
On 60 testes analysed, 20 presented focal lesions studied with CEUS and in 12 conscious dogs, confirmed histologically for ICT, the procedure was fine for qualitative and quantitative analysis. In all cases the procedure was well tolerated and no adverse effects were noted.
B-mode ultrasonography revealed for all twelve dogs the presence of a focal lesion of prevalent hyperechogenicity of the parenchyma, not prominent, sometimes with small anechoic areas inside, and with diameter around 1cm; Colour Doppler showed a prominent vascularization of this lesions with inner vessels.
Contrast-enhanced ultrasound showed the wash-in around 25-30 seconds, at the same time of surrounding tissue: lesions were hyperenhancing and inhomogeneous with rim enhance, prominent inner vessels inside, but also with no enhancement of small parts, corresponding to the anechoic areas detected in B-mode. (Figure 6.1)
Mean PI% in lesions was 12.8 +/- 9 and in non-pathologic tissue was 6,4 +/- 4,3. Mean RBV in lesions was 748 +/- 417 and in non-pathologic tissue was 357 +/- 263. Mean RBF in lesions was 12.68 +/- 10 (range 2-33) and 6 +/- 4.7 (range 2-20) in surrounding tissue. Mean TTP in lesions was 44 +/- 11 (range 25-62) and 44 +/- 10.8 (range 33-62) in surrounding tissue. Mean MTT in lesions was 54.94 +/- 15.59 (range 32-77) and 51.73 +/- 13.56 (range 38-85) in surrounding tissue. Quantitative analysis provides significantly higher PI% (P=0.005), RBV (P=0.02) and RBF (P=0.007) in lesions than surrounding tissue; no differences were found for TTP and MTT. (Figure 6.2)

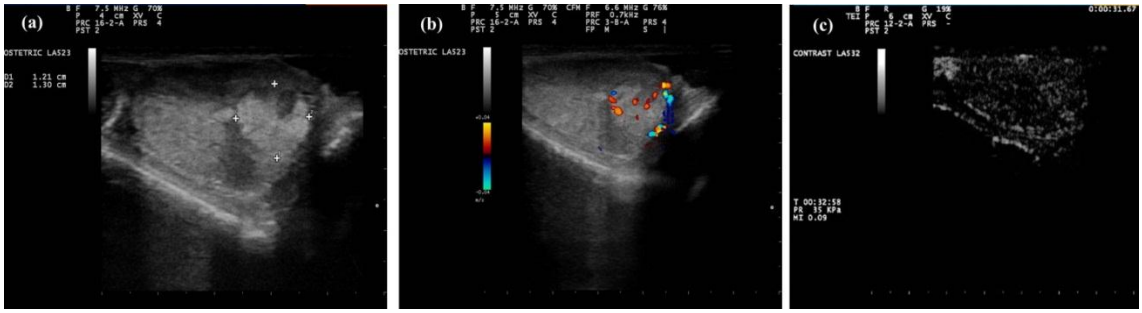

Figure 6.1 CEUS appearance of ICT on clinical case n°1. B-mode image of left testicle with a nodular lesion hyper-echoic, with dimension of 1.21X1.30cm of diameter (a). Lesion was vascularized on Doppler US (b). CEUS show a vascularized lesion almost hyso- hyper- enhancement to surrounding tissue at 13 seconds after injection of contrast medium (c).

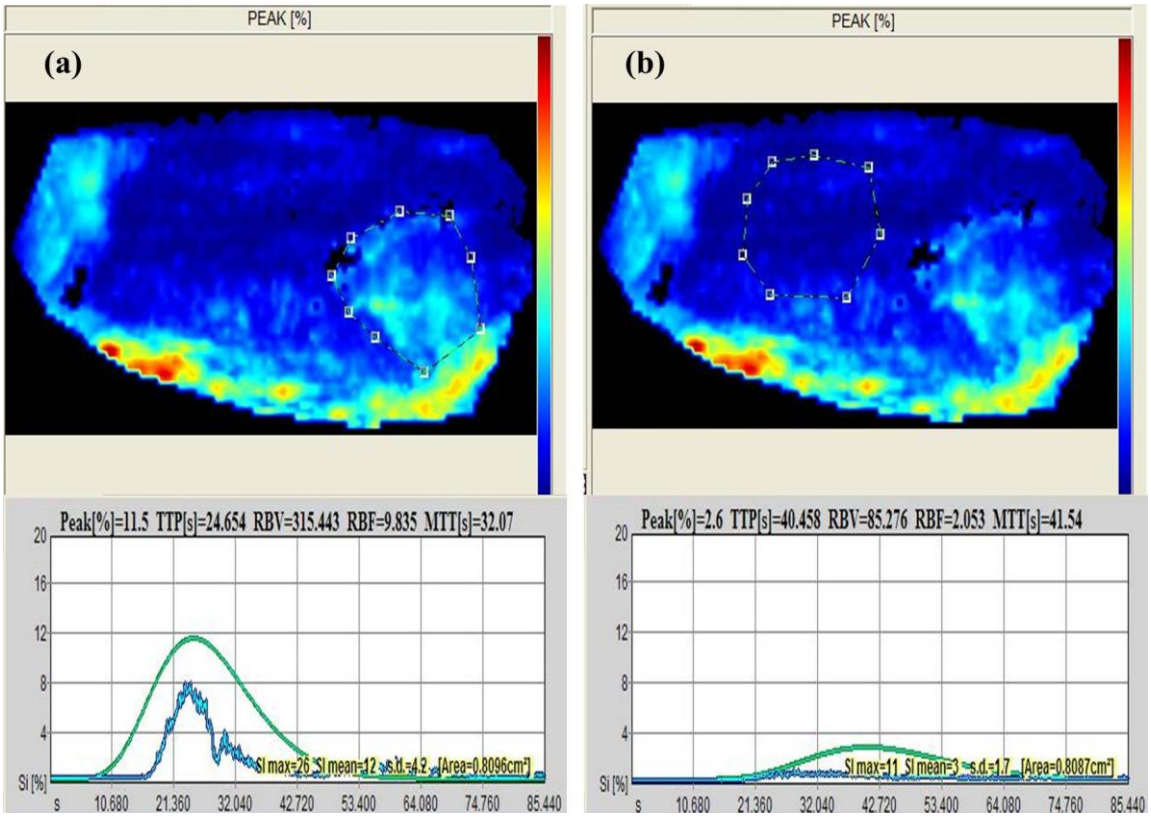

Figure 6.2 Quantitative analysis of ICT(clinical case 1). Quantitative analysis of CEUS using Qontrast®. Two ROI were designed: one in lesion (a) and one in normal tissue (b), different data were obtained generating TICs.

Table 6.2 Quantitative data obtained with *Qontrast*®. All quantitative data obtained from quantitative analysis of CEUS of ICT were summary in this table, including Mean, Standard deviation (SD), Maximum (Max) and Minimum (Min) value. For each clinical case were showed data for lesion (L) and normal (N) tissue.

CASE	PEAK L	PEAK N	TTP L	TTP N	RBV L	RBV N	RBF L	RBF N	MTT L	MTT N
1	11,5	2,6	25	40	315	85	9,835	2,053	32,07	41,54
2	13,2	7,5	38	36	494,42	266	11	6	44,48	43,72
3	9,7	5,1	62	53	799	243,31	10	4	76,81	60,46
4	30,8	8,2	43	34	2338,528	445	33	9	70,51	50,09
5	8,9	5,3	50	59	424	315	8	5	50,64	60,07
6	3,9	3,8	41	36	145	121	3	3	43,61	39,5
7	11	2,3	25	41	324	69	10	2	33,97	41,8
8	13,5	7,6	39	35	511	264	11	6	44,97	43,18
9	8,9	5,2	58	45	680	355,44	9	6	71,92	58,69
10	30,6	18,9	43	59	2.330	1.667	33	20	70,56	84,56
11	9,1	6,2	51	62	501	311	11	7	65,2	59,55
12	2,4	4,6	55	33	109	142	2	4	54,6	37,67
MEAN	12,79167	6,441667	44	44	748	357	12,67817	6,15675	54,945	51,73583
SD	8,982352	4,345836	11,79211	10,8813	766,4542	428,1922	9,99552	4,769916	15,5997	13,56071
MAX	30,8	18,9	62	62	2.339	1.667	33	20	77	85
MIN	2,4	2,3	25	33	109	69	2	2	32	38

6.4 Discussion

In human medicine, CEUS helps to differentiate ICT from other testicular tumours, particularly for earlier and higher enhancement related to Seminoma (Cantisani, et al., 2015). The first study in dogs reveals hyperenhancing and heterogeneous lesions, with rim enhancement or inner vessels, both in ICT that in SCT (Volta, et al., 2014).
Also in our study, a perfusion pattern of hyperenhancement was similar in focal lesions of ICT and rim enhancement, prominent inner vessels and no enhanced small parts were evident.
Mean peak intensity (PI%) is lowest than mean values reported for various neoplasms by Volta, et al., (2014), however, perfusion parameters of ICT lesions were significantly higher than the healthy parenchyma as in that study, suggesting hyper-vascularization of neoplastic tissue.
Mechanical Index, that we used, was lower than that used (max 0.15) by Volta et al. (2014), so this could be one of the factors responsible for the lower PI value. A low mechanical index (0.08-0.09) was chosen to minimize microbubble disruption and allow accumulation of microbubbles in the microvasculature, which has been suggested to avoid variability in clinical applications of CEUS. Again, considering that the entire testes were only 3-4 cm of depth, a low MI is necessary to obtain a diagnostic image quality avoiding pitfalls concerning the insonation power (Dietrich, et al., 2011). Experimentally, using *SonoVue*®, was found an increase of about 50% of signal intensity from an MI of 0.05 to 0.1 (Tang, et al., 2011).
Among the benefits of using contrast-enhanced ultrasound as a potential diagnostic method in veterinary medicine there is the not obligation to perform anaesthesia, but in uncooperative patients sedative drug administration is necessary. The action of dexmedetomidine implies a decrease of the PI in the renal cortex but not in the spleen, liver and intestines according with Restitutti et al. (2013); conversely, Rossi et al. (2016) observe a significant reduction of splenic enhancement with dexmedetomidine and contraindicate the use as sedatives for splenic CEUS procedures in dog; administration of butorphanol as sedative agent without following anaesthesia does not modify perfusion of the spleen. Pharmacologic features of butorphanol show systemic analgesia without significant changes on myocardial contractility and vascular tone, while medetomidine gives a reduced perfusion in peripheral organs (Pawson, 2008). In this study, ICT showed in conscious non-sedated dogs a similar CEUS pattern to that described in dogs after medetomidine (10 µg/kg) and butorphanol (0.2 mg/kg) intramuscularly administration. The lower peak intensity and RBF in awake dogs could be related to technical or methodology differences of the two studies but not speculated through the known pharmacologic action of the sedatives used in the recent study (Volta, et al., 2014).
In conclusion, CEUS seems to be a feasible imaging technique also in not sedated dogs with ICT, the testis had hyperenhancing pattern whit rim or inner vessels.
Further studies about contrast enhanced ultrasound on canine testicular tumours, including a larger number of animals, are needed to standardize technical variability.

--SPECIAL SECTION TWO: OTHER APPLICATIONS---

7 Liver

The liver is the largest gland in the body.
The porta of the liver is the hilus of the organ. The hepatic vessels and nerves and the hepatic ducts
communicate with the gland through the porta. The nerves and arteries enter the porta dorsally, the hepatic ducts leave ventrally, and the portal vein enters between the two of them. It is located on the dorsal third of the visceral surface, ventrodextral to the attachment of the papillary process.
Vessels structure include, in the centres of the lobules, the single central veins. Adjacent central veins fuse to form the interlobular veins. The interlobular veins unite with each other to form finally the hepatic veins, which empty into the CVC.
The portal vein brings the functional blood to the liver from the stomach, intestines, pancreas, and spleen.
In the fetal pup there is a shunt from the umbilical vein to the hepatic venous system, known as the ductus venosus, that become fibrous. (Evans & De Lahunta, 2013, p. 327-331)

The US evaluation of the liver must include several parameters: size and borders, parenchymal echogenicity, vascularization, ultrasound-beam attenuation, as well as the distribution of abnormalities.
The ultrasonography vasculature of liver includes a dual afferent vascular flow, with a larger proportion coming from the PV and the rest coming from the hepatic arteries.
The efferent flow follows the hepatic veins into the CVC.
On B-mode, can be seen only the hepatic and PVs as anechoic, branching, smoothly tapering tubular structures. The walls of the PVs appear hyperechoic, regardless of the orientation of the ultrasonographic beam, facilitating their identification. However, the walls of the hepatic veins can also appear hyperechoic when the ultrasonographic beam is directed perpendicularly.
The use of colour Doppler facilitates the identification and distinction of hepatic vessels. (Penninck & D'Anjou, 2015, p. 183-212)

According to EFSUMB recommendation giving first indication for CEUS about focal liver lesions, CEUS of the liver permits clear improvements in the characterization and detection when compared to unenhanced US, based on characteristic enhancement patterns throughout the vascular phases.
Tissue enhancement resulting exclusively from the hepatic artery supply usually starts from 10–20 seconds post-injection into a peripheral vein and lasts for approximately 10–15 seconds.
This is followed by the portal venous phase which usually lasts until 2 minutes after UCA injection. The late phase lasts until the clearance of the US contrast agent from the hepatic parenchyma,
up to approximately 4–6 minutes post injection for *SonoVue*® and 15 to 20 minutes for *Levovist*® (sinusoid pooling and RES/Kupffer cells uptake).
The arterial phase provides information on the degree and pattern of vascularity. The portal and late phase provide information about the wash out of UCA from the lesion compared to normal liver tissue.
Benign solid lesions are characterized by persistence of contrast enhancement during the portal-venous and late phase and can be further characterized by enhancement

patterns during the arterial phase, (e. g. enhancement of the whole lesion (focal nodular hyperplasia, adenoma) or initial peripheral globular-nodular enhancement).
Malignant lesions are characterized by wash out of microbubbles during the portal and late phase.
CEUS is indicated in all patients with uncertain liver lesions, particularly including the following clinical situations: incidental findings on routine US, lesions or suspected lesion in chronic hepatitis or liver cirrhosis, lesions or suspected lesion in patient with a known history of malignancy, patient with inconclusive MRI/CT or cytology/histology results. (Albrecht, et al., 2004, p. 249-256)

In 2003 were studied, with *Definity*®, eight adult dogs with no evidence of liver disease giving baseline data those may prove useful in the evaluation of dogs with diffuse hepatic disease: data acquisition and analysis from constant rate infusions were more cumbersome than for bolus, and results were less repeatable. (Ziegler, et al., 2003)

O'Brien, et al., (2004) studied thirty-two dogs with spontaneous hepatic nodules with *Definity*® or *SonoVue*®. There was improved conspicuity of malignant nodules after contrast enhancement compared with conventional imaging and increased numbers of malignant nodules were often noted. There was decreased conspicuity of benign nodules and no additional nodules were seen after contrast enhancement.
The results indicate improved conspicuity of malignant masses compared with normal liver. All malignant masses were hypoechoic compared with the surrounding liver at peak normal liver enhancement. Benign lesions had decreased conspicuity during contrast enhancement and, except for one nodule, were uniformly isoechoic to the surrounding normal contrast-enhanced liver.
Metastatic hemangiosarcoma is very conspicuous as it remains distinctly hypoechoic throughout the enhancement of the surrounding normal liver. (O'Brien, et al., 2004)

In a study of 2005, 11 healthy dogs with CEUS were individuating reproducible liver perfusion data and *SonoVue*® like safe and well tolerated agent for use in dogs.
They differentiated *SonoVue*® from *Imagent*® and *Definity*® using the time–intensity curves to compare the effects of administration rate, bolus vs. continuous rate infusion: they report a faster time to peak enhancement for their bolus injection curves than studied with *SonoVue*®, because other contrast agents are not strict blood pool agents but may be taken up by the RES of the liver and may therefore be concentrated in the liver for a longer period of time than strict blood pool agents. (Nyman, et al., 2005)

The perfusion of liver in normal dogs has been described (Ziegler, et al., 2003 - Nyman, et al., 2005). The mean time to peak perfusion (TTP) varied from 22.9 to 46.3 s and the variability may be related to dose of contrast, agent used, injection protocol and various machine settings. Additional variables include patient size and age: evidence indicates that portal circulation (TTP) is faster in smaller and younger patients.
The diagnosis of malignancy of hepatic nodules is very challenging. There is no specific echo pattern for either benign or malignant nodules except epithelial cysts. (Ohlerth & OBrien, 2007)

The results from a human study confirm the excellent performance of real-time contrast-enhanced ultrasound for focal liver lesion characterization which is clearly superior to that of unenhanced ultrasound. Furthermore, this study demonstrates, that the diagnostic accuracy of *SonoVue*®-enhanced ultrasound is even better than that of contrast-enhanced CT and MRI.

For the diagnosis of benign lesions correct diagnosis is the only issue since usually no further activities are required. (Trillaud, et al., 2009)

A human review of 2009 summarizes the characteristics of liver lesions including haemangioma, focal nodular hyperplasia, hepatic adenoma, complex cyst, hepatocellular carcinoma, metastasis, as in the following table. (Jang, et al., 2009)

Table 7.1 Lesions of liver. Some lesions characteristics of CEUS according to Jang, Yu, & Kim, (2009).

LESION	CEUS FINDINGS
Haemangioma	in the arterial phase, usually it demonstrates strong, nodular enhancement at the periphery of the lesion. The pools of enhancement expand in a centripetal pattern during the portal venous phase and beyond, progressing to complete fill-in of the lesion except areas of thrombosis or fibrosis. Sustained enhancement through the portal venous phase and beyond is a prerequisite for confident diagnosis. The rapidity of enhancement of haemangioma varies greatly. Focal nodular hyperplasia is proliferation of non-neoplastic hepatocytes with an abnormal arrangement and is frequently associated with a central fibrous scar and anomalous arteries.
Focal nodular hyperplasia	strong, brisk, homogeneous enhancement in the arterial phase. CEUS frequently demonstrates central stellate arteries in the early arterial phase, and the direction of intratumoral enhancement is typically centrifugal, from the centre to the periphery over time. Recognition of initial arterial vascular morphology and sustained enhancement of periphery is important for the correct diagnosis of focal nodular hyperplasia.
Hepatic adenoma	homogeneous arterial enhancement. A large lesion can show heterogeneous enhancement. Intratumoral not-enhancing areas which may represent necrosis or haemorrhage are occasionally seen and may be mistaken as a central scar of focal nodular hyperplasia if they are central in location. Adenomas usually show sustained enhancement in the portal venous phase, but occasionally show mild washout more commonly than focal nodular hyperplasia. Careful observation of the early arterial phase filling pattern is important to characterize these masses; adenoma typically shows peritumoral arteries with centripetal or diffuse filling of Intratumoral enhancement, in contrast to a central stellate artery with centrifugal filling of focal nodular hyperplasia. Neoplastic cysts and cystic metastasis or biliary cystic neoplasm: vascular flow within the septa or solid component.
Non-neoplastic complex cysts and haemorrhagic cysts or hydatid-cysts	show the absence of intralesional enhancement.
Hepatocellular carcinoma	The majority of moderately differentiated Hepatocellular carcinomas show classic enhancement features of arterial phase hypervascularity and later washout; well-differentiated and poorly differentiated Hepatocellular carcinomas account for the majority of iso- or hypovascular variations of enhancement. Absence of portal venous washout is rare in advanced Hepatocellular carcinomas. However, lack of washout should not be considered diagnostic of a benign lesion in a cirrhotic liver since approximately half of well-differentiated tumours fail to show washout. Arterial hypervascularity alone raises a high suspicion of Hepatocellular carcinoma in the setting of cirrhosis.
Regenerative and dysplastic nodules	Generally, show no hypervascularity in the arterial phase. They are usually isoechoic to the parenchyma during all phases on CEUS with or without transient arterial hypovascularity. They may show mild negative enhancement during the portal venous phase. However, increasing hypoechogenicity, or progressive washout, in the portal venous phase even in the absence of prior arterial hypervascularity is a highly suspicious finding for Hepatocellular carcinoma.
Peripheral cholangiocarcinoma	has enhancement pattern on imaging similar to metastatic adenocarcinomas as is the microscopic morphology. It shows rapid and complete washout within 60 s regardless of arterial phase vascularity
Metastases	show very brief arterial enhancement, peripheral or diffuse, followed by rapid washout in the early portal phase. The mean peak enhancement of metastasis on CEUS is reported at 15 s delay and washout commences earlier than 25 s delay after the bolus injection. As virtually all metastases show early complete washout and are seen as punched out defects contrasted with the well-perfused background liver on CEUS, liver survey during portal venous phase is very effective for the detection of additional small metastases which may not be on unenhanced ultrasound or prior imaging.

According to Nakamura, et al., (2010), *Sonazoid*®, contrast agent, should be used for liver CEUS to differentiate between malignant tumours and benign nodules with high accuracy.

In normal dogs, *Sonazoid*® led to enhanced signal from the portal vein and hepatic parenchyma immediately after injection. Uniform contrast enhancement was maintained for at least 30 min in the liver parenchyma. The signal intensity from the portal vein was the highest at 1 min after injection and then enhancement of the portal vein decreased gradually and disappeared at 7min after injection. So, they defined the portal phase as 1min after injection and the parenchymal phase as 7–30 min after injection. Hepatic

arteries were too thin to evaluate. They defined the arterial phase as the moment when the echogenicity of the portal vein started to rise. In clinical patients, malignant nodules were clearly filling defects following *Sonazoid*® injection. Parenchymal enhancement in rat liver following *Sonazoid*® injection is due to the distribution of the microbubbles in the Kupffer cells and not in the sinusoids. The filling defect during the parenchymal phase created by the malignant nodule is then due to a decrease in the number of Kupffer cells. Arterial imaging was also useful to differentiate between malignant and benign lesions. In the present study, nodular hyperplasia was isoechoic and hepatocellular carcinoma was hyperechoic during the arterial phase. On the other hand, all haemangiosarcomas were hypoechoic during all three phases. In this study, hepatocellular carcinoma had a branching vasculature pattern.(Nakamura, et al., 2010)

In a human medicine case report, CEUS of hepatic angiosarcoma metastasis showed findings comparable to those described for CT and MR imaging of primary liver angiosarcoma and hepatic soft tissue angiosarcoma metastasis. (Rauch, et al., 2014)

In a human medicine study of 2015 the authors used *SonoVue*®: they see a certain amount of microbubble left in liver after 5-6 minutes of low MI CEUS scanning.
According to this it was easier detect a specific "mosaic" or "nodule in nodule" sign on US post-CEUS than US pre-CEUS because the remaining microbubbles in blood pool enhanced the contrast of different histological structures or differentiated component of tumour immediately after CEUS. The tumour border, halo sign, and heterogeneous appearance were better displayed on US post-CEUS, which helped us to get accurate diagnosis.
In the analysis of the conventional US scanning before and after CEUS in 43 hepatic metastases, they found improvement of imaging characteristics including margin definition and contrast resolution. The clinical value of US post-CEUS in detecting small lesions and guiding biopsy or local treatment of the lesion. The main advantage of US post-CEUS lied in the improvement of visibility of lesion border and inner architecture: this information helped us to accurately diagnose haemangioma. The US post-CEUS optimized the display of tumour boundary and internal structures compared with conventional grey-scale US, thus providing additional information about pathological characteristic of liver lesions. (Yang, et al., 2015)

In a study of 2015 was used CEUS to investigate perfusion change to evaluate liver fibrosis based on biliary obstruction using an animal model**:** New Zealand white rabbits underwent bile duct ligation to form a biliary obstruction model and was performing CEUS attending that the peak signal intensity was association with liver fibrosis grades. (Shin, et al., 2015)

Guidelines indication from (Albrecht, et al., 2004) suggests that low MI contrast specific techniques allow dynamic imaging with subsequent evaluation of the three different vascular phases using a low solubility gas UCA.
The steps recommended in the investigational procedure are as follows:

1. Baseline investigation in B-Mode, potentially including colour and Doppler techniques
2. After identification of the target lesion(s) the transducer is kept in a stable position while the imaging mode is changed to low MI contrast specific imaging.
3. Adjust the MI setting to provide sufficient tissue cancellation with maintenance of adequate depth penetration. Major vascular structures and some anatomical landmarks like the diaphragm should remain barely visible.

4. UCA is administered as a bolus injection followed by a 5– 10 ml saline flush. The needle diameter should not be smaller than 20 Gauge to avoid loss of bubbles due to mechanical impact during injection. A stop clock should be started at time of UCA injection.
5. Continuous scanning for 60–90 seconds is recommended to continuously assess the arterial and portal-venous phase. For assessment of the late phase scanning may be used intermittently until the disappearance of the UCA from the liver microvasculature has been observed.
6. Because of the dynamic nature of real time CEUS, it is recommended to document the investigation on video or digital media.

High MI techniques in which microbubbles are deliberately destroyed are probably more useful for focal liver lesion detection but can be used for characterization. When required intermittent scanning of the lesion is performed during all 3 phases. (Albrecht, et al., 2004)

According to the human guidelines we performed CEUS as written in chapter 4: General Procedures.

Qualitative criteria adopted for interpretation of the results were:

- The arterial phase provides information on the degree and pattern of vascularity. The portal and late phase provide information about the wash out of UCA from the lesion compared to normal liver tissue. (Note: Guidelines for liver application - *SonoVue*® - human) (Albrecht, et al., 2004)
- Malignant masses: hypoechoic compared with the surrounding liver at peak normal liver enhancement.
  Benign lesions: decreased conspicuity during contrast enhancement and were uniformly isoechoic to the surrounding normal contrast-enhanced liver.
  Metastatic hemangiosarcoma: very conspicuous as it remains distinctly hypoechoic throughout the enhancement of the surrounding normal liver. (Note: *Definity*® - dogs) (O'Brien, et al., 2004)
- Arterial imaging was also useful to differentiate between malignant and benign lesions. Nodular hyperplasia: isoechoic during the arterial phase.
  Hepatocellular carcinoma: hyperechoic during the arterial phase and had a branching vasculature pattern.
  Hemangiosarcomas: hypoechoic during all three phases. (Note: *Sonazoid*® - dogs). (Nakamura, et al., 2010)

In our experience, some evaluation on liver were done and are included in the following Figures 7.1-7.2-7.3.

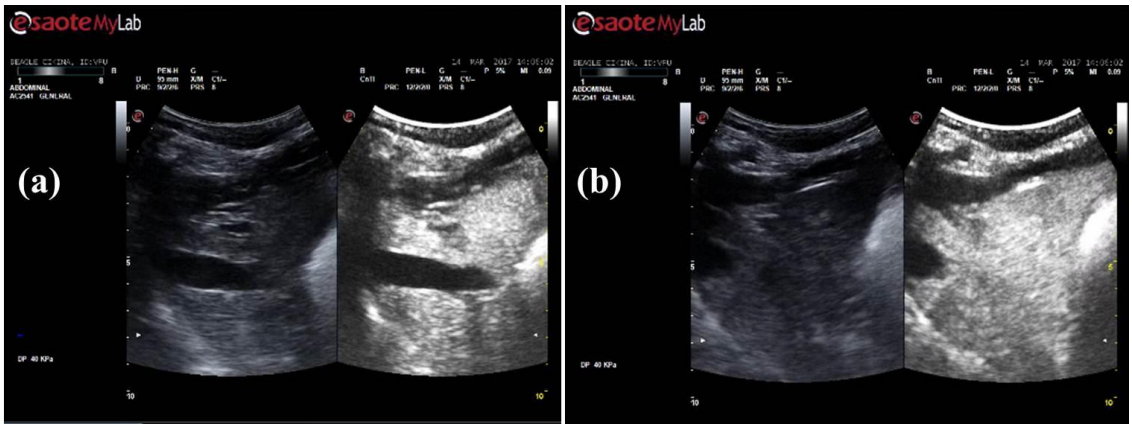

Figure 7.1 Physiological CEUS of liver. CEUS in physiological liver (a)(b): image example.

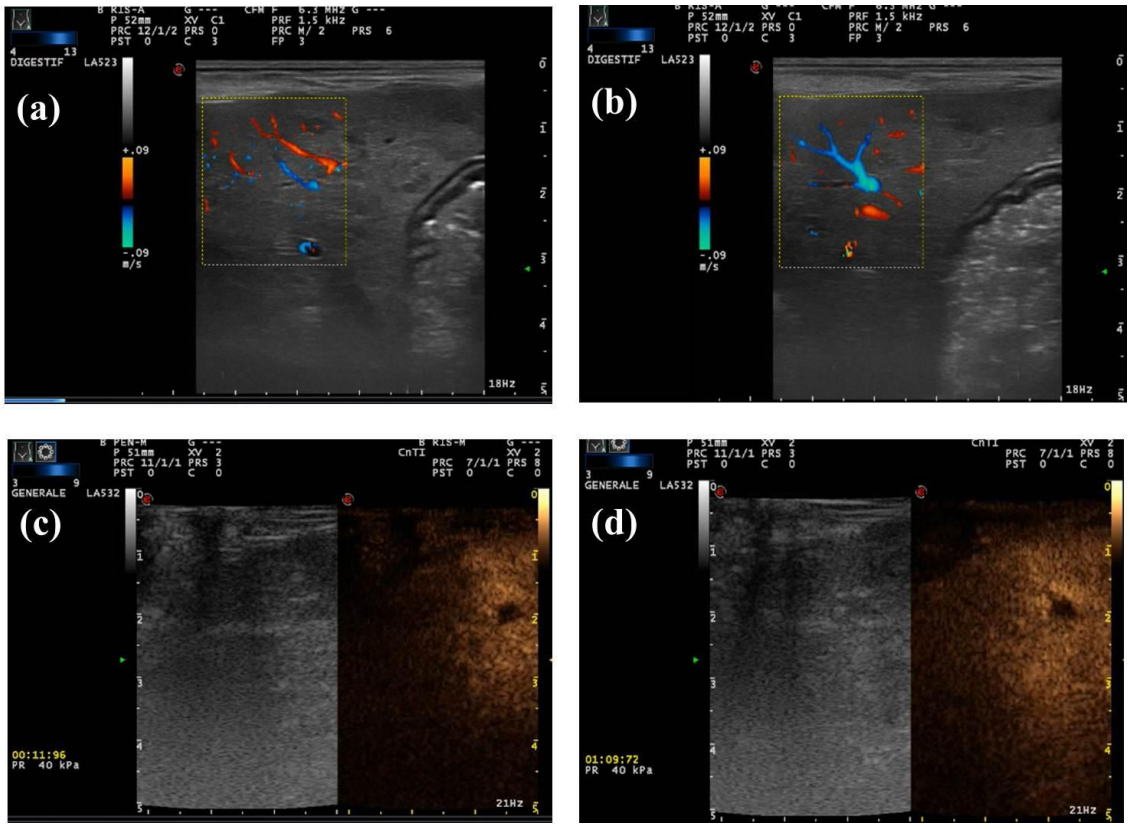

Figure 7.2 Benign lesion on liver. Benign evaluation of nodular diffuse lesion on Doppler (a)(b) and benign CEUS appearance in arterial phase (c) and late phase(d).

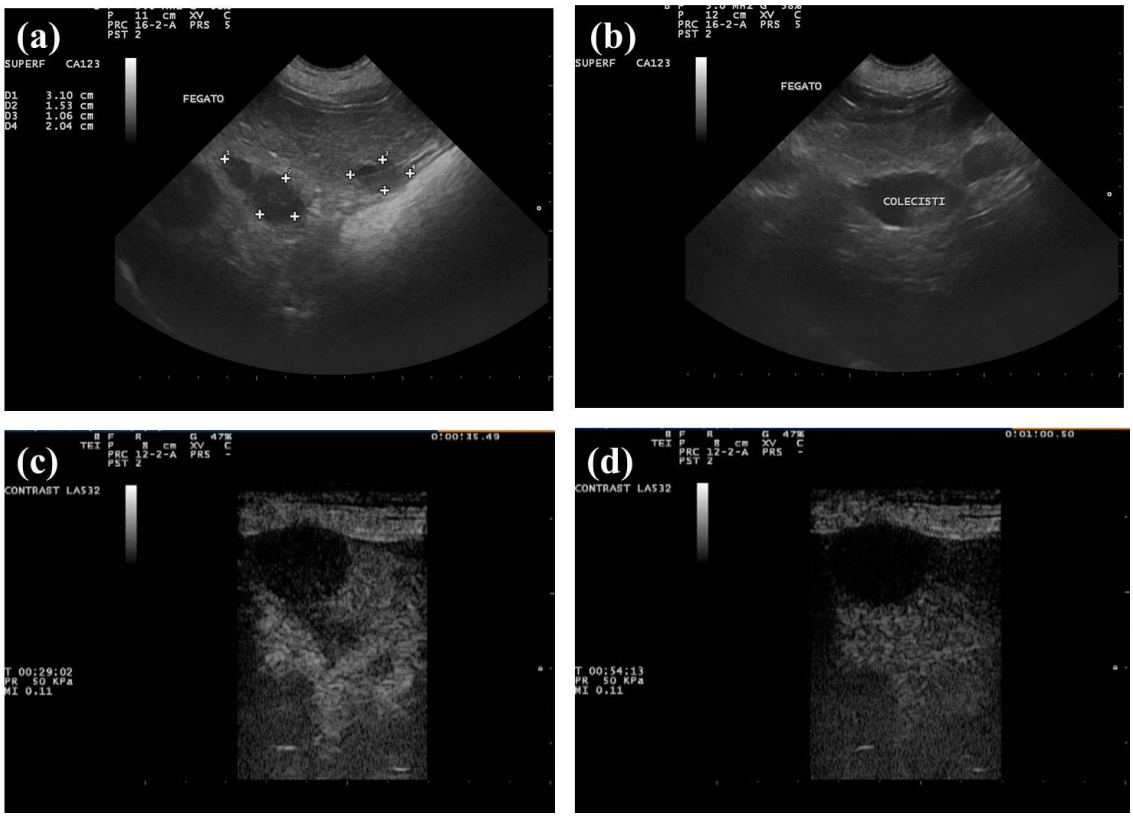

Figure 7.3 Histiocytic Sarcoma in liver. Multi-nodular lesions in liver seen on B-mode (a)(b) and having in CEUS a malignant appearance in portal phase(c) and late phase(d).

According to literature, the benign lesion showed decreased conspicuity during contrast enhancement and were uniformly isoechoic to the surrounding normal contrast-enhanced liver while in malignant case we had hypoechoic lesion compared with the surrounding liver for all three phases.
Useful application of CEUS were done that should be applied in daily clinical practice.

8 Gallbladder

The gallbladder stores and concentrates the bile. Vascularization of gallbladder depends from the hepatic artery. (Evans & De Lahunta, 2013, p. 331-332)

Some pathologies of GB have to be detected with US and basically evaluation have to be done about wall and content: presence of obstruction, inflammation, necrosis, presence of sludge, mucocele. (Penninck & D'Anjou, 2015, p. 213-223)

In our knowledge CEUS was used in dogs with a study of 44 patients that had intact wall underwent medical management and all achieved complete remission of signs. So, is supported the use of CEUS for surgical planning in dogs with suspected gallbladder necrosis/ rupture. (Bargellini, et al., 2016)

In human medicine in a metanalysis the authors identified that the sensitivity of CEUS for lesions of 1 cm or small was lower of that for lesions bigger of 1 cm, similar to the results from CT and MRI and is confirmed the use of CEUS for detecting gallbladder carcinoma. (Wang, et al., 2016)

CEUS can assessed the difference between tumours and sludge and polypoid changes on CEUS being in the arterial phase mainly. (Tsuji, et al., 2012)

Possible diagnosis on CEUS of wall correspond to biliary lithiasis, gallbladder polyp, part of the duodenal wall or wall collaterals. (Liu, et al., 2015 - Si, et al., 2013 - Tang, et al., 2013)

The definitive diagnosis of GB perforation is observation of a defect or “hole sign” in the GB wall. Because CEUS clearly depicts disruption of the GB wall at the site of perforation, in addition to any accompanying pericholecystic hepatic abscess, it may be more accurate than conventional US for the diagnosis of GB perforation. Therefore, CEUS may be the preferable imaging option for the initial evaluation of patients suspected to have GB perforation. (Tang, et al., 2013)

In human medicine were studied with CEUS some pathology including: Polypoid lesions, GB adenomas, GB sludge, Adenomyomatosis, Acute cholecystitis, GB malignant tumours, difference between benign and malignant lesions, summarized in Table 8.1. (Spârchez & Radu, 2012)

Table 8.1 Characteristics of some gallbladder lesions. Some gallbladder lesions are described according to human medicine (Spârchez & Radu, 2012)

LESION	CEUS FINDINGS
Polypoid lesions	On CEUS, hyper-enhancement most present during the early phase. Cholesterol polyps: dotted- or branched-type tumour vessels on CEUS with hypo- or iso- enhancement in the late phase.
Adenomas	during the early phase can appear homogeneous hyper-enhanced and isoenhanced while during the late phase they appear iso- and hypo-enhanced.
Sludge	the mass appears not- enhanced in all phases.
Adenomyomatosis	during arterial phase, the wall has characteristics moth-eaten enhanced while the not affected wall is normally enhanced.
Acute cholecystitis	On CEUS examination during the arterial phase, the enhancement of the wall will be seen earlier than the enhancement of the adjacent liver parenchyma. In the late phase, the thickened wall will have an obvious "wash-out" comparative with the liver parenchyma.
Gallbladder malignant tumours	On CEUS examination, the arterial branches that supply the gallbladder carcinoma tend to show irregularly tortuous extension. The late phase washout of the contrast agent within 35-60 seconds after administration may be a key for differential diagnosis. Improved gallbladder wall visualization following contrast administration and the malignant feature of late-phase hypovascularity relative to the hepatic parenchyma may provide sharp demarcation of tumour outline. Should be the disruption of the gallbladder wall integrity and On CEUS examination, in the arterial phase the wall disruption is better visualized.

In a study about comparisons between malignant and benign GB diseases there was significant difference between malignant and benign GB diseases in enhancement extent during the arterial phase. GB wall destruction beneath the lesions and liver infiltration were more often encountered in malignant GB diseases. (Liu, et al., 2012)

CEUS was performed according to chapter 4 General Procedures. Firstly visualized on B-mode and Doppler, after was performed CEUS.

Objective of our study about GB is to use CEUS in normal clinical practice to enhance the wall in case of sludge or some suspect of lesion.

The referral criteria, established, according to our literature research include:

- Only 2 phases can be followed: arterial phase (10–20 s after bolus injection) and late phase (31–180 s after contrast injection). The late phase persists for a short time in comparison with that for the liver. Enhancement is assessed by comparing the echogenicity of a lesion with the echogenicity of the liver parenchyma.

  Difference between benign and malignant lesions: In the arterial phase, most of the lesions are hyper-enhanced in the early phase of CEUS and no difference between them is detected. The benign lesions show dotted vessel enhancement whereas malignant lesions tortuous vessel enhancement. Although the late phase is important in establishing the nature of the hepatic lesion, for gallbladder this algorithm is not always applicable. The combination of enhancement pattern (hyperenhancement or iso-enhancement in the early phase with hypo-enhancement within 35 s after contrast agent administration) and lesion's size in diagnosing malignancy. (Note: *SonoVue*® - human) (Spârchez & Radu, 2012)
- Comparisons between malignant and benign diseases: The washout time for the malignant gallbladder diseases seams quicker than that for the benign. During the arterial phase, the intralesional blood vessels seam more often to be branched or linear in the malignant gallbladder diseases whereas dotted in the benign diseases. Homogeneous enhancement seam more easily to be found in benign gallbladder diseases whereas inhomogeneous enhancement in malignant gallbladder diseases. There was significant difference between malignant and

benign GB diseases in enhancement extent during the arterial phase (Note: *SonoVue*® - human) (Liu, et al., 2012)

- Necrosis/rupture: focal lack of enhancement of the gallbladder wall on CEUS. (Note: *SonoVue*® - dogs) (Bargellini, et al. 2016).

Our clinical practice had few cases of application of CEUS to GB, according to General Procedure (see chapter 4).

One example of application includes a clinical case of sludge, visible on B-mode and Doppler, with not vascularization. CEUS was performed: contrast agent enhances only the wall and still after 1 minute was visible the absence of content inside GB and a normal wall perfusion that means no presence of lesions and confirm sludge diagnosis (Figure 8.1).

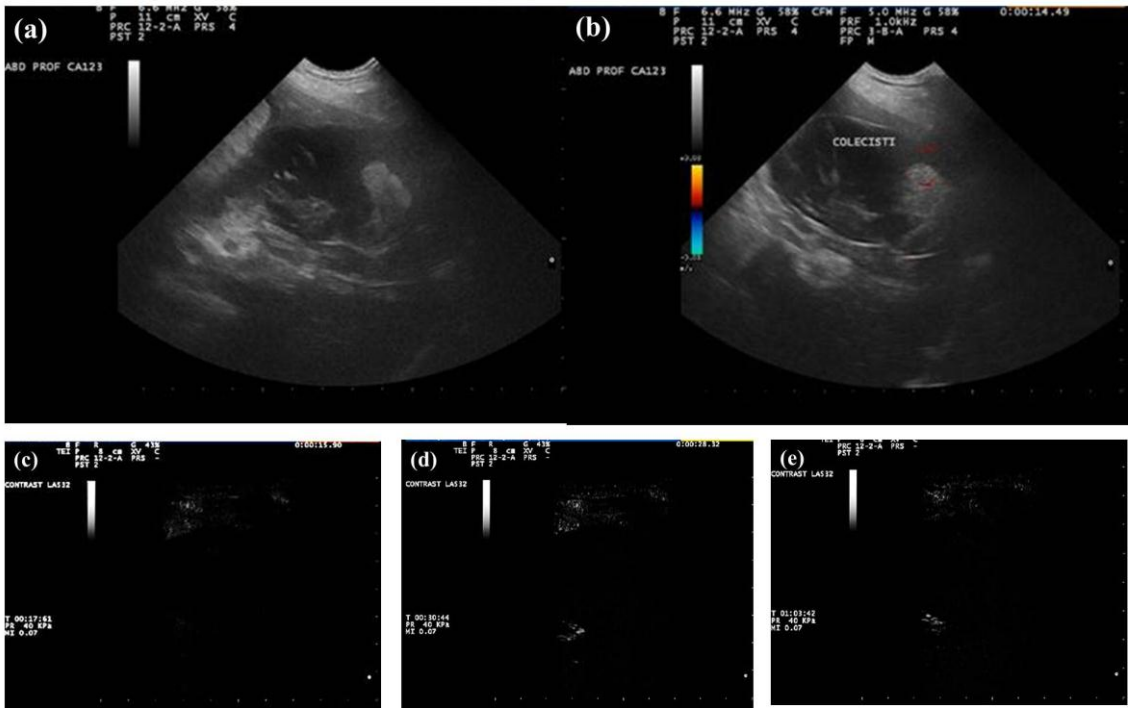

Figure 8.1 Sludge in gallbladder: CEUS evaluation. Clinical case of sludge, visible on B-mode (a) and Doppler (b), with not vascularization. CEUS was performed: wash-in time 17seconds (c), contrast enhances only the wall at 36seconds (d), still after 1 minute (e) is visible the absence of content inside GB and a normal wall perfusion that means no presence of lesions and confirm sludge diagnosis.

Clinical use of CEUS to evaluate GB alteration of content and wall should be a good, economically, easy to perform technique with no side effects.

9 Adrenal

Adrenal glands, organized in cortex and medulla, influence markedly the organism's response to both acute and chronic stress. The arterial supply of the adrenal gland arises from several major vessels. The branches from these vessels passing to the adrenal gland are numerous and of small calibre. They include cranial adrenal branches from the caudal phrenic and cranial abdominal arteries or their common trunk, middle adrenal branches from the abdominal aorta, caudal adrenal branches from the lumbar and renal arteries. These provide 20 to 30 contributing arterioles those approach the gland from all surfaces, enter the fibrous portion of the capsule, and anastomose to form a network. Numerous vessels plunge from the capsular network into the cortex.
The sinusoids of the cortex and medulla become confluent, as outlined previously, and join to form the large medullary sinuses and a plexus venosus medullae. The adrenal veins of each gland terminate differently because of their position relative to the CVC. The right adrenal vein joins directly with the CVC, but the left adrenal vein enters the left renal vein. There is also a well-developed lymphatic plexus surrounding the central vein of the medulla. (Evans & De Lahunta, 2013, p. 418-421)

With Basic- ultrasonography the normal adrenal glands are hypoechoic to the surrounding fat and well defined. They may also exhibit a thin hyperechoic rim running parallel to the capsule, representing the junction between cortex and medulla, or a more uniformly hyperechoic medulla.
The left gland has an elongated bilobed shape, frequently described as resembling a peanut.
The right adrenal gland has a more complex shape: its cranial pole is often folded or V-shaped, and is therefore more difficult to clearly visualize.
The phrenico-abdominal vein may be seen as two fine, hyperechoic parallel lines obliquely crossing the mid-body of the adrenal gland. The phrenico-abdominal vessels may be quite small and not seen on B-mode images, but blood flow can usually be seen with colour Doppler examination.
The sonographic appearance of adrenal nodules and masses is non-specific. The differential diagnosis for solid lesions includes cortical adenoma, cortical adenocarcinoma, pheochromocytoma, myelolipoma, metastasis, and hyperplasia. Adrenal nodules and masses vary in size and echogenicity. Ultrasound represents a good screening tool for identifying invasion of the caudal vena cava. "Incidentalomas" are adrenal nodules and small masses and have become more common incidental findings, cause no clinical signs, and a diagnosis is never confirmed. (Penninck & D'Anjou, 2015, p. 387-391)

In human medicine, no one CEUS criteria that can reliably differentiate between benign (endocrine tumours and adenomas) and malignant adrenal masses are known and indeed (Piscaglia, et al., 2012), the specificity of CEUS in the diagnosis of malignant adrenal masses was low (70%), but however, use of CEUS, considered a big tool for malignant differentiation. (Friedrich-Rust, et al., 2011)
Malignant adrenal tumours may infiltrate and occlude the adrenal vein. The vascularity of a tumour thrombus can be shown by UCA and thus its character be demonstrated. CEUS may demonstrate characteristic hypervascularity of some adrenal gland tumours, e. g. pheochromocytoma, which typically also have necrotic regions with no contrast enhancement. (Piscaglia, et al., 2012) (Dietrich, et al., 2010)

Bargellini et al. (2013) studied CEUS characteristics of adrenal glands in dogs with pituitary dependent hyperadrenocorticism giving an important contribute to literature.
In healthy dogs and during the initial wash-in phase, the adrenal vascularization pattern was characterized by the first appearance within the medulla of a central longitudinal vessel parallel to the major axis of the gland, approximately 8 s (range 7–12) after contrast agent injection. This was followed by perfusion of small vessels directed from the central artery to the periphery with a radial centrifugal distribution. During this latter phase, the US contrast agent was distributed homogeneously and with increased intensity from the medulla to the cortex of the adrenal glands. In the washout phase, there was a gradual and homogeneous decrease of the enhancement of the entire adrenal gland.
In dogs with PDH, regardless of adrenal gland dimensions, the CEUS examination demonstrated a rapid, chaotic, and simultaneous perfusion of US contrast agent into both the adrenal medulla and cortex. Three distinctive abnormal vascular patterns are summarized in the following Table 9.1. (Bargellini, et al., 2013)

Table 9.1. Vascular pattern of adrenals glands. Three types of vascular pattern are described according to Bargellini et al. (2013).

TYPE	DESCRIPTION
I	ACTH-stimulated cortisol levels below 24 μg/dl, case in which only the central longitudinal artery of the medulla was seen, but it was barely visible.
II	It was found in another group of ten dogs with ACTH-stimulated cortisol levels above 24 μg/dl, but in this case the perfusion of the adrenal gland by the contrast agent was so fast and disordered that the central longitudinal artery was not detectable, even in the initial wash-in stages.
III	was a nodular pattern characterized by the presence of abnormal vessels forming nodular lesions together with homogeneous, but chaotic enhancement of the contrast agent within the whole adrenal parenchyma similar to that of type II.

All PDH dogs were characterized by a uniform distribution of the contrast agent during the late wash-in phase and the entire gland became iso-enhanced, followed by slow and progressive washout, similar to that of the remaining adrenal parenchyma.
About quantitative CEUS parameters, within each group of clinically normal or PDH dogs, CEUS quantitative parameters did not differ between cortical and medullar ROIs but significant differences between control and PDH dogs were found in several parameters, such us Peak perfusion intensity in dogs with PDH was approximately twice ($P < 0.05$) that of controls (28.90 ± 10.36 vs. 48.47 ± 15.28, respectively), in dogs with PDH, the regional blood volume of the left adrenal medulla was almost fourfold ($P < 0.05$) greater than that of control dogs, the regional blood flow volumes of the left adrenal gland for both cortical and medulla ROIs were approximately twofold higher ($P < 0.05$) in dogs with PDH vs. those of clinically normal dogs, and, finally SI maximal and mean values, and the area under the curve were approximately twice as high ($P < 0.05$) in cortical and medulla regions of adrenal glands in dogs with PDH.
Contrast-enhanced ultrasonography represents a valuable alternative to invasive diagnostic procedures such as fine needle aspiration and core biopsy, as well as more expensive imaging techniques such as CT and MRI.
Based on this study, although limited in the number of cases examined, they proposed that CEUS should be considered in the diagnostic algorithm when it is necessary to confirm the presence of PDH, especially for dogs that have normal adrenal dimensions. (Bargellini, et al., 2013)

Important considerations about use of CEUS in case of adrenal masses were established by Bargellini, et al. (2016).

With simple B-mode evaluation the adrenal lesions were not precisely localizable within cortical or medullary region.
Adrenocortical adenomas had well-defined margins, while most adenocarcinomas showed nonhomogeneous parenchyma characterized by anechoic areas, hyperechoic spots, septa, and areas of different echogenicity defined margins. It should invade the surrounding tissue. Metastases were detected in surrounding renal and lumbar aortic lymph nodes of one dog and in the lung of another one.
The pheochromocytoma invaded the CVC and, in these cases, the diagnosis could be made by B-mode ultrasound.
In the dog with adrenal lipoma, ultrasound scanning characterized a well-defined mass in the caudal pole of left adrenal gland with hyperechoic margins and hypoechoic core; the adrenal surface was deformed by this mass, but there was no apparent invasion of surrounding tissues.
By using irregular adrenal margins of the lesions as the criteria, the B-mode accuracy in differentiating malignant versus benign tumours was 75%, with a sensitivity of 71.4% and a specificity of 80%. There were no statistical differences in the other qualitative ultrasound variables among the diagnosis groups or between benign and malignant adrenal lesions.
By performing CEUS all adenomas and adenocarcinomas had a reduced enhancement and all pheochromocytomas had an increased enhancement. About The distribution of the ultrasound contrast agent within the adrenal lesions was also different (P , 0.05), showing either homogenous, heterogeneous, or nodular patterns, depending on tumour type. In two adrenal adenomas, local perfusion defects were evidenced by the absence of contrast enhancement. Non-vascularized areas were identified in all adrenal adenocarcinomas and also in four pheochromocytomas.
In most adenomas, the enhancement arose simultaneously from different small arteries, which maintained a ramified but centripetal direction. The vascularization showed a disordered pattern in most adrenocortical adenocarcinomas and in all pheochromocytomas.
In addition, CEUS examination allowed a detailed view of those adrenal lesions that invaded the surrounding tissues and/or the CVC. In these latter cases, the microbubbles were clearly visualized in the arterial vessels of the pheochromocytoma
inside the CVC during the early wash-in phase; only later did they appear within the venous system, allowing the illumination of the entire CVC. Compared to the normal adrenal parenchyma, the perfusion pattern of all adrenal adenomas and adenocarcinomas was characterized by slow wash-in and fast wash-out phases, whereas that of pheochromocytomas had a slow wash-out phase, regardless of their size. The perfusion pattern of the lipoma was characterized by greatly reduced enhancement of the contrast agent during the different phases of its vascular distribution. During the arterial phase, two vessels entering the lesions from the periphery were visualized.
Their results indicate that this technique is useful in distinguishing between benign and malignant adrenal mass lesions, allowing the differential diagnosis between adrenocortical adenoma, adenocarcinoma, and pheochromocytoma.
The diagnostic accuracy of CEUS relies on specific vascularization patterns that characterize and distinguish between nodular hyperplasia, adrenocortical adenoma, adenocarcinoma, and other types of adrenal tumours, such as pheochromocytoma and lipoma. Wider application of CEUS in the diagnostic approach for the differentiation of adrenal lesions will likely reduce the number of dogs requiring unnecessary diagnostic procedures such as fine-needle aspiration and core biopsy and/or other imaging techniques such as CT and MRI without compromising accurate diagnosis. (Bargellini, et al., 2016)

To study adrenal CEUS can be performed following indications of chapter 4 General Procedures.

From literature, we are able to focalize some qualitative criteria for interpretation of the results:

- Healthy dogs: during the initial wash-in phase, the adrenal vascularization pattern was characterized by the first appearance within the medulla of a central longitudinal vessel parallel to the major axis of the gland, approximately 8 s (range 7–12) after contrast agent injection. This was followed by perfusion of small vessels directed from the central artery to the periphery with a radial centrifugal distribution. During this latter phase, the US contrast agent was distributed homogeneously and with increased intensity from the medulla to the cortex of the adrenal glands. In the washout phase, there was a gradual and homogeneous decrease of the enhancement of the entire adrenal gland. (Note: *SonoVue*® - dogs) (Bargellini et al 2013).
- Dogs with PDH: rapid, chaotic, and simultaneous perfusion of US contrast agent into both the adrenal medulla and cortex.
  Three distinctive abnormal vascular patterns could be discerned.
  The type I pattern corresponded to ACTH-stimulated cortisol levels below 24 μg/dl, case in which only the central longitudinal artery of the medulla was seen, but it was barely visible.
  The type II was found in another group of ten dogs with ACTH-stimulated cortisol levels above 24 μg/dl, but in this case the perfusion of the adrenal gland by the contrast agent was so fast and disordered that the central longitudinal artery was not detectable, even in the initial wash-in stages.
  The type III was a nodular pattern characterized by the presence of abnormal vessels forming nodular lesions together with homogeneous, but chaotic enhancement of the contrast agent within the whole adrenal parenchyma similar to that of type II.
  All PDH dogs were characterized by a uniform distribution of the contrast agent during the late wash-in phase and the entire gland became iso-enhanced, followed by slow and progressive washout, similar to that of the remaining adrenal parenchyma
  (Note: *SonoVue*® - dogs) (Bargellini et al 2013).
- Adenomas and adenocarcinomas: reduced enhancement
  Pheochromocytomas: increased enhancement.
  In two adrenal adenomas, local perfusion defects were evidenced by the absence of contrast enhancement. Non-vascularized areas were identified in all adrenal adenocarcinomas and also in four pheochromocytomas. In most adenomas, the enhancement arose simultaneously from different small arteries, which maintained a ramified but centripetal direction. The vascularization showed a disordered pattern in most adrenocortical adenocarcinomas and in all pheochromocytomas.
  Adrenal lesions that invaded the surrounding tissues and/or the CVC: the microbubbles were clearly visualized in the arterial vessels of the pheochromocytoma inside the CVC during the early wash-in phase; only later did they appear within the venous system, allowing the illumination of the entire CVC. Compared to the normal adrenal parenchyma, the perfusion pattern of all adrenal adenomas and adenocarcinomas was characterized by slow wash-in and fast wash-out phases, whereas that of pheochromocytomas had a slow wash-out

phase, regardless of their size. The perfusion pattern of the lipoma was characterized by greatly reduced enhancement of the contrast agent during the different phases of its vascular distribution. During the arterial phase, two vessels entering the lesions from the periphery were visualized. (Note: *SonoVue*® - dogs) (Bargellini, et al., 2016)

In our experience adrenal was used just for clinical applications with few cases (Figure 9.1).

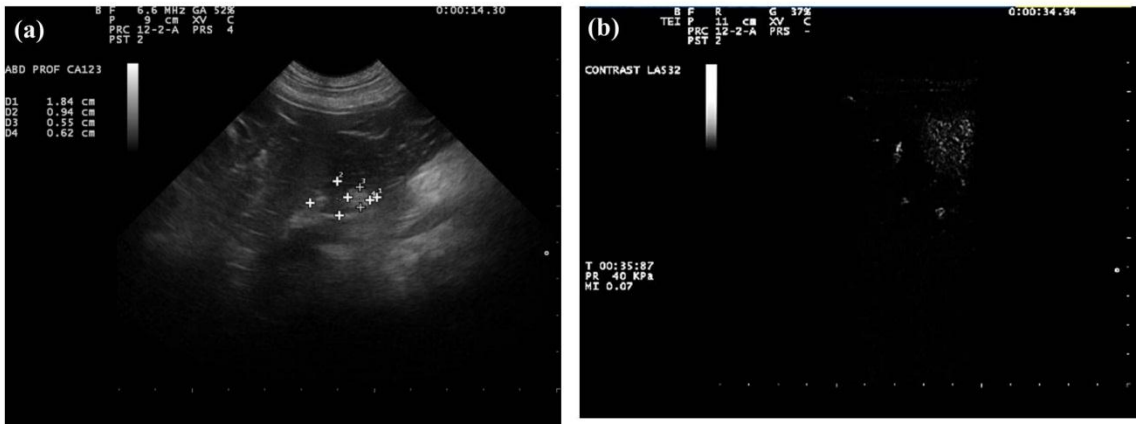

Figure 9.1 Clinical case of suspected PDH. On B-mode (a) is visible 1.84 longitudinal left adrenal with a hyperechoic nodule inside the hypoechoic structure. On CEUS (b) at 35 seconds is visible the structure with an hypoenhanced areas corresponded to a part of parenchymal adrenal.

CEUS better perform the evaluation of US add more information to B-mode and Doppler. The case is still in course of diagnosis. According to Bargellini, et al., (2013-2016) in this case there was a rapid, chaotic, and simultaneous perfusion of US contrast agent into both the adrenal medulla and cortex; a focal part individuated like hyperenhancement not exclude the possible presence of a nodular lesion.

Use of CEUS, following the established criteria, should be a good daily use to evaluate adrenals.

10 Gastro-enteric tract

CEUS technique give important information to use in gastro-enteric tract.

Firstly, it is important clarify the organization of vascularization in stomach and intestine in dogs (see following).
The main arteries to the stomach are the left and right gastric arteries, which run along the lesser curvature, and the left and right gastro-epiploic arteries, which run along the greater curvature. The larger left gastric artery anastomoses with the right gastric at the beginning of the pyloric antrum. The epiploic vessels anastomose with each other on the greater curvature of the body of the stomach. In addition to these arteries, two or more long branches leave the terminal part of
the splenic artery and supply a portion of the fundus of the stomach by short gastric arteries. The arterial branches that actually enter the musculature of the organ along the greater curvature run greater distances under the serosa and are more nearly vertical to the parent trunks than the comparable branches along the lesser curvature. The veins from the stomach are satellites of the arteries supplying the organ. The left gastric and left gastro- epiploic veins are tributaries of the splenic vein. The right gastric and right gastro-epiploic veins are tributaries of the gastro-duodenal vein. The blood from the stomach enters the liver through the portal vein.
The large middle portion of the small intestine, the jejunum, is supplied by 12 to 15 jejunal arteries, which are branches of the cranial mesenteric. The duodenal branches from both the cranial and caudal pancreatic-duodenal arteries supply the duodenum, the most proximal jejunal artery anastomosing with the most distal duodenal branch of the caudal pancreatico-duodenal artery. The ileum is supplied on its mesenteric side by ileal branches from the ileo-colic artery and on its anti-mesenteric side it is supplied by the anti-mesenteric ileal branches of the cecal artery. The main antimesenteric ileal branch runs in the areolar tissue, connecting the cecum to the ileum. Upon leaving the adhered area between the two viscera, it continues in the ileo-cecal fold along the whole ileum and anastomoses with the most distal jejunal artery in the musculature of the small intestine. From the terminal arcades that lie closely adjacent to the intestine the short, irregular vasa recti, upon reaching the intestine, run on the mesenteric half of the musculature and supply the submucosa and the mucosa. (Evans & De Lahunta, 2013, p. 318-323)

With US can be easily evaluated the wall thickness and layering, and relative motility of different segments of the GI tract The thickness of the GI tract can be measured by placing callipers on the outer aspect of the serosa and on the mucosal inner border. Abnormalities of wall and content con be focalized in B-mode and Doppler. (Penninck & D'Anjou, 2015, p. 259)

EFSUMB examination of Gastrointestinal tract provides that Higher contrast doses (e. g. 2.4 – 4.8 ml *SonoVue*®) should be used.
The arrival time in the intestinal capillaries is usually 10 – 20 sec after injection. Peak enhancement is reached after 30 – 40 sec and this arterial phase is followed by a venous phase that lasts from 30 to approximately 120 sec.
Before intravenously UCA administration, the intestines must be examined in B-mode and Doppler US to detect any pathology.
CEUS is indicated in the following clinical situations:
1. Estimation of disease activity in inflammatory bowel disease.
2. Discerning between fibrous and inflammatory strictures in Crohn’s disease.

3. Characterisation of suspected abscesses.
4. Confirming and following the route of fistulas. (Piscaglia, et al., 2012)

CEUS is gaining in popularity for the study of inflammatory bowel disease, particularly Crohn's disease in human medicine. The ability of CEUS to investigate bowel wall microcirculation has therefore generated great interest. Rapid wash-in and slow wash-out at CEUS were consistent with active disease at endoscopy and histological evaluation; on the contrary, slow wash-in and rapid wash-out indicated quiescent disease. Quantitative evaluation of enhancement proved useful to assess the response to medical therapy and to predict recurrence after medical therapy and surgery. (Cantisani, et al., 2015)

In our knowledge Nisa, et al. (2017) give some referral about CEUS in study of duodenal perfusion in healthy dogs studying six healthy beagles underwent CEUS three times within one day (4-hour intervals) and on two different days (1-week interval). All dogs were sedated with a combination of butorphanol (0.2 mg/kg) and midazolam (0.1 mg/kg) prior to CEUS using *Sonazoid*®.

We summarize some criteria to follow the interpretation of CEUS in GE tract.

- The arrival time in the intestinal capillaries is usually 10 – 20 sec after injection, particularly in the submucosal layer. Peak enhancement is reached after 30 – 40 sec and this arterial phase is followed by a venous phase that lasts from 30 to approximately 120 sec. (Note: *SonoVue*® - human)(Piscaglia, et al., 2012)
- If areas of a significant size close to or within an affected bowel wall are completely devoid of microbubble signals, these lesions likely represent abscesses rather than inflammatory infiltrates, particularly if adjacent tissue shows hyperenhancement. Similar findings also apply to abscesses caused by other diseases, e. g. diverticulitis. (Note: *SonoVue*® - human)(Piscaglia, et al., 2012)
- Acute disease: hyperenhancement.
  Wash-in and wash-out were defined as "rapid" when micro-bubbles filled the wall within 20 s after the injection, and when the reduction in enhancement occurred within 60–80 s, respectively. A "slow" wash-out was defined in case of persistent enhancement during the late phase (180 s). Rapid wash-in and slow wash-out at CEUS were consistent with active disease at endoscopy and histological evaluation; on the contrary, slow wash-in and rapid wash-out indicated quiescent disease. (Note: *SonoVue*® - human) (Cantisani, et al., 2015)

In our experience, we applied CEUS to study intestine wall in only two cases of thickening by chronic inflammatory bowel disease.

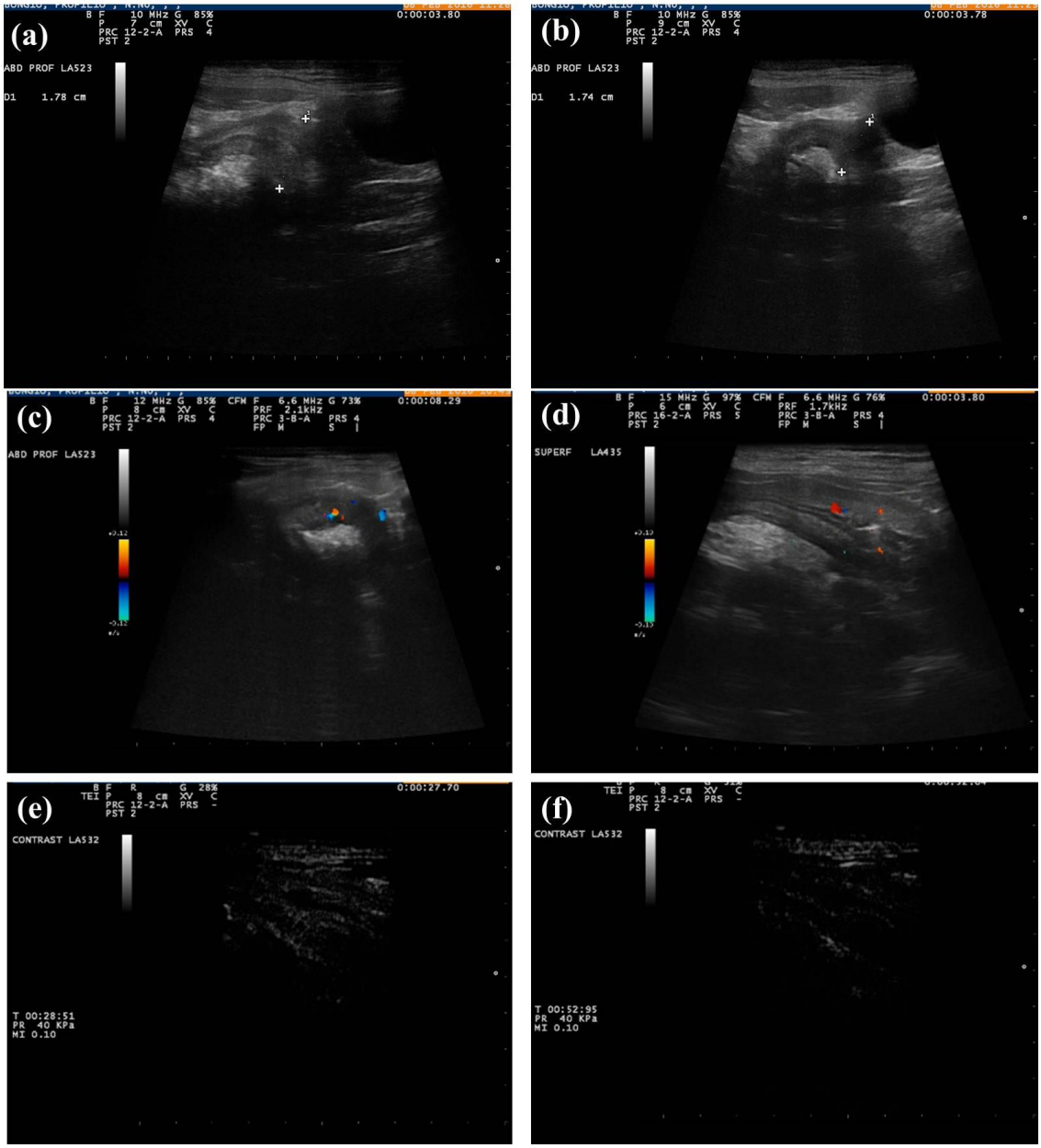

Figure 10.1 Thickening of enteric wall by chronic inflammatory bowel disease on CEUS. B-mode images of intestinal tract with thickening (a)(b) – Doppler evaluation of wall perfusion (c)(d) – CEUS of wall perfusion (e)(f).

Performing this clinical case, it is clear that CEUS can be a useful technique to evaluate some wall alteration.
Clinical examination was positive for colitis untreatable, after colonoscopy and biopsy the final diagnosis was a severe linpho-plasmocitic colitis.
On B-mode and Doppler was visible just the thickening of the bowel and visible perfusion.
On CEUS there was an hyperenhancement areas in bowel, thickening and homogeneous to the surrounding parts.
Few cases are studied and more needed to establish criteria for different lesions in dogs.

11 Ovary

The ovary, or female gonad, is a paired oval organ, attached by a mesovarium to the body wall and the mesosalpinx.
The ovary is supplied with blood through the ovarian artery. The ovarian artery arises from the aorta approximately one-third to one-half the distance from the renal arteries to the deep circumflex iliac arteries. Usually the right ovarian artery arises slightly cranial to the left. The degree of uterine development determines the tortuosity and size as well as the position of the artery. In a nulliparous animals the artery extends laterally almost at right angles from the aorta, whereas in late pregnancy it is drawn cranio-ventrally, along with the ovary, by the enlarged, heavy uterus. In addition, to supplying the ovary, the ovarian artery supplies branches to the adipose and fibrous capsules of the kidney. In addition, small tortuous branches supply the uterine tube and uterus. Caudally, the uterine branch of the ovarian artery anastomoses with the uterine artery, a branch of the vaginal artery (formerly urogenital artery). Through this anastomotic connection, the uterine artery may be considered as a supplementary source of arterial blood to the ovary. The arteries to the ovary supply the parenchyma of the medulla and cortex as well as the thecae of the follicles. Capillary loops become extensive during follicular enlargement but recede or disappear during corpus luteum regression.
The right and left ovarian veins have different terminations.
The right vein drains into the CVC, whereas the left enters the left renal vein. Similar to the corresponding arteries, the uterine vein and ovarian vein anastomose among the peritoneal layers of the broad ligament. The ovarian vein receives a tributary that comes from the medial edge of the suspensory ligament of the ovary and the lateral surface of the kidney. In some instances, the vein will also anastomose with the deep circumflex iliac vein. (Evans & De Lahunta, 2013, p. 387-390)

The US appearance of the ovary varies during the oestrus cycle.
On the day of ovulation , the contour of the ovary may be bumpy and a scant amount of fluid may be seen surrounding it. During oestrus the contour of the ovary remains bumpy, and fluid-filled corpora lutea may be seen (mean of three per ovary). Corpora lutea are 5–9mm diameter and tend to be thicker-walled and more variable in shape compared with preovulatory follicles. During dioestrus, the ovarian contour remains bumpy and size reduces. Around 10–14 days after ovulation, the corpora lutea appear solid and remain as such for the duration of dioestrus.
Ovarian cysts appear as anechoic, well-circumscribed, and thin-walled structures with distal enhancement. Hormonally inactive cysts arising from the ovarian bursa and hormone-producing follicular and luteinizing cysts cannot be differentiated through ultrasonography. Large follicles and corpora lutea may be confused with ovarian cysts and can only be ultrasonographically differentiated by serial ultrasound examinations. Follicles should not persist longer than 30 days and corpora lutea for no more than 60 days. The finding of fluid-filled structures associated with the ovary has to be interpreted in light of the clinical presentation when serial examinations are not being performed.
Ovarian tumours (epithelial tumours, sex-cord stromal tumours, and germ-cell tumours), which appear as nodules or masses of variable size and echogenicity, may have a cystic or mineral component.
Tumour types cannot be differentiated ultrasonographically, although teratomas and teratocarcinomas have the tendency to become very large and contain bone or mineral.
Common concurrent findings include ascites, pyometra, and cystic endometrial hyperplasia. (Penninck & D'Anjou, 2015, p. 403-406)

In human medicine, since 2010, they used CEUS to detect ovarian lesions: CEUS improved diagnostic confidence in the characterization of liquid-corpuscular lesions where conventional US is inconclusive. CEUS can be proposed as a valid alternative to CT and MR. However, information obtained by CEUS influences the therapy in a limited percentage of cases (24.6%). (Sconfienza, et al., 2010)

In a study of human medicine, they aimed at investigating the efficacy of CEUS in exploring the vascularity of the ovarian tumours or tumour-like lesions to assess the relationship between the parameters of the peak intensity and area under curve on CEUS and diameter in ovarian masses: their results showed clear differences in enhancement patterns between benign and malignant ovary tumours or tumour-like lesions.
In benign tumours or tumour-like lesions, CEUS ring-like enhancement was seen in cystic wall and/or papillae of the ovarian cyst and abscess, while solid tumours or tumour-like lesions showed either internal scattered mild enhancement or branching regular moderate low enhancement. In malignant tumours, CEUS showed overall heterogeneous enhancement or dendritic, rapidly increased enhancement. Peak intensity and area under curve were significantly higher in malignant tumours than those in the benign group, which suggested that malignant ovarian tumours were rich in blood perfusion. (Wang, et al., 2011)

Ovarian artery perfusion increases during ovulation. This change directs blood to the ovaries and increases intra-ovarian artery perfusion on the day after ovulation.
Doppler ultrasound has been widely used in female and the purpose is to provide information about the physiology of ovulation in this species; contribute to reproductive biotechnology, and provide an experimental model for wild canids.
Ovarian US and uterine and ovarian artery Doppler measurements are specifically altered during the peri-ovulatory phase. (Barbosa, et al., 2013)

In a study using fourteen German Shepherd bitches, monitored three times a week from the first day of cytological dioestrus until parturition or the end of dioestrus by colour Doppler, pulsed wave spectral Doppler, and power Doppler ultrasonography, the authors studied the relationship between hemodynamic changes in the ovary and luteal function in pregnant and not pregnant bitches.
The results of this study confirm the reliability of the Doppler ultrasound examination as a valuable, non-invasive diagnostic aid for monitoring ovarian vascularization in the pregnant and not pregnant dog. The use of PD for measuring intra-ovarian blood flow may represent an additional parameter to predict the luteal function together with those already employed. (Polisca, et al., 2013)

CEUS was evaluated in human medicine about the accuracy for differential diagnosis of benign and malignant ovarian tumours: the results revealed the high clinical value of CEUS in differential diagnosis of benign and malignant ovarian tumours. (Qiao, et al., 2015)

Criteria, according to literature that we suggest to follow include:

- Difference between malignant and benign lesions: malignant lesions were characterized by significantly higher peak enhancement intensity and significantly shorter peak enhancement times than benign tumours. This phenomenon might be related to the high velocity flow through the arterio-

venous shunts that are typical of malignant neovascularization and seems to be more pronounced in carcinomas, where the increased vascularization is thought to decrease the arrival time of the contrast agent (Note: *SonoVue*® - human) (Sconfienza, et al., 2010)

In benign tumours or tumour-like lesions, CEUS ring-like enhancement was seen in cystic wall and/or papillae of the ovarian cyst and abscess, while solid tumours or tumour-like lesions showed either internal scattered mild enhancement or branching regular moderate low enhancement. (Note: *SonoVue*® - human) (Wang, et al., 2011)

In malignant tumours, CEUS showed overall heterogeneous enhancement or dendritic, rapidly increased enhancement. PI and AUC were significantly higher in malignant tumours than those in the benign group, which suggested that malignant ovarian tumours were rich in blood perfusion. (Note: *SonoVue*® - human) (Wang, et al., 2011)

- Doppler ultrasonography: ovarian artery perfusion increases during ovulation. This change directs blood to the ovaries and increases intra-ovarian artery perfusion on the day after ovulation. (Note: dogs) (Barbosa, et al., 2013)

  Difference between follicles and corpora lutea on Doppler: appeared to follow the anechoic (preovulatory follicles) to hypoechoic (ovulated follicles) to anechoic (developing CL) pattern. y reported. (Note: dogs) (Bergeron, et al., 2013)

In our experience, we start to study ovary perfusion in oestrus time.
Vascularization of ovary should be increased during oestrus time, and for this we use CEUS to show micro-vascularization, like in the following example.

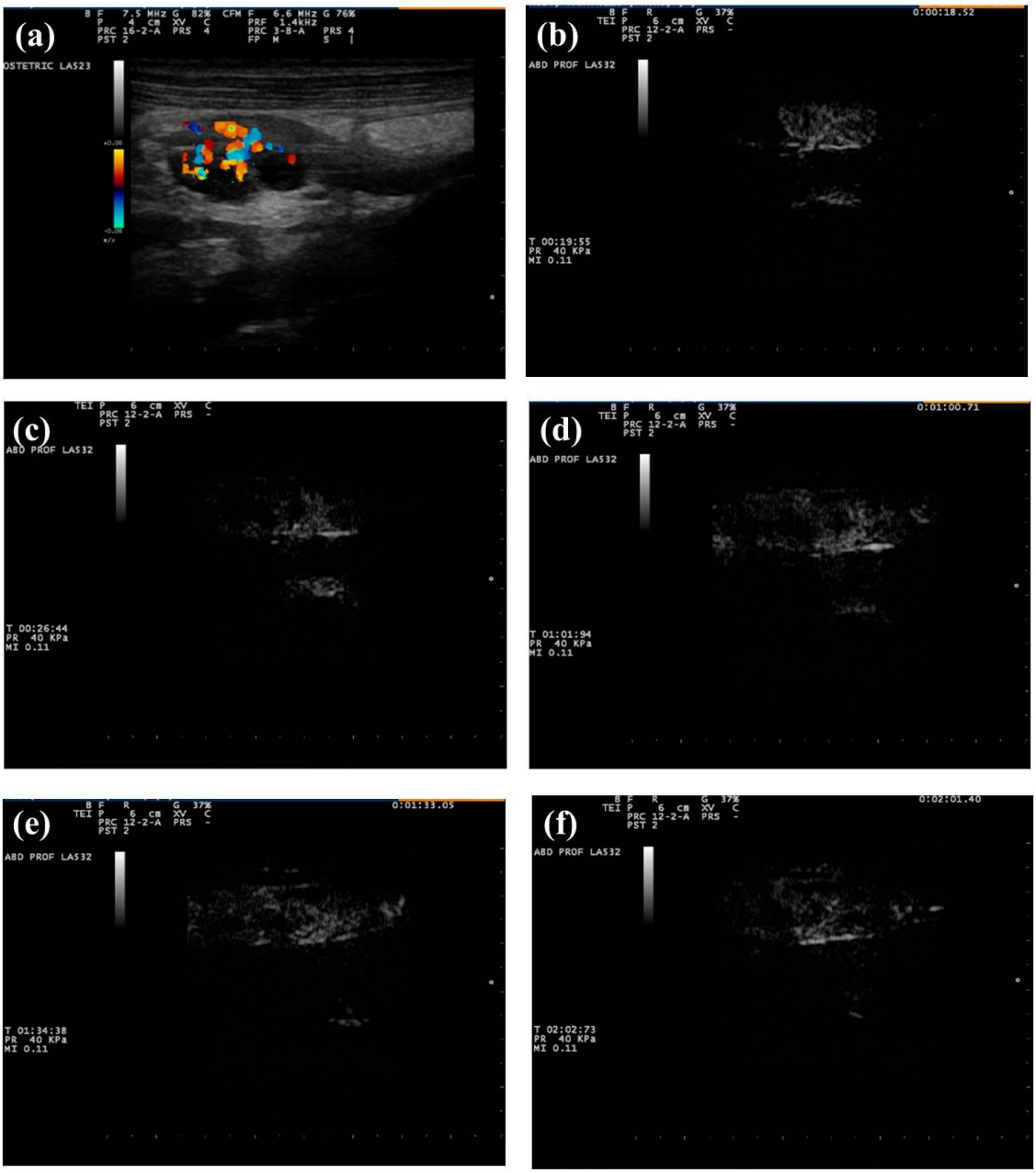

Figure 11.1 Ovary appearance of CEUS. Vascularization of estrus period with Doppler(a) and CEUS (b)(c)(d)(e)(f): it's visible a micro-vascularization not revealed in Doppler.

In this example micro-vascularization of ovary, it's clearly showed, not clearly showed on Doppler.
More studies should be done, trying to identify with CEUS the different phases.

12 Soft tissue

One study of human medicine in 2015 evaluate the usefulness of contrast-enhanced ultrasonography (CEUS) in the bioptic sampling of soft tissue tumours compared with unenhanced ultrasonography alone in 40 patients and in conclusion CEUS, due to its ability to evaluate micro-vascular areas, has proven to be a promising method in guiding bioptic sampling of soft tissue tumour, directing the needle to the most significant areas of the tumour. (Coran, et al., 2015)

In our experience CEUS was used to study a clinical case of a soft tissue lesion: a nodular skin lesion of 1.5cm of diameter on the left chest region near armpit. Doppler evaluation of a lesion gives some indication of a vascularized lesion. On CEUS, the lesion was characterized by a capsule perfused with septae directly to the centre but inside there was a non-enhanced content. Final diagnosis, after surgery excision, with histology was an ascessualized Swannoma tumour (Figure 12.1).

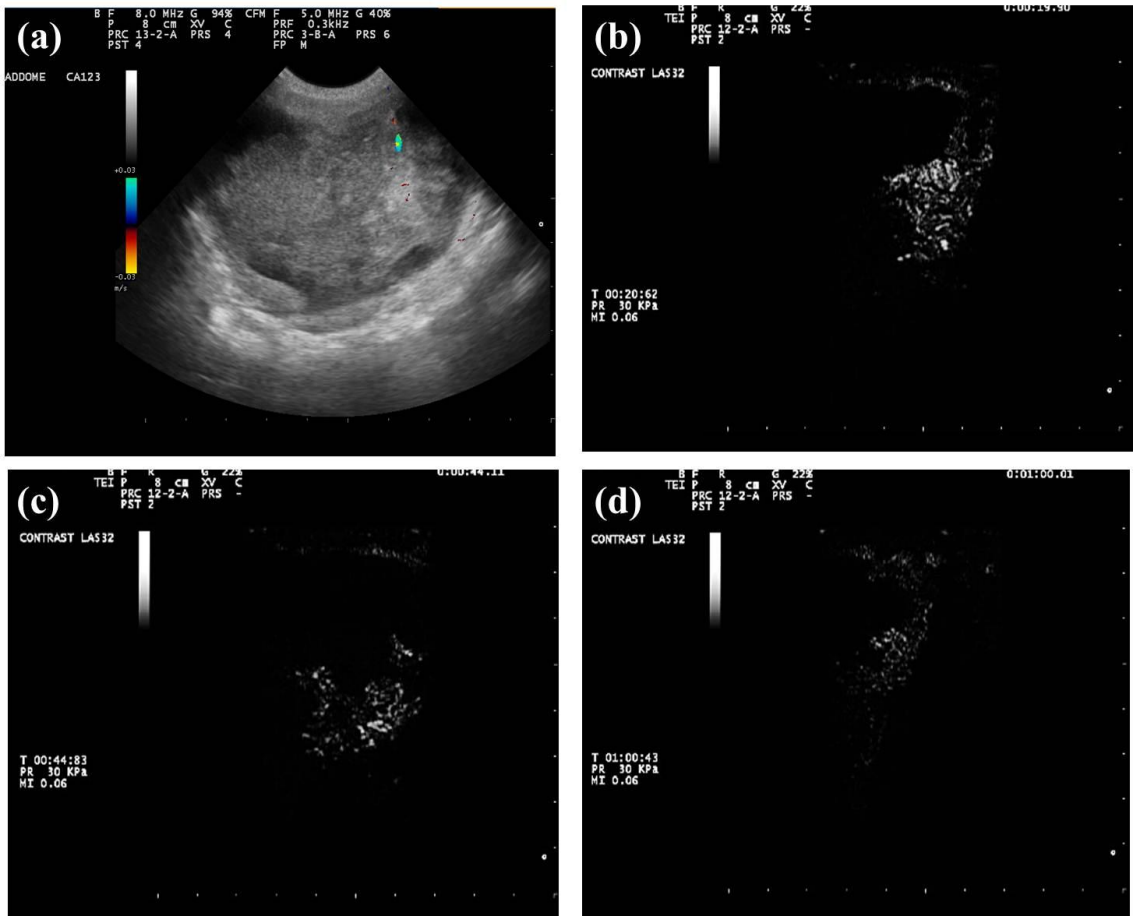

Figure 12.1 Soft Tissue lesion with CEUS. Study of a nodular skin lesion of 1.5cm of diameter on the left chest region near armpit. Doppler (a) evaluation of lesion give some indication of a vascularized lesion. On CEUS (b)(c)(d) the lesion was characterized by a capsule perfused with septae directly to the centre but inside there was a not-enhanced content. Final diagnosis, after surgery excision, with histology was an ascessualized Swannoma tumour.

According to our experience CEUS can be useful to study nodular lesion.

---FINAL SECTION---

13 General Discussion and Conclusions

CEUS method, in the last years, was often used, properly to show the organs perfusion, in human medicine (Claudon, et al., 2008 - Piscaglia, et al., 2012) and in veterinary medicine (Ohlerth & OBrien, et al., 2007).
The guidelines about use of CEUS in human medicine were written in 2012 (Piscaglia, et al., 2012) after some referral about liver given in 2004 and 2008 (Albrecht, et al., 2004 - Claudon, et al., 2008).
Assessed the most accuracy of CEUS compared to Doppler US to detect the perfusion also compared with CT and MR imaging, CEUS has some advantages, being less expensive, portable, and rapidly performed, without ionizing radiation exposure. (Piscaglia, et al., 2012 - Rossi, et al., 2008).
Important reason to use CEUS in these years was, in fact, the safety of the technique without side effects for patients (Piscaglia & Bolondi, 2006 - Haar ter, 2009) confirmed, also, in veterinary medicine (Seiler, et al., 2013 - Ohlerth & OBrien, 2007).
SonoVue® is the UCA used during our clinical experiences; our choice to use a second generation of contrast medium is justified from by the safety studies existing, the microbubble characteristics of blood pool agent, the easily administration. (EMA: European Medicines Agency, 2017)
CEUS have to be performed routinely after B-mode and Doppler when basic US is not sufficient to give information about perfusion characteristics of organs (Piscaglia, et al., 2012).
The procedure has to be organized and conducted by minimum two operators, expert of CEUS and able to set machine, to use the contrast medium, to perform US, to recognize CEUS artefacts (Dietrich, et al., 2010). Of course, the most challenging part of CEUS is the qualitative and quantitative analysis of video clips.
The ROI's placement is the most important critical point in the quantitative analysis: from ROI derive the TIC and software calculate the values of PI, TTP, RBV, RBF, MTT with Parametric Maps and Error Maps.

- Our experience included 20 cases of splenic BNH and some cases of hemangiosarcoma, lymphoma, histiocytic sarcoma.
  If for the few case of malignant lesions, heterogeneity, prominent and tortuous vessels and hypoenhancement were confirmed as previously reported in literature, different data were collected in case of BNH. The simultaneous wash-in lesion with surrounding tissue (with homogeneous or heterogeneous pattern with small anechoic areas) and early wash-out of the nodules were reported. The evidence of hypoenhancement of benign nodular lesions in our study can open new considerations about the specificity, emerged in previous studies, of this pattern for malignant splenic lesions. Probably, alterations of vascular system responsible of the same detection of this perfusion pattern may be not exclusive of neoplastic lesions therefore, we think that new investigations on benign nodular hyperplasia vascularization may help CEUS patterns interpretation.

- The most important use of CEUS in bladder is the evaluation of lesion originating from the wall: in TCC cases, muscle layer involvement was fundamental for the interpretation of malignancy of these lesions.
  Although the small number of dogs enrolled, we believe that CEUS can improve diagnostic accuracy in detection of bladder wall involvement in case of TCC. Very

interesting would be the evaluation of the bladder wall in the course of hyperplastic cystitis using CEUS.

- Aim of our experience about CEUS in kidney failure (IRIS classification) was to determine the usefulness of CEUS in the visualization of peritubular capillaries and changes in enhancement with renal dysfunction. A lower perfusion was noted in comparison to a control group.
  The kidney's failure cases were, however, few, but we think this should be a good point to start to use CEUS for evaluation of vascular alteration associated to kidney disease.

- Topic of our research was also the study of ICT in not sedated subject, starting from referring data about testis tumours in veterinary medicine (Volta, et al., 2014).
  In our study, the pattern of enhancement was similar in focal lesion of ICT with rim enhancement, prominent inner vessels, and compared to Volta et al., 2014, the mean PI was lowest. In other applications, our tool was to show some possibilities to apply CEUS in other organs with the same principles based to the evaluation of perfusion.

In conclusion CEUS may provide a useful tool to evaluate the perfusion of abdominal organs and lesions, becoming an important clinical technique to be used in daily practice. CEUS must be used to complete B-mode and Doppler US and the other diagnostic imaging techniques.

References

Albrecht, T., Blomley, M., Bolondi, L., Claudon, M., Correas, J., Cosgrove, D., Greiner, L., Jager, K., de Jong, N., Leen, E., Lencioni, R., Lindsell, D., Martegani, A., Solbiati, L., Thorelius, L., Tranquart, F., Weskott, H.P., Whittinghamet, T. (2004).
Guidelines for the use of contrast agents in ultrasound. January 2004.
Ultraschall in der Medizin, 25, 249–256.

Barbosa, C., Souza, M., Scalercio, S., Silva, T., Domingues, S., Silva, L. (2013).
Ovarian and uterine periovulatory Doppler ultrasonography in bitches.
Pesquisa Veterinària Brasileira, 33(9), 1144-1150.

Bargellini, P., Orlandi, R., Dentini, A., Paloni, C., Rubini, G., Fonti, P., Diana, A.; Peterson, M.E., Boiti, B., (2016).
Use of Contrast-Enhanced Ultrasound in the Differential Diagnosis of Adrenal Tumors in Dogs.
Journal of the American Animal Hospital Association, 52, 132–143.

Bargellini, P., Orlandi, R., Paloni, C., Rubini, G., Fonti, P., Peterson M.E., Rishniw, M., Boiti, C. (2016).
Evaluation of Contrast-Enhanced Ultrasonography as a method for detecting gallbladder necrosis or rupture in dogs.
Veterinary Radiology and Ultrasound, 57(6), 611-620.

Bargellini, P., Orlandi, R., Paloni, C., Rubini, G., Fonti, P., Peterson, M.E., Boiti, C (2013).
Contrast-Enhanced Ultrasonographic characteristics of adrenal glands in dogs with pituitary dependent hyperadrenocorticism.
Veterinary Radiology and Ultrasound, 54(3), 283-292.

Bergeron, L., Nykamp, S., Brisson, B., Madan, P., & Gartley, C. (2013).
An evaluation of B-mode and colour Doppler ultrasonography for detecting periovulatory events in the bitch.
Theriogenology, 79, 274-283.

Brunereaua, L., Bruyère, F., Linassier, C., & Baulieu, J. (2012).
The role of imaging in staging and monitoring testicular cancer.
Diagnostic and Interventional Imaging, 93, 310-318.

Bude, R., Rubin, J., & Adler, R. (1994).
Power versus conventional Doppler sonography: comparison in the depiction of normal Intrarenal vasculature.
Radiology, 192, 777–780.

Cantisani, V., Bertolotto, M., Weskott, H. P., Romanind, L., Grazhdani, H., Passamonti, M., Drudi, F.M., Malpassini, F., Isidori, A., Meloni, F.M., Calliada, F., D'Ambrosio, F. (2015).
Growing indications for CEUS: The kidney, testis, lymph nodes, thyroid, prostate, and small bowel.
European Journal of Radiology, 84, 1675–1684.

Caruso, G., Salvaggio, G., Campisi, A., Melloni, D., Midiri, M., Bertolotto, M., Lagalla, R. (2010).
Bladder Tumor Staging: Comparison of Contrast-Enhanced and Gray-Scale Ultrasound.
American Journal of Roentgenology, 96, 151-156.

Choi, S., Jeong, W., Lee, Y., & Choi, H. (2016).
Contrast enhanced ultrasonography of kidney in conscious and anesthetized beagle dogs
The Journal of Veterinary Medicine Science, 78(2), 239-244.

Claudon, M., Cosgrove, D., Albrecht, T., Bolondi, L., Bosio, M., Calliada F., Correas, J.M., Darge, K., Dietrich, C., D'Onofrio, M., Evans, D.H., Filice, C., Greiner, L., Jäger, K., Jong, N., Leen, E., Lencioni, R., Lindsell, D., Martegani, A., Meairs, S., Nolsøe, C., Piscaglia, F., Ricci, P., Seidel, G., Skjoldbye, B., Solbiati, L., Thorelius, L., Tranquart, F., Weskott, H.P., Whittingham, T.
Guidelines and good clinical practice recommendations for contrast enhanced ultrasound (CEUS) - update 2008.
Ultraschall in der Medizine 29(1),28-44

Cole, P. (2012).
Association of canine splenic hemangiosarcomas and hematomas with nodular lymphoid hyperplasia or siderotic nodules.
Journal of Veterinary Diagnostic Investigation, 24(4), 759-762.

Coran, A., Di Maggio, A., Rastrelli, M., Alberioli, E., Attar, S., Ortolan, P., Bortolanza, C., Tosi, A., Montesco, M.C., Bezzon, E., Rossi, C.R., Stramare, R. (2015).
Core needle biopsy of soft tissue tumors, CEUS vs US guided: a pilot study.
Journal of Ultrasound, 18(4), 335-342.

Corbin, E., Cavanaugh, R., Schwartz, P., Zawadzki, K., & Donovan, T. (2017).
Splenomegaly in small-breed dogs: 45 cases(2005–2011) .
Journal American Veterinary Medical Association, 250, 1148–1154.

Costa, H., Goto, F., Saldanha, L., Silva, S., Sinhorini, I., Silva, T., Guerra, J.L. (2003).
Histopathologic Patterns of Nephropathy in Naturally Acquired Canine Visceral Leishmaniasis.
Veterinary Pathology, 40 677–684

D'Onofrio, M., Gallotti, A., Principe, F., & Pozzi Mucelli, R. (2010).
Contrast-enhanced ultrasound of the pancreas.
World Journal of Radiology, 2(3), 97-102.

Diana, A., Linta, N., Cipone, M., Fedone, V., Steiner, J., Fracassi, F., Grandis, A., BaronToaldo, M., (2015). Contrast-enhanced ultrasonography of the pancreas in healthy cats.
BioMedical Central Veterinary Research, 11:64

Dietrich, C., Ignee, A., Barreiros, A., Schreiber-Dietrich, D., Sienz, M., Bojunga, J., Braden, B. (2010).
Contrast-Enhanced Ultrasound for Imaging of Adrenal Masses.
Ultraschall in der Medizine, 31, 163-168.

Dietrich, C., Ignee, A., Hocke, M., Schreiber-Dietrich, D., & Greis, C. (2011).
Pitfalls and artefacts using contrast enhanced ultrasound.
Zeitschrift Fur Gastroenterologie, *49*, 350-356.

Dong, Y., Wang, C. W., Fan, P., & Lin, X. (2013).
Quantitative Evaluation of Contrast-Enhanced Ultrasonography in the Diagnosis of Chronic Ischemic Renal Disease in a Dog Model.
Plos One 8(8)

Drudi, F., Di Leo, N., Maghella, F., Malpassini, F., Iera, J., Rubini, A., Orsogna, N., D'Ambrosio, F. (2014). CEUS in the study of bladder, method, administration and evaluation, a technical note .
Journal of Ultrasound, 17, 57-63.

Drudi, F., Di Leo, N., Malpassini, F., Antonini, F., Corongiu, E., & Iori, F. (2012).
CEUS in the differentiation between lowand high-grade bladder carcinoma.
Journal of Ultrasound, 15, 247-251.

Eriksson, R., Persson, H., Dymling, S., & Lindstrom, K. (1991).
Evaluation of Doppler ultrasound for blood perfusion measurements.
Ultrasound in Medicine and Biology, 17, 445-452.

EMA: European Medicines Agency. (2017): http://www.ema.europa.eu.

Evans, H. E., & De Lahunta, A. (2013).
Miller's anatomy of the dog.
Elsevier Saunder.

Fine, L., & Norman, J. (2008).
Chronic hypoxia as mechanism of progression of chronic kidney diseases: from hypothesis to novel therapeutics.
Kidney International, 74(7), 867-872.

Fine, L., Bandyopadhay, D., & Norman, J. (2000).
Is there a common mechanism for the progression of different types of renal diseases other than proteinuria? Towards the unifying theme of chronic hypoxia.
Kidney International, 75, 22-26.

Friedrich-Rust, M., Glasemann, T., Polta, A., Eichler, K., Holzer, K., Kriener, S., Herrmann, E., Nierhoff, J., Bon, D., Bechstein, W.O., Vogl, T., Zeuzem, S., Bojunga, J. (2011).
Differentiation between Benign and Malignant Adrenal Mass using Contrast-Enhanced Ultrasound.
Ultraschall in der Medizine, 32, 460-471.

Girometti, R., Stocca, T., Serena, E., Granata, A., & Bertolotto, M. (2017).
Impact of contrast-enhanced ultrasound in patients with renal function impairment.
World Journal of Radiology , 9(1), 10-16.

Grieco, V., Riccardi, E., Greppiy, G., Teruzzi, F., Iermano`, V., & Finazzi, M. (2008).
Canine Testicular Tumours: a Study on 232 Dogs . 2008, Vol. 138, 86-89.

Journal of Comparative Pathology 138, 86-89.

Haar ter, G. (2009).
Safety and bio-effects of ultrasound contrast agents.
Medical and Biological Engineering Computing, 47, 893–900.

Haers, H., Daminet, S., Smets, P., Duchateau, L., Aresu, L., & Saunders, J. (2013).
Use of quantitative contrast-enhanced ultrasonography to detect diffuse renal changes in Beagles with iatrogenic hypercortisolism.
American Journal of Veterinary Research, 74, 70-77.

Haers, H., Vignoli, M., Paes, G., Rossi, F., Taeymans, O., Daminet, S., Saunders, J.H. (2010).
Contrast Harmonic Ultrasonographic Appearance Of Focal Space-Occupying Renal Lesions.
Veterinary Radiology & Ultrasound, 51(5), 516-522.

Hayes, H., & Pendergrass, T. (1976).
Canine testicular tumors: epidemiologic features of 410 dogs.
International Journal of Cancer, 18(4), 482-487.

Ivančić, M., Long, F., & Seiler, G. S. (2009).
Contrast harmonic ultrasonography of splenic masses and associated liver nodules in dogs.
Journal of the American Veterinary Medical Association, 234(1), 88-94.

Jang, H., Yu, H., & Kim, T. (2009).
Contrast-enhanced ultrasound in the detection and characterization of liver tumors.
Cancer Imaging, 9, 96-103.

Kennedy, P. (1998).
Histological classifications of tumors of the genital system of domestic animals.
Armed Forced Istitute of Pathology, 4, 17-18.

Kinns, K., Aronson, L., Hauptman, J., & Seiler, G. (2010).
Contrast-Enhanced Ultrasound Of The Feline Kidney.
Veterinary Radiology & Ultrasound, 51(2), 168-172.

Leinonen, M., Raekallio, M., Vainio, O., & O'Brien, R. (2011).
Effect of anaesthesia on contrast-enhanced ultrasound of the feline spleen.
The Veterinary Journal, 190,273.

Lim, S., Nakamura, K., Morishita, K., Sasaki, N., Murakami, M., Osuga, T., Ohta, H., Yamasaki, M., Takiguchi, M. (2014).
Qualitative and Quantitative Contrast-Enhanced Ultrasonographic Assessment of Cerulein-Induced Acute Pancreatitis in Dogs.
Journal of Veterinary Internternal Medicine, 28, 496-503.

Lim, S., Nakamura, K., Moroshita, K., Sasaki, N., Murakami, M., Osuga, T., Ohta, H., Yamasaki, M., Takiguchi, M. (2013).

Qualitative and Quantitative Contrast Enhanced Ultrasonography of the Pancreas Using Bolus Injection and Continuous Infusion Methods in Normal Dogs.
The Journal of Veterinary Medical Science, 75(12), 1601–1607.

Liu, L., Zhao, Y., Zhang, Y., & Liu, J. (2015).
Differential diagnosis between benign and malignant gallbladder diseases with contrast-enhanced ultrasound.
Ultrasound in Medicine and Biology, 41, 99-105.

Liu, L.N., Xu, H.X., Lu, M.D., Xie, X.Y., Wang, W.P., Hu, B., Yan, K., Ding, H., Tang, S.S., Qian, L.X., Luo, B.M., Wen, Y.L. (2012).
Contrast-Enhanced Ultrasound in the Diagnosis of Gallbladder Diseases: A Multi-Center Experience.
Plos One.

Löffler, C., Sattler, H., Uppenkamp, M., & Bergner, R. (2016).
Contrast-enhanced ultrasound in coxitis.
Joint Bone Spine, 669-674.

Macrì, F., Di Pietro, S., Liotta, L., & al., e. (2016).
Effects of size and location of regions of interest examined by use of contrast-enhanced ultrasonography on renal perfusion variables of dogs.
American Journal of Veterinary Research, 77(8), 869-876.

Mattoon, J., & Nyland, T. (2015).
Small animal diagnostic ultrasound.
Elsevier Saunders.

Miele, V., Piccolo, C., Galluzzo, M., Ianniello, S., Sessa, B., & Trinci, M. (2016).
Contrast-enhanced ultrasound (CEUS) in blunt abdominal trauma.
The British Journal of Radioly, 89.

Mitchelld, S., Toald, R., Danield, G., & Rohrbacvh, B. (1998).
Evaluation Of Renal Hemodynamics In Awake and Isoflurane-Anesthetized Cats With Pulsed-Wave Doppler and Quantitative Renal Scintigraphy.
Veterinary Radiology & Ultrasound, 39(5), 451-458.

Nakamura, K., Lim, S., Ochiai, K., Yamasaki, M., Ohta, H., Morishita, K., et al. (2015).
Contrast-Enhanced Ultrasonographic Findings In Three Dogs With Pancreatic Insulinoma.
Veterinary Radiology and Ultrasound, 55(1), 55-62.

Nakamura, K., Sasaki, N., Murakami, M., Bandula Kumara, W. R., Ohta, H., Yamasaki, M., Takagi, S., Osaki, T., Takiguchi, M. (2010).
Contrast-Enhanced Ultrasonography for Characterization of Focal Splenic Lesions in Dogs.
Journal of Veterinary Internal Medicine 24:1290–1297.

Nakamura, K., Sasaki, N., Yoshikawa, M., Ohta, H., Hwang, S.J., Mimura, T., Yamasaki, M., Takiguchi, M. (2009).
Quantitative Contrast-Enhanced Ultrasonography Of Canine Spleen.

Veterinary Radiology & Ultrasound, 50(1), 104-108.

Nakamura, K., Takagi, S., Sasaki, N., Kumara, W., Murakami, M., Ohta, H., Yamasaki, M., Takiguchi, M. (2010).
Contrast-Enhanced Ultrasonography For Characterization Of Canine Focal Liver Lesions.
Veterinary Radiology & Ultrasound, 51(1), 79-85.

Nangaku, M. (2006).
Chronic Hypoxia and Tubulointerstitial Injury: A Final Common Pathway to End-Stage Renal Failure.
Journal of the American Society of Nephrology 17, 17-25.

Nicolau, C., Bunesch, L., Peri, L., Salvador, R., Corral, J., Mallofre, C., Sebastia, C. (2011).
Accuracy of contrast-enhanced ultrasound in the detection of bladder cancer .
The British Journal of Radiology, 94, 1091–1099.

Nisa, K., Lim, S.Y., Shinohara, M., Nagata, N., Sasaoka, K., Dermlim, A., Leela-Arporn, R., Morita, T., Yokoyama, N., Osuga, T., Sasaki, N., Morishita, K., Nakamura, K., Ohta, H., Takiguchi, M. (2017)
Repeatability And Reproducibility Of Quantitative Contrast-Enhanced Ultrasonography For Assessing Duodenal Perfusion In Healthy Dogs
The Journal Of Veterinary Medical Science

Nyman, H., Kristensen, A., Kjelgaard-Hansen, M., & Mcevoy, F. (2005).
Contrast-Enhanced Ultrasonography In Normal Canine Liver. Evaluation Of Imaging And Safety Parameters .
Veterinary Radiology & Ultrasound, 46(3), 243-250.

O'Brien, R., Iani, M., Matheson, J., Delaney, F., & Young, K. (2004).
Contrast Harmonic Ultrasound Of Spontaneous Liver Nodules In 32 Dogs .
Veterinary Radiology & Ultrasound, 45(6), 547-553.

Oh, T., Lee, Y., & Seo, I. (2014).
Diagnostic Efficacy of Contrast-Enhanced Ultrasound for Small Renal Masses . *Korean Journal of Urology*.

Ohlerth, S., & OBrien, R. (2007).
Contrast ultrasound: General principles and veterinary clinical applications. *The Veterinary Journal, 174*, 501-512.

Ohlerth, S., Dennler, M., Rüefli, E., Hauser, B., Poirier, V., Siebeck, N., Roos, M., Kaser-Hotz, B. (2008).
Contrast harmonic imaging characterization of canine splenic lesions.
Journal of Veterinary Internal Medicine, 22(5), 1095-1102.

Ohlerth, S., Ru¨ Efli, E., Poirier, V., Roos, M., & Kaser-Hotz, B. (2007).
Contrast Harmonic Imaging Of The Normal Canine Spleen.
Veterinary Radiology & Ultrasound, 48(5), 451-456.

Paefgen, V., Doleschel, D., & Kiessling, F. (2015).
Evolution of contrast agents for ultrasound imaging and ultrasound-mediated drug delivery Frontiers in Pharmacology vol6 n197 2015.
Frontiers in Pharmacology, 6(197).

Pawson, P. (2008). Sedatives.
In Maddison, J., Steven, P., Church, D.
Small animal clinical pharmacology (p. 113-125).
Elsevier Saunders.

Peddu, P., Shah, M., & Sidhu, P. (2004).
Splenic abnormalities: a comparative review of ultrasound, microbubble-enhanced ultrasound and computed tomography
Clinical Radiology, 59, 777-792.

Penninck, D., & D'Anjou, M. (2015).
Atlas of Small Animal Ultrasonography (Second ed.).
JohnWiley & Sons.

Piscaglia, F., & Bolondi, L. (2006).
The safety of Sonovue in abdominal applications: retrospective analysis of 23188 investigations.
Ultrasound in Medicine and Biology, *32*, 1369–1375.

Piscaglia, F., Nolsøe, C., Dietrich, C., Cosgrove, D., Gilja, O., Bachmann Nielsen, M., Albrecht, T., Barozzi, L., Bertolotto, M., Catalano, O., Claudon, M., Clevert, D.A., Correas, J. M., D ́Onofrio, M., Drudi, F. M., Eyding, J., Giovannini, M., Hocke, M., Ignee, A., Jung, E.M., Klauser, A.S., Lassau, N., Leen, E., Mathis, G., Saftoiu, A., Seidel, G., Sidhu, P.S., ter. Haar, G., Timmerman, D., Weskott H.P.(2012).The EFSUMB Guidelines and Recommendations on the Clinical Practice of Contrast Enhanced Ultrasound (CEUS): Update 2011 on non-hepatic applications.
Ultraschall in der Medizine, 33, 33–59.

Polisca, A., Zelli, R., Troisi, A., Orlandi, R., Brecchia, G., & Boiti, C. (2013).
Power and pulsed Doppler evaluation of ovarian hemodynamic changes during diestrus in pregnant and nonpregnant bitches.
Theriogenology, 79, 219–224.

Pollard, R., Watson, K., Hu, X., Ingham, E., & Ferrara, K. (2017).
Feasibility of quantitative contrast ultrasound imaging of bladder tumors in dogs.
Canadian Veterinary Journal, 58, 70-72.

Qiao, J., Yu, J., Yu, Z., Li, N., Song, C., & Li, M. (2015).
Contrast-Enhanced Ultrasonography in Differential Diagnosis of Benign and Malignant Ovarian Tumors . *Plos One*.

Quaia, E. (2005).
Contrast Media in ultrasonography. Basic Principles and Clinical Applications.
Springer.

Rademacher, N., Ohlerth, S., Scharf, G., Laluhova, D., Sieber-Ruckstuhl, N., Alt, M., Roos, M., Grest, P., Kaser-Hotz, B. et al. (2008).
Contrast-Enhanced Power and Colour Doppler Ultrasonography of the Pancreas in Healthy and Diseased Cats.
Journal of Veterinary Internternal Medicine, 22, 1310-1316.

Rademacher, N., Schur, D., Gaschen, F., Kearney, M., & Gaschen, L. (2016).
Contrast-Enhanced Ultrasonography Of The Pancreas In Healthy Dogs And In Dogs With Acute Pancreatitis.
Veterinary Radioloy and Ultrasound, 57(1), 58-64.

Rauch, M., Schild, H., & Strunk, H. (2014).
Contrast enhanced ultrasound of a hepatic soft tissue angiosarcoma metastasis. Case report.
Medical Ultrasonography, 16(3), 271-273.

Recaldini, C., Carrafiello, G., Bertolotti, E., Angeretti, M., & Fugazzola, C. (2008).
Contrast-Enhanced Ultrasonograpic Findings In Pancreatic Tumors.
International Journal of Medical Science, 5, 203-208.

Restitutti, F., Laitinen, M., Raekallio, M., Vainionp, M., O'Brien, R., Kuusela, E., Vainio, O.M (2013).
Effect of K-467 on organ blood flow parameters detected by contrast-enhanced ultrasound in dogs treated with dexmedetomidine.
Veterinary Anaesthesis analgesia, 40(6), 48-56.

Rossi, F., Fina, C., Stock, E., Vanderperren, K., Duchateau, L., & Saunders, J. (2016).
Effect of sedation on contrast-enhanced ultrasonography of the spleen in healthy dogs.
Veterinary Radiology and Ultrasound, 57(3), 276-81.

Rossi, F., Leone, V. F., Vignoli, M., Laddaga, E., & Terragni, R. (2008).
Use of contrast-enhanced ultrasound for characterization of focal splenic lesions.
Veterinary Radiology & Ultrasound, 49(2), 154-164.

Rossi, F., Rabba, S., Vignoli, M., Haers, H., Terragni, R., & Saunders, J. H. (2010).
B-Mode And Contrast-Enhanced Sonographic Assessment Of Accessory Spleen In The Dog.
Veterinary Radiology & Ultrasound, 51(2), 173-177.

Salwei, R., O'Brien, R., Matheson, J., (2005).
Characterization of lymphomatous lymph nodes in dogs using contrast harmonicand Power Dopplerultrasound.
Vet Radiol Ultrasound, 46(5), 411-416.

Schneider, A., Goodwin, M., Schelleman, A., Michael Bailey, M., Johnson, L., & Bellomo, R. (2014).
Contrast-enhanced ultrasonography to evaluate changes in renal cortical microcirculation inducedby noradrenaline: a pilot study.
Critical Care, 18(6):653.

Sconfienza, L., Perrone, N., Delnevo, A., Lacelli, F., Murolo, C., Gandolfo, N., Serafini, G. (2010)
Diagnostic value of contrast-enhanced ultrasonography in the characterization of ovarian tumors.
Journal of Ultrasound, 13, 9-15.

Seiler, G., Brown, J., Reetz, J., Taeymans, O., Bucknoff, M., Rossi, F., Ohlerth, S., Alder, D., Rademacher, N., Tod Drost, W., Pollard, R.E., Travetti, O., Pey, P., Saunders, J.H., Shanaman, M.M, Oliveira, C.R., O'Brien, R.T., Gaschen, L. (2013).
Safety of contrast-enhanced ultrasonography in dogs and cats: 488 cases (2002-2011).
Journal of American Veterinary Medicine Association, 242(9), 1255-9.

Sharpley, J. L., Marolf, A. J., Reichle, J. K., Bachand, A. M., & Randall, E. K. (2012).
Color And Power Doppler Ultrasonography For Characterization Of Splenic Masses In Dogs.
Veterinary Radiology and Ultrasound, 53(5), 586-590.

Shin, H., Chang, E., Lee, H., Hong, J., Park, G., Kim, H., Kim, M.J., Lee, M.J. (2015).
Contrast-enhanced ultrasonography for the evaluation of liver fibrosis after biliary obstruction .
World Journal of Gastroenterology, 21(9), 2614-2621.

Si, Q., Qian, X., Wang, F., & al, e. (2013).
Real-Time Grey Scale Contrast-Enhanced Ultrasonography in Diagnosis of Gallbladder Cancer.
Ultrasound in Medicine and Biology, 39, 86-91.

Solano-Gallego, L., Miró, G., Koutinas, A., Cardoso, L., Pennisi, M., Ferrer, L., Bourdeau, P., Oliva, G., Baneth, G. (2011).
LeishVet guidelines for the practical management of canine leishmaniasis.
Parasites & Vectors.

Spangler, W., & Culbertson, M. (1992).
Prevalence, type, and importance of splenic diseases in dogs: 1,480 cases (1985-1989).
Journal of American Veterinary Medical Association.

Spârchez, Z., & Radu, P. (2012).
Role of CEUS in the diagnosis of gallbladder disease.
Medical Ultrasonography, 14(4), 326-330.

Stock, E., Vanderperren, K., Bosmans, T., Dobbeleir, A., Duchateau, L., Hesta, M., Lybaert, L., Peremans, K., Vandermeulen, E., Saunders, J.H. (2016).
Evaluation of Feline Renal Perfusion with Contrast-Enhanced Ultrasonography and Scintigraphy.
PlosOne, 11(10).

Stock, E., Vanderperren, K., Van der Vekens, E., Hendrik Haers, H., Duchateau, L., Polis, I., Hesta, M., Saunders, J.H. (2014).
The effect of anesthesia with propofol and sedation with butorphanol on quantitative contrast enhanced ultrasonography of the healthy feline kidney.
The Veterinary Journal, 637–639.

Taeymans, O., & Penninck, D. (2011).
Contrast Enhanced Sonographic Assessment Of Feeding Vessels As A Discriminator Between Malignant Vs. Benign Focal Splenic Lesions.
Veterinary Radiology & Ultrasound, 52(4), 457-461.

Tang, M. X., Mulvana, H., Gauthie, T., Lim, A. K., Cosgrove, D. O., Eckersley, R. J., Stride, E. (2011).
Quantitative contrast-enhanced ultrasound imaging: a review of sources of variability.
Interface Focus(1), 520-539.

Tang, S., Wang, Y., & Wang, Y. (2013).
Contrast-enhanced ultrasonography to diagnose gallbladder perforation.
American Journal of Emergency Medicine, 31, 1240-1243.

Trillaud, H., Bruel, J., Valette, P., Vilgrain, V., Schmutz, G., Oyen, R., Jakubowski, W., Danes, J., Valek, V., Greis C.(2009).
Characterization of focal liver lesions with SonoVue®- enhanced sonography: International multicenter-study in comparison to CT and MRI.
World Journal of Gastroenterology, 15(30), 3748-3756.

Troisi, A., Orlandi, R., Bargellini, P., Menchetti, L., Borges, P., Zelli, R., Polisca, A. (2015). Contrast-enhanced ultrasonographic characteristics of the diseased canine prostate gland.
Theriogenology, 84(8), 1423-30.

Tsuji, S., Sofuni, A., Moriyasu, F., Itokawa, F., Ishii, K., Kurihara, T., Tsuchiya, T., Ikeuchi, N., Umeda, J., Tanaka, R., Itoi, T. (2012).
Contrast-enhanced ultrasonography in the diagnosis of gallbladder disease.
Hepatogastroenterology, 59, 336-340.

Tsuruoka, K., Yasuda, T., Koitabashi, K., Yazawa, M., Shimazaki, M., Sakurada, T., Shirai, S., Shibagaki, Y., Kimura, K., Tsujimoto, F. (2010).
Evaluation of renal microcirculation by contrast-enhanced ultrasound with Sonazoid as a contrast agent.
International Heart Journal, *51*(3), 176-82.

Volta, A., Manfredi, S., Vignoli, M., Russo, M., England, G., Rossi, F., Bigliardi, E., Di Ianni, F., Parmigiani, E., Bresciani, C., Gnudi, G. (2014). Use of Contrast-Enhanced Ultrasonography in Chronic Pathologic Canine Testes.
Reproduction in Domestic Animals, *49*, 202-209.

Waller, K., O'brien, R., & Zagzebski, J. (2007).
Quantitative Contrast Ultrasound Analysis Of Renal Perfusion In Normal Dogs.
Veterinary Radiology & Ultrasound, 48(4), 373-377.

Wang, J., Lv, F., Fei, X., Cui, Q., Wang, L., Gao, X., Yuan, Z., Lin, Q., Lv, Y., Liu, A. (2011).
Study on the Characteristics of Contrast-Enhanced Ultrasound and Its Utility in Assessing the Microvessel Density in Ovarian Tumors or Tumor-Like Le-sions.
International Journal of Biological Sciences, 7, 600-606.

Wang, W., Fei, Y., & Wang, F. (2016).
Meta-analysis of contrast-enhanced ultrasonography for the detection of gallbladder carcinoma.
Medical Ultrasonography, 18(3), 281-287.

Wang, X., Wang, Y., & Lei, C. (2011).
Evaluating the perfusion of occupying lesions of kidney and bladder with contrast-enhanced ultrasound .
Clinical Imaging, 447–451.

Xue, L., Lu, Q., Huang, B., Ma, J., Yan, L., Wen, J., et al. (2014).
Contrast-enhanced ultrasonography for evaluation of cystic renal mass: in comparison to contrast-enhanced CT and conventional ultrasound .
Abdominal Imaging, 39, 1274–1283.

Yamaya, Y., Niizeki, K., Kim, J., Entin, P., Wagner, H., & Wagner, P. (2004).
Anaphylactoid response to Optison and its effects on pulmonary function in two dogs.
The Journal of Veterinary Medical Science, 66(11), 1492-32.

Yang, W., Chen, M., Wu, W., Dai, Y., & Fan, Z. (2015).
Effects of Gray-Scale Ultrasonography Immediate Post-Contrast on Characterization of Focal Liver Lesions.
BioMed Research International.

Zatelli, A., Borgarelli, M., Santilli, R., Bonfanti, U., Nigrisoli, E., Zanatta, R., Tarducci, A., Guarraci, A. (2003).
Glomerular lesions in dogs infected with Leishmania organisms.
American Journal of Veterinary Research, 64(5), 558-561.

Zhang, Z., Hong, Y., Liu, N., & Chen, Y. (2017).
Diagnostic accuracy of contrast enhanced ultrasound in patients with blunt abdominal trauma presenting to the emergency department: a systematic review and meta-analysis.
Scientific Report, 30(7).

Zhao, C., Jiang, Y., Li, J., Xu, Z., Zhang, Q., Su, N., et al. (2017).
Role of Contrast-enhanced Ultrasound in the Evaluation of Inflammatory Arthritis.
Chinese Medical Journal (Engl), 130(14), 1722-1730.

Zhou, X., Chen, L., Feng, C., Li, B., Tang, J., Liu, A., Lv, F., Li, T. (2013).
Establishing an animal model of intracerebral hemorrhage under the guidance of ultrasound.
Ultrasound in Medicine and Biology, 39(11), 2116-2122.

Ziegler, L., O'Brien, R., Waller, K., & Zagzebski, J. (2003).
Quantitative Contrast Harmonic Ultrasound Imaging Of Normal Canine Liver .
Veterinary Radiology & Ultrasound, 44(4), 451-454.